

**POLYMER FILMS AS MEDIA FOR ORGANOMETALLIC CHEMISTRY,
AND
THE PREPARATION AND CHARACTERIZATION OF AN ELECTRICALLY
CONDUCTING POLY(3-ALKYLTHIOPHENE)-IRON(II) COMPLEX**

A THESIS

by

JIAN PING GAO

Submitted to the Faculty of Graduate Studies and Research in Partial Fulfillment of the
Requirements for the Degree of

Doctor of Philosophy

Department of Chemistry
McGill University
Montreal, Quebec, Canada
H3A 2K6

July, 1989 ©

To my grandmother,

Yian Dang,

to my parents,

and to my husband,

Zhi Yuan

**POLYMER FILMS AS MEDIA FOR ORGANOMETALLIC CHEMISTRY,
AND
THE PREPARATION AND CHARACTERIZATION OF AN ELECTRICALLY
CONDUCTING POLY(3-ALKYLTHIOPHENE)-IRON(II) COMPLEX**

by JIAN PING GAO

ABSTRACT

The thesis is divided into two parts. In part I, the monomeric and dimeric metal carbonyl complexes, $M(CO)_6$ ($M = Cr, Mo, W$), $CpMn(CO)_3$ ($Cp = \eta^5-C_5H_5$), $(\eta^6-C_6H_6)Cr(CO)_3$, $[CpFe(CO)_2]_2$, $[CpMo(CO)_3]_2$, $Mn_2(CO)_{10}$ and *trans*- $Ir(CO)Cl(PPh_3)_2$, have been embedded into polystyrene (PS), poly(methylmethacrylate) (PMMA) and poly(styrene-acrylonitrile) (PSAN) polymer film matrices. The environments experienced by the metal complexes as a function of the polymer type have been characterized by vibrational spectroscopy and have been compared with those of the structurally-related solvents toluene, ethyl acetate and acetonitrile, respectively. Several of films have been subjected to UV irradiation in order to study the solid-state photochemistry of metal carbonyls in donor and non-donor polymer matrices and the effect of the polymer microstructure on the photodecomposition of the complexes. Iodine oxidation of the dimeric complexes in different polymer films and the chemical reactivity of Vaska's complex in PS upon exposure to the simple molecular gases, H_2 , O_2 , CO , SO_2 and I_2 have also been examined.

In part II, treatment of an electrically-nonconducting copolymer of 3-methyl- and 3-hexylthiophene with $[CpFe(CO)_2(H_2C=CMe_2)]BF_4$ gave an electrically-conducting material ($\sigma = 10^{-3}-10^{-4} \Omega^{-1} cm^{-1}$). The IR, UV and NMR spectra of this material and of model complexes suggest that $[CpFe(CO)_2]^+$ residues, which are attached to the sulfur atoms of the thiophene rings of the copolymer backbone, induce the improved conductivity.

**FILMS POLYMERIQUES COMME MILIEUX EN CHIMIE ORGANOMETALLIQUE,
ET
PREPARATION ET CARACTERISATION D'UN COMPLEXE
POLY(ALKYL-3 THIOPHENE)-FER(II) ELECTRIQUEMENT CONDUCTEUR**

par *JIAN PING GAO*

RESUME

La thèse est divisée en deux sections. Premièrement, les complexes métal-carbonyle monomériques et dimériques $M(CO)_6$ ($M = Cr, Mo, W$), $CpMn(CO)_3$ ($Cp = \eta^5-C_5H_5$), $(\eta^6-C_6H_6)Cr(CO)_3$, $[CpFe(CO)_2]_2$, $[CpMo(CO)_3]_2$, Mn_2CO_{10} et *trans*- $IrCl(CO)(PPh_3)_2$, ont été noyés dans des films polymériques constitués de matrices de polystyrène (PS), polymétacrylate de méthyle (PMMA) et du copolymère polystyrène/polyacrylonitrile (PSAN). Les interactions entre les complexes métalliques et leur environnement ont été caractérisées par spectroscopie vibrationnelle et ont été comparées avec celles obtenues dans les solvants apparentés: le toluène, l'acétate d'éthyle et l'acétonitrile respectivement. Plusieurs films ont été soumis à l'irradiation par UV pour étudier la photochimie des carbonyles métalliques dans différentes matrices polymériques ainsi que l'effet de la microstructure du polymère sur la photodécomposition des complexes. L'oxydation par l'iode des complexes dimériques dans différents films de polymères et la réactivité du complexe de Vaska dans le PS suite à l'exposition aux gaz moléculaires simples tels H_2 , O_2 , CO , SO_2 et I_2 a aussi été examinée.

Dans la deuxième partie, le traitement avec $[CpFe(CO)_2CH_2=CMe_2]BF_4$ d'un copolymère électriquement non-conducteur constitué de méthyl-3 et d'hexyl-3 thiophène a donné un matériau conducteur ($\sigma = 10^{-3} \cdot 10^{-4} \Omega^{-1}cm^{-1}$). Les spectres IR, UV et RMN de ce matériau ainsi que de complexes modèles suggèrent que les résidus $[CpFe(CO)_2]^+$, qui sont attachés aux atomes de soufre des anneaux thiophène intégrés dans la chaîne du copolymère induisent l'amélioration de la conductivité.

CONTENTS

ABSTRACT	i
RESUME	ii
CONTENTS	iii
ACKNOWLEDGEMENTS	vii
GLOSSARY OF ABBREVIATIONS	viii
FIGURES	x
TABLES	xiii

PART I.

POLYMER FILMS AS MEDIA FOR ORGANOMETALLIC CHEMISTRY

	Page
CHAPTER 1. General Introduction	1
CHAPTER 2. Vibrational Spectra and Photochemistry of Some Monomeric Organometallic Carbonyl Complexes in Polymer Matrices	
2.1 Introduction	11
2.2 Experimental	12
2.3 Results and Discussion	15
2.3.1 Microscopy Studies	15

2.3.2 Vibrational Spectra	16
a. IR Spectra	16
b. ATR-FT-IR Spectra	20
c. Raman Spectra	22
2.3.3 Photolysis Experiments	24
a. Room-temperature Photolysis	24
b. Low-temperature Photolysis	32
2.4 Conclusions	34

CHAPTER 3. Vibrational Spectra, Photochemistry and Iodine Oxidation Reactions of Dimeric Metal Carbonyl Complexes in Polymer Matrices

3.1 Introduction	36
3.2 Experimental	37
3.3 Results and Discussion	38
3.3.1 IR Spectra	38
3.3.2 Photochemistry	42
3.3.3 Iodine Oxidation Reactions	49
3.3.4 Polarized FT-IR Studies	52
3.4 Conclusions	57

CHAPTER 4. Reactions of Organometallics Embedded in Polystyrene Matrices With Gases

4.1 Introduction	58
------------------	----

4.2 Experimental	59
4.3 Results and Discussion	61
4.3.1 Substitution Reactions of CpRu(COD)Cl in PS Films	61
4.3.2 Addition Reactions of <i>trans</i> -Ir(CO)Cl(PPh ₃) ₂ in PS Films	
a. H ₂ addition	64
b. O ₂ addition	66
c. SO ₂ addition	67
d. CO addition	69
e. I ₂ addition	71
4.3.3 ATR-IR Studies	71
4.4 Conclusions	73

PART II.

THE PREPARATION AND CHARACTERIZATION OF AN ELECTRICALLY CONDUCTING POLY(3-ALKYLTHIOPHENE)-IRON(II) COMPLEX

CHAPTER 5. General Introduction	74
5.1 Conducting Polymers	74
5.2 Conductivity Mechanisms of Solid Materials	83
a. Electronic Conductivity	83
b. Ionic Conductivity	87
c. Conducting Polymers	88

CHAPTER 6. Synthesis and Characterization of an Electrically Conducting Poly(3-alkylthiophene)-Iron(II) Complex	
6.1 Introduction	91
6.2 Experimental	92
6.3 Results	100
a. Preparation of 3-Alkylthiophene polymers	100
b. I ₂ -Doping	104
c. Thiophene-iron Model Complexes	106
d. [CpFe(CO) ₂] ⁺ -doping	107
6.4 Discussion	115
6.5 Conclusions	117
6.6 Suggestions for Future Work	117
SUMMARY AND CONTRIBUTIONS TO KNOWLEDGE	118
PUBLICATIONS	120

ACKNOWLEDGEMENTS

I would like to express my deepfelt gratitude to my two research directors, Dr. *Ian S Butler* and Dr. *Alan Shaver*, for their guidance, patience and encouragement during this research. Many friendly, interesting discussions with them have made my studies at McGill University especially rewarding.

I would also like to thank:

McGill University for the award of a Major Fellowship (Balbir Bindra) and the Department of Chemistry for financial support in the form of teaching and research assistantships;

Dr. *J. Chun* for allowing the use of his UV-VIS instrument;

Dr. *A. Eisenberg* for providing the facilities to prepare polymer films;

Dr. *G. Eccles* for his help with various instruments;

Dr. *D F R. Gilson* and Dr. *J. Harrod* for their suggestions;

Dr. *A. Ismail* for access of his Bomem FTIR instrument and for many useful discussions;

Dr. *B. Lennox* for his useful suggestions;

Dr. *F. Sauriol* for her instruction and aid in running the NMR spectra;

Miss *N. Kawai*, *B. Soo Lum*, *H. Uhm*, *A. Wei* and Ms. *H.Q. Li*, for their friendship and assistance in proofreading this thesis;

Drs. *G. Lord*, *R.M. Paroli* and *Z.H. Xu* for their considerable help during my early days here;

Mr. *J. Demers* for translating the abstract of this thesis into French;

Mr. *S. Barnett*, *G. Emo*, *Y.N. Huang*, *J. Haines*, Dr. *I. Wharf* and all the members of rooms 335 and 435 of the Otto Maass Chemistry Building for their friendly assistance.

GLOSSARY OF ABBREVIATIONS

Ac	acetyl
AC	alternating current
AIBN	α , α' -azobisisobutyronitrile
ANAL.	elemental analysis
ATR	attenuated total reflectance
br	broad
bridg	bridging
<i>n</i> -Bu ₂ O	<i>n</i> -butyl ether
Calcd	calculated
COD	cycloocta-1,5-diene
COP	3-methyl-(3-hexylthiophene)copolymer
Cp	η^5 -cyclopentadienyl
DC	direct current
d_p	penetration depth
dppp	1,3-bis(diphenylphosphino)propane
DTGS	deuterium triglycine sulfate
Eq	equation
Et ₂ O	diethyl ether
Fig	figure
h	hour(s)
Ir/PS	PS film containing <i>trans</i> -Ir(CO)Cl(PPh ₃) ₂
Ir ¹³ CO/PS	PS film containing <i>trans</i> -Ir(¹³ CO)Cl(PPh ₃) ₂
KRS-5	TlI·TlBr
m	medium

min	minute(s)
PE	polyethylene
PMMA	polymethylmethacrylate
PP	polypyrrole
PPP	poly(<i>p</i> -phenylene)
PPS	poly(<i>p</i> -phenylene sulphide)
PT	polythiophene
PS	polystyrene
PSAN	poly(styrene-acrylonitrile)
PTFE	polytetrafluoroethylene
PVC	poly(vinyl chloride)
s	strong
sh	shoulder
THF	tetrahydrofuran
vs	very strong
vw	very weak
w	weak

Figures

Figure

- 2-1 Electron micrograph (6000 X) of transparent PS film embedded with $W(CO)_6$ (10%). 15
- 2-2 The IR spectrum in the $\nu(CO)$ region of $W(CO)_6$ in PMMA film. 18
- 2-3 Transmission IR and ATR-IR spectra in the $\nu(CO)$ region of $Cr(CO)_6$ in PS and $(\eta^6-C_6H_6)Cr(CO)_3$ in PSAN film. 21
- 2-4 The Raman spectra in the $\nu(CO)$ region of (a) crystalline $W(CO)_6$; (b) $W(CO)_6$ (21%)-PSAN film; (c) $W(CO)_6$ (40%)-PSAN film and (d) pure PSAN film. 23
- 2-5 The IR spectra in the $\nu(CO)$ region of $W(CO)_6$ in PS film before irradiation, after irradiation (Pyrex filter) for 10 min and after allowing the latter sample to stand for 20 min. 28
- 2-6 The IR spectra in the $\nu(CO)$ region of $W(CO)_6$ in PMMA film before irradiation, after irradiation (Pyrex filter) for 10 min and after allowing the latter sample to stand for 8 h. 28
- 2-7 The IR spectra in the $\nu(CO)$ region of $W(CO)_6$ in PSAN film before irradiation, after irradiation (Pyrex filter) for 10 min and after allowing the latter sample to stand for 8 h. 29
- 2-8 The IR spectra in the $\nu(CO)$ region of $CpMn(CO)_2(PSAN)$ produced by UV irradiation (Pyrex filter) of $CpMn(CO)_3$ in PSAN for 30 min. 32
- 2-9 The IR spectra in the $\nu(CO)$ region of $W(CO)_6$ in PS film (a) at $-145^\circ C$ before irradiation; (b) after irradiation for 30 min at $-145^\circ C$ and (c) after allowing the latter sample to warm up to room temperature. 33

- 3-1 The IR spectra in the $\nu(\text{CO})$ region of $[\text{CpFe}(\text{CO})_2]_2$ in PS and PSAN showing the effect of the polymer on the relative amounts of the *cis* and *trans* isomers. 41
- 3-2 The IR spectra in the $\nu(\text{CO})$ region of $[\text{CpFe}(\text{CO})_2]_2$ in PSAN: (a) before irradiation; (b) after irradiation for 4 h and (c) spectrum (a) subtracted from spectrum (b). 47
- 3-3 The IR spectrum in the $\nu(\text{CO})$ region of $\text{eq-Mn}_2(\text{CO})_9(\text{PSAN})$ in PSAN. 48
- 3-4 The IR spectra in the $\nu(\text{CO})$ region of $[\text{CpFe}(\text{CO})_2]_2$ in PS: before exposure to I_2 , after exposure to I_2 for 1 day and 10 days. 50
- 3-5 (a) The parallel polarized IR spectrum in the $\nu(\text{CO})$ region of $\text{Mn}_2(\text{CO})_{10}$ soaked in PE film after stretching; (b) dichroic IR spectra (A_{\parallel} - A_{\perp}) of $\text{Mn}_2(\text{CO})_{10}$ in PE after stretching and (c) before stretching. 55
- 3-6 The parallel and perpendicular polarized IR spectra in the low-frequency region of $\text{Mn}_2(\text{CO})_{10}$ in PE film after stretching. 56
- 4-1 The IR spectra in the $\nu(\text{CO})$ region of $\text{CpRu}(\text{CO})_2\text{Cl}$ and $\text{CpRu}^{13}\text{CO}_2\text{Cl}$. 62
- 4-2 The IR spectra in the $\nu(\text{CO})$ region of Ir/PS upon treatment with H_2 for 5 days, followed by exposure to vacuum for 3 days and followed by exposure to air for 3 days. 65
- 4-3 The IR spectra in the $\nu(\text{CO})$ region of Ir/PS upon treatment with O_2 for 5 days, followed by exposure to vacuum for 3 days and followed by exposure to air for 3 days. 66
- 4-4 The IR spectra in the $\nu(\text{CO})$ region of Ir/PS upon treatment with SO_2 before treatment, treatment for 3h and followed by exposure to vacuum for 15 h. 68
- 4-5 The IR spectra in the $\nu(\text{CO})$ region of Ir ^{13}CO /PS upon treatment with

	CO (a) before treatment; (b) after treatment for 20 min and (c) followed by exposure to vacuum for 30 min.	70
4-6	The IR and ATR-IR spectra in the $\nu(\text{CO})$ region of Ir/PS upon treatment with I_2 for 3 h.	72
6-1	Schematic diagram of the in-line four-probe conductivity measurement apparatus.	99
6-2	$^1\text{H-NMR}$ spectrum of 3-methyl-(3-hexylthiophene)copolymer in CDCl_3 .	102
6-3	IR spectra of COP and I_2 -oxidized COP.	103
6-4	UV-VIS absorption spectra of COP in CH_2Cl_2 and cast on a quartz surface.	104
6-5	The IR spectra of (a) COP, (b) $[\text{CpFe}(\text{CO})_2\text{-COP}]\text{BF}_4$, (c) $\text{CpFe}(\text{CO})_2\text{I-COP}$. and $\text{CpFe}(\text{CO})_3\text{BF}_4\text{-COP}$.	110
6-6	UV-VIS spectra of $[\text{CpFe}(\text{CO})_2\text{-COP}]\text{BF}_4$, $[\text{CpFe}(\text{CO})_2(3\text{-methylthiophene})]\text{BF}_4$ and COP.	111
6-7	$\text{Log } \sigma$ as a function of the number of $[\text{CpFe}(\text{CO})_2]^+$ residues attached to every 100 thiophene rings.	112
6-8	The current of $[\text{CpFe}(\text{CO})_2\text{-COP}]\text{BF}_4$ as a function of time under constant DC conditions (200 V).	113

Tables

Table

2-1	Observed carbonyl stretching modes of the monomeric metal carbonyl complexes in various solvents.	16
2-2	Observed carbonyl stretching modes of the monomeric metal carbonyl complexes in polymer film matrices.	17
2-3	Assignment of the CO stretching modes of the species generated by UV irradiation of the monomeric metal carbonyl complexes embedded in polymer matrices.	27
3-1	Observed carbonyl stretching modes of $[\text{CpFe}(\text{CO})_2]_2$, $[\text{CpMo}(\text{CO})_3]_2$ and $\text{Mn}_2(\text{CO})_{10}$ in different media.	39
3-2	Consumption of metal carbonyl starting material (as percentage) by photoreaction (30 min) as a function of polymer and film thickness (mm).	45
3-3	Consumption of metal carbonyl starting material (as percentage) by iodine oxidation (10 days) as a function of polymer and film thickness (mm).	51
4-1	The carbonyl stretching frequencies of <i>trans</i> - $\text{Ir}(\text{CO})\text{Cl}(\text{PPh}_3)_2$ and selected adducts and of $\text{CpRu}(\text{CO})_2\text{Cl}$ in PS and other media.	63

PART I.
POLYMER FILMS AS MEDIA FOR ORGANOMETALLIC
CHEMISTRY

CHAPTER 1. General Introduction

Metal-polymer systems are important from both practical and theoretical standpoints. Current research is directed towards the optical, electrical, photochemical, mechanical, catalytic and biomedical applications of these materials.¹ For example, thermal-decomposition of $W(CO)_6$ in polycarbonate polymer solution produces a dark blue mixture and castings of this polymer solution are capable of absorbing near-IR radiation and are useful as optical, e.g., ophthalmic lenses.² Reaction of poly(Vbpy) (Vbpy = 4-Methyl-4'-vinyl-2,2'-bipyridine) with *cis*- $Ru(bpy)_2Cl_2$ (bpy = 2,2'-bipyridine) gives rise to the polymer pendant $[Ru(bpy)_3]^{2+}$, which is a potential catalyst for solar energy conversion.³ In addition, heme and 1-(2-phenylethyl)imidazole embedded in polystyrene reversibly bind O_2 in the presence of water,⁴ while polyacetylene containing ferrocenyl groups becomes a much better electrical conductor when exposed to I_2 .⁵ From a theoretical point of view, the latter two examples are valuable as models to understand the biochemical processes occurring in nature and the conduction mechanisms in polymers.

There are several different ways of incorporating metal complexes into organic polymers.⁶ For instance, the metal species can be attached to the polymer via reaction of pendant functional groups with metal complexes [Scheme 1-1].

1. (a) Zeldin, M.; Wynne, K.J.; Allcock, H.R.(eds) *Inorganic and Organometallic Polymers* American Chemical Society, Washington, DC, 1988. (b) Sheats, J.E.; Carraher, C.E.; Pittman, C.U.Jr.(eds) *Metal-Containing Polymeric Systems* Plenum Press, New York, 1985. (c) Carraher, C.E.Jr.; Sheats, J.E.; Pittman, C.U.Jr. (eds) *Advances in Organometallic and Inorganic Polymer Science* Marcel Dekker, Inc. New York, 1982.

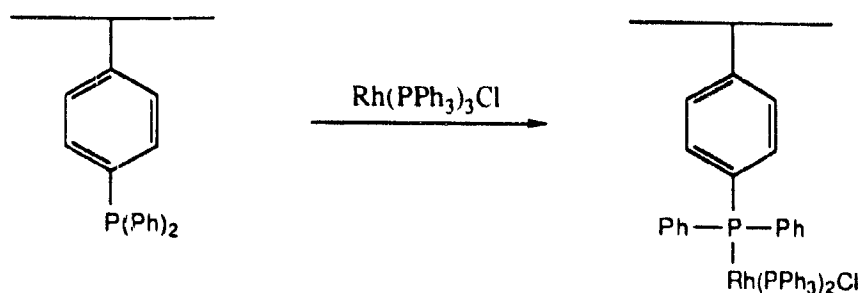
2. Vance, J.D. US Patent 4464 525, 1984.

3. Kaneko, M.; Yamada, A. In ref. 1(b), p249.

4. Wang, J.H. *J. Am. Chem. Soc.* 1958, 80, 3168.

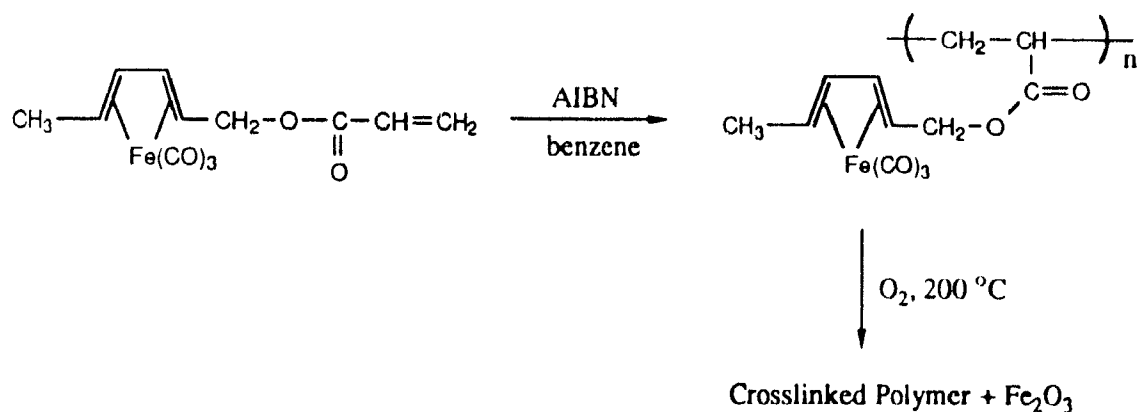
5. Camus, A.; Faruffini, V.; Furlani, A.; Marsich, N.; Ortaggi, G.; Paolesse, R.; Russo, M.V. *Appl. Organomet. Chem.* 1988, 2, 533.

6. Clair, A.K.St.; Taylor, L.T. in ref. 1(c), p95.



Scheme 1-1

Polymerization of the vinyl group attached to metal moieties has been studied extensively, particularly by Pittman and coworkers.⁷ They have prepared and copolymerized several monomers such as: (styrene)tricarbonylchromium(0), π -(2,4-hexadien-1-yl acrylate)-tricarbonyliron(0), and (vinyl-cyclopentadienyl)tricarbonylmanganese(I). They have also thermally decomposed polymers containing $\text{Fe}(\text{CO})_3$ or $\text{Cr}(\text{CO})_3$ fragments in air to give Fe_2O_3 and Cr_xO_y as fine powders [Scheme 1-2].⁸ This is an interesting method of preparing metals or metal oxides highly dispersed in a polymer medium.

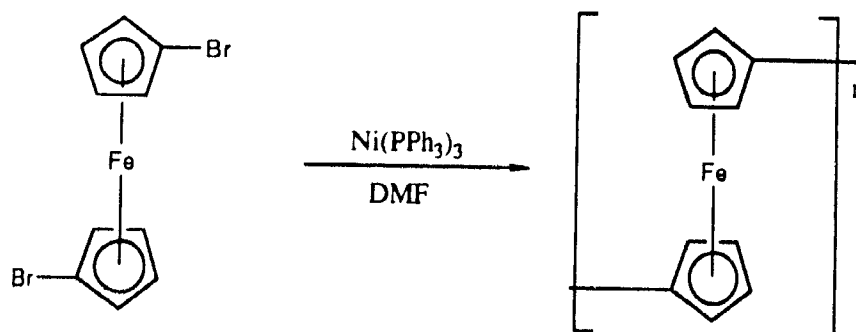


Scheme 1-2

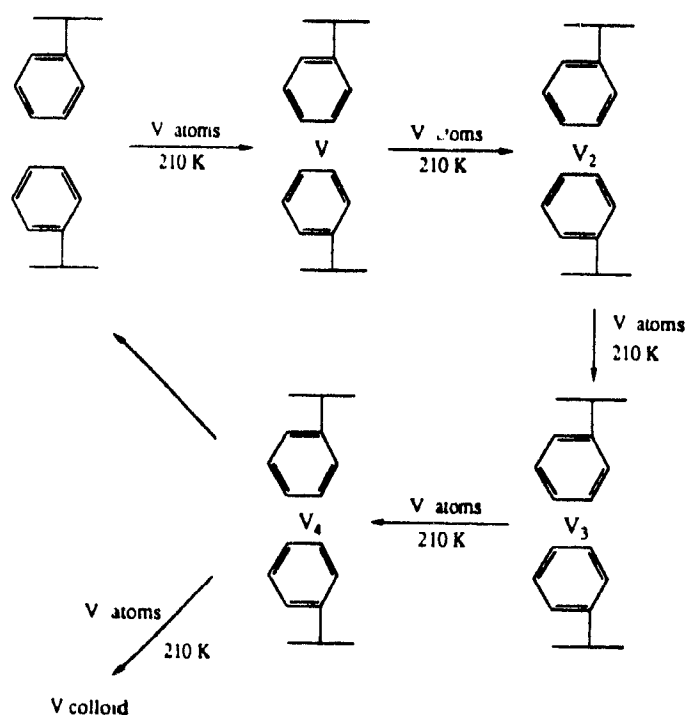
7. Pittman, C.U.Jr.; Rausch, M.D. *Pure & Appl. Chem.*, **1986**, *58*, 617.

8. (a) Pittman, C.U.Jr.; Ayers, O.E.; McManus, S.P. *Macromolecules*, **1974**, *7*, 737. (b) Pittman, C.U.Jr.; Ayers, O.E.; McManus, S.P. *J. Macromol. Sci.-Chem.* **1973**, *A7(8)*, 1563.

Polymers with metal-containing groups on the main chain (e.g., poly-1,1'-ferrocenylene) can be made by various monomer coupling reactions [Scheme 1-3].⁹ Recently, the metal vapour deposition method has been applied to the formation of metal-containing polymers and polymer-supported cluster species [Scheme 1-4].¹⁰



Scheme 1-3



Scheme 1-4

(Adapted from ref.10.)

9. Neuse, E.W. in ref. 1(c), p3.

10. Francis, C.G.; Ozin, G.A. in ref. 1(c), p167.

The chemistry of organometallic complexes embedded in solid polymer matrices is another interesting area that has received relatively little attention and constitutes the focus of the first part of this thesis. The practice of embedding organometallic compounds into polymer matrices in order to study their photochemistry dates back to 1961 Massey and Orgel¹¹ reported that dissolution of group VIB metal hexacarbonyls ($M(CO)_6$, $M = Cr, Mo, W$) in a benzene solution of polymethylmethacrylate (PMMA) followed by evaporation of the solvent leaves a film containing the organometallic [Scheme 1-5]. This method, known as solvent casting, has become the most commonly used method to embed organometallic complexes in polymer films. Subsequent UV irradiation of the PMMA films at room temperature caused them to change from colourless to yellowish, presumably because of the formation of $M(CO)_5$ photofragments. Over the next 15 years, little additional work¹² was done until Galembeck, De Paoli and coworkers reported their results of the effects of UV light on polytetrafluoroethylene (PTFE) and polyethylene (PE) films containing $Fe(CO)_5$ in the absence and presence of ligands such as olefins, dienes and acrylic acid.^{13,14,15,16} To prepare their samples, they soaked the polymer film first in liquid $Fe(CO)_5$ for 24 h, and then in neat alkene (L), or placed it under alkene gas for 24 h [Scheme 1-6]. On the basis of their IR spectra in the carbonyl stretching region, the photoproducts were identified as $Fe_2(CO)_9$, $Fe(CO)_4L$, $Fe(CO)_3L_2$. Presumably, the monomeric species have either the high mobility or the high concentration in the polymer bulk necessary for the occurrence of a bimolecular photoreaction.

11. Massey, A.G.; Orgel, L.E. *Nature(London)* **1961**, 1387.

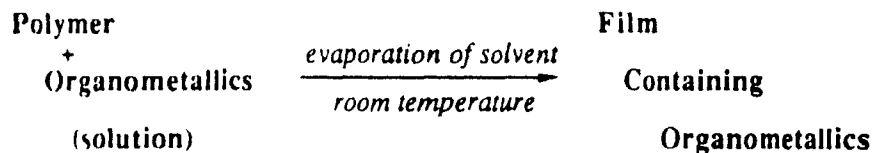
12. McIntyre, J.A. *J. Phy. Chem.* **1970**, *74*, 2403.

13. Galembeck, F. *J. Polym. Sci. Polym. Chem. Ed.* **1978**, *16*, 3015.

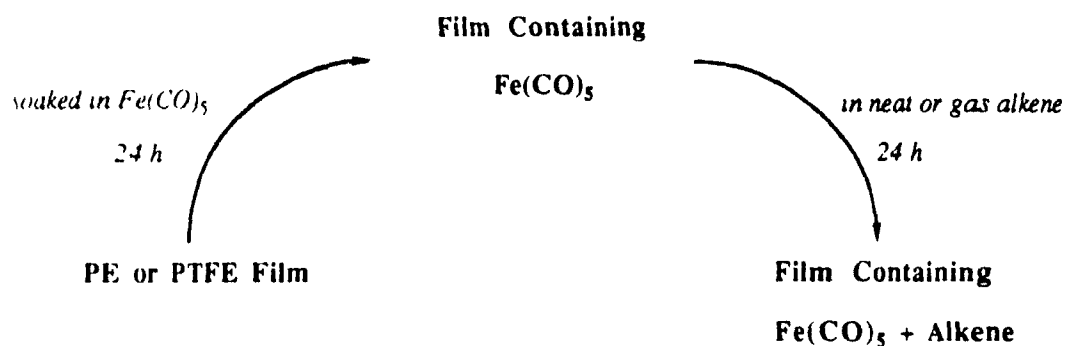
14. De Paoli, M.A.; Tamashiro, T.; Galembeck, F. *J. Polym. Sci. Polym. Lett. Ed.* **1979**, *17*, 391.

15. Galembeck, F.; Galembeck, S.E.; Vargas, H.; Ribeiro, L.A.; Miranda, L.C.M.; Glizoni, C.C. In: *Surface Contamination* Mittal, K.L.(ed.), Plenum Press, New York, **1979**, Vol. 1, p 57.

16. De Paoli, M.A.; Oliveira, M.; Galembeck, F. *J. Organomet. Chem.* **1980**, *193*, 105.



Scheme 1-5



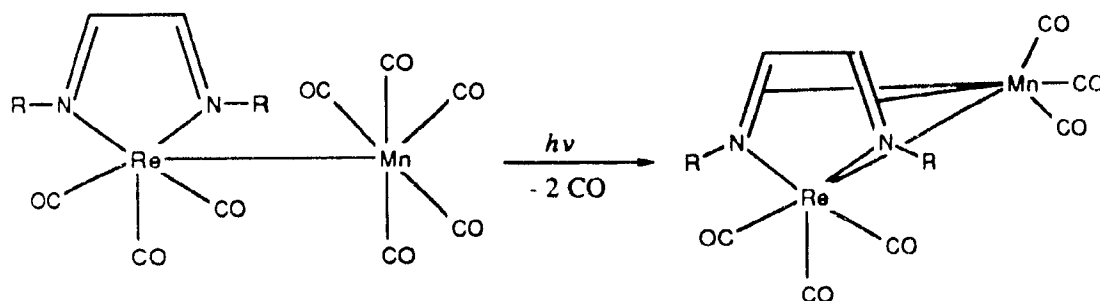
Scheme 1-6

The low-temperature gas matrix isolation method has been extensively used to study photochemical processes of transition metal carbonyls and to isolate rather air-sensitive, unstable species.¹⁷ For example, $\text{Cr}(\text{CO})_5$ -matrix (matrix = Ne, Ar and CH_4) can be generated in the corresponding matrix by UV photolysis of $\text{Cr}(\text{CO})_6$.¹⁸ Low-temperature matrices such as the inert gases, CH_4 and N_2 , necessitate expensive cryogenic equipment and a special high-vacuum system. Matrix isolation in a polymer was first regarded as a simple and inexpensive potential alternative method that could be used over a wide temperature range. Rest and colleagues have studied the photochemistry of organometallic

17. (a) Burdett, J.K.; Downs, A.J.; Gaskill, G.P.; Graham, M.A.; Turner, J.J.; Turner, R.F. *Inorg. Chem.* **1978**, *17*, 523. (b) Crayston, J.A.; Almond, M.J.; Downs, A.J.; Poliakoff, M.; Turner, J.J. *Inorg. Chem.* **1984**, *23*, 3051.

18. Perutz, R.N.; Turner, J.J. *J. Am. Chem. Soc.* **1975**, *97*, 4791.

complexes in cast polymer films throughout the 12-300K temperature range.¹⁹ This research team used poly(vinyl chloride) (PVC),^{20,21,22} poly(vinyl alcohol),²³ paraffin wax, and Nujol mull as matrices.²⁴ Intermediates such as $\text{CpFe}(\text{CO})_3\text{FeCp}$ with three bridging carbonyls and free CO were observed upon irradiating $[\text{CpFe}(\text{CO})_2]_2$ in PVC film at low temperature. Photolysis of $\text{CpM}(\text{CO})_3\text{R}$ ($\text{M} = \text{Mo}, \text{W}$, $\text{R} = \text{CH}_3, \text{CH}_2\text{CH}_3$) in PVC at room temperature led to the detection of several products (e.g., $\text{CpM}(\text{CO})_3\text{Cl}$, $\text{CpM}(\text{CO})_3\text{H}$, $[\text{CpM}(\text{CO})_3]_2$) by IR spectroscopy. Tannenbaum, Goldberg and Flenniken²⁵ have utilized the method of decomposing $\text{Fe}(\text{CO})_5$ in cast polymer films by UV irradiation or thermal heating to prepare uniform composites of polymer and metal or metal oxide with small particle size. Finally, Stufkens, Oskam and colleagues²⁶ have investigated the photochemistry of the metal-metal bonded species such as $(\text{CO})_5\text{ReMn}(\text{CO})_3(i\text{-Pr-DAB})$ ($\text{DAB} = 1,4\text{-diazabutadiene}$) in PVC films to yield $(\text{CO})_3\text{Mn}(i\text{-Pr-DAB})\text{Re}(\text{CO})_3$ [Scheme 1-7].



Scheme 1-7

19. Hitam, R.B.; Hooker, R.H.; Mahmoud, K.A.; Narayanaswamy, R.; Rest, A.J. *J. Organomet. Chem.* **1981**, 222, C9.

20. Hooker, R.H.; Rest, A.J. *J. Organomet. Chem.* **1983**, 249, 137.

21. Hooker, R.H.; Rest, A.J. *J. Chem. Soc., Dalton Trans., Chem.* **1984**, 761.

22. Hooker, R.H.; Mahmoud, K.A.; Rest, A.J. *J. Chem. Soc., Chem. Commun.* **1983**, 1022.

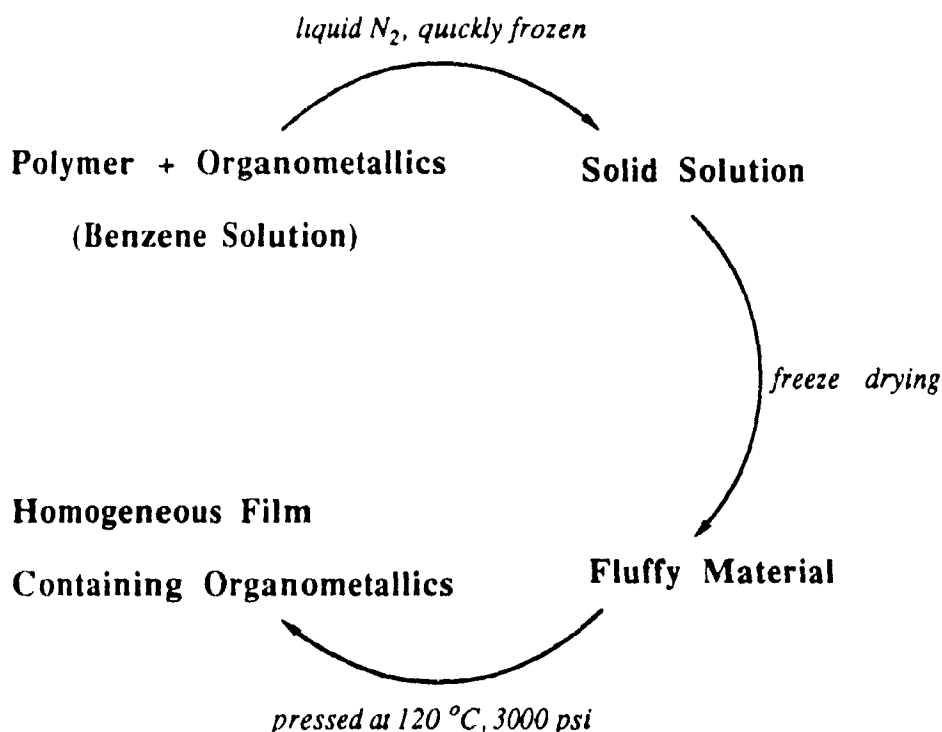
23. Bloyce, P.E.; Hooker, R.H.; Lane, D.A.; Rest, A.J. *J. Photochem.* **1985**, 98, 525.

24. Mascetti, J.; Rest, A.J. *J. Chem. Soc., Chem. Commun.* **1987**, 221.

25. Tannenbaum, R.; Goldberg, E.P.; Flenniken, C.L. in ref. 1(b), p303.

26. Kokkees, M.W.; Stufkens, D.J.; Oskam, A. *Inorg. Chem.* **1985**, 24, 4411.

Initial interest in this area in our laboratory arose from studies of the mechanical spectra of polystyrene strips containing organometallic complexes dispersed as solid solutions throughout the polymer.²⁷ In addition, $\text{Cr}(\text{CO})_6$ embedded in PS has been shown to be a useful calibrant for IR spectra.²⁸ Some preliminary work on embedding monomeric metal carbonyls, such as $(\eta^6\text{-C}_6\text{H}_6)\text{Cr}(\text{CO})_2\text{L}$ ($\text{L} = \text{CO}, \text{P}(\text{n-Bu})_3$), $(\eta^6\text{-C}_6\text{H}_5\text{NH}_2)\text{Cr}(\text{CO})_3$, $(\eta^6\text{-o-C}_6\text{H}_4(\text{NH}_2)\text{Me})\text{Cr}(\text{CO})_3$ and $\text{CpFe}(\text{CO})\text{LR}$ ($\text{L} = \text{CO}, \text{PPh}_3$; $\text{R} = \text{Me}, \text{C}(\text{O})\text{Me}$) into polystyrene (PS), poly(methylmethacrylate) (PMMA), poly(styrene-methyl methacrylate) (PSPMMA) and poly(styrene-acrylonitrile) (PSAN) polymers was performed by Fong, Uhm and Klein.²⁹



Scheme 1-8

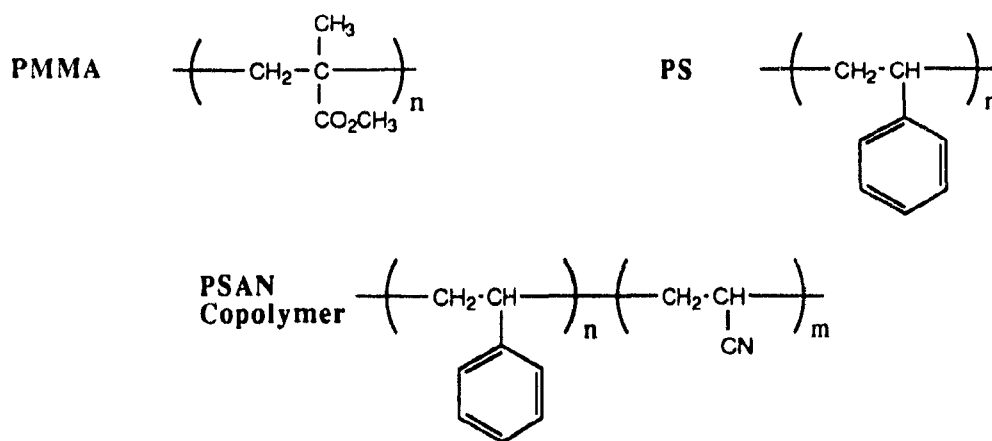
27. (a) Eisenberg, A.; Shaver, A.; Tsutsui, T. *J. Am. Chem. Soc.* **1980**, *102*, 1416. (b) Shaver, A.; Eisenberg, A.; Yamada, K.; Clark, A. J. F.; Farrokyzad, S. *Inorg. Chem.* **1983**, *22*, 4154.

28. Butler, I.S.; Shaver, A.; Fong, B.; Eisenberg, A. *Appl. Spectrosc.* **1984**, *38*, 601.

29. Shaver, A.; Butler, I.S.; Eisenberg, A.; Gao, J.P.; Xu, Z.H.; Fong, B.; Uhm, H.; Klein, D. *Appl. Organomet. Chem.* **1987**, *1*, 383.

The embedding process employed in our group involves freeze-drying a benzene solution of the polymer and complex (1g : 0.05g mixture in 70 mL benzene) and then pressing the resulting fluffy product above the glass-transition temperature of the polymer at about 3000 psi [Scheme 1-8] to give clear, mechanically-robust films. The technique is quite general and suitable for a wide range of polymers and complexes

Earlier work has demonstrated that polymer films provide a matrix that can be used over a wide temperature range for investigating photochemical processes of transition-metal carbonyls and isolating photogenerated species. Such films also afford an additional way of preparing uniform polymer-metal or metal oxide composites. However, many polymers used in previous studies were restricted to simple and inert ones, such as PE, PTFE, PVC and PMMA. Most chemical reactions of the complexes embedded in polymer matrices were photoinduced. The films (cast or soaked) have relatively large amorphous sites and the embedded compounds have quite a high degree of motion in the matrices. The uniformity of these types of film are limited because of their mode of preparation.



scheme 1-9

In the work presented here, series of monomeric and dimeric metal carbonyl complexes have been embedded into PS, PMMA and PSAN polymer matrices [Scheme 1-9]. Most polymers have a "window" of low absorptivity in the region of the IR spectrum where bands due to carbonyl stretching vibrations of metal carbonyls are detected. Therefore, it is reasonable to probe the chemistry of such complexes in polymers using IR spectroscopy. The objectives of this project were:

(1) to characterize by vibrational spectroscopy the environments experienced by metal complexes as a function of the polymer type,

(2) to study the photochemistry of metal carbonyls in non-donor (PS, PMMA) and donor (PSAN) polymer matrices and the effect of the polymer microstructure on photodecomposition of the complexes,

(3) to examine iodine oxidation of dimeric complexes, such as $[\text{CpFe}(\text{CO})_2]_2$, $[\text{CpMo}(\text{CO})_3]_2$ and $\text{Mn}_2(\text{CO})_{10}$, in different polymer films, and

(4) to investigate the chemical reactivity of Vaska's complex *trans*- $\text{Ir}(\text{CO})\text{Cl}(\text{PPh}_3)_2$ embedded in solid PS matrices, when molecular gases, such as H_2 , O_2 , CO and SO_2 are permitted to diffuse through the films.

CHAPTER 2. Vibrational Spectra and Photochemistry of Some Monomeric Organometallic Carbonyl Complexes in Polymer Matrices

2.1 Introduction

The vibrational spectra of the metal hexacarbonyls $M(\text{CO})_6$ ($M = \text{Cr}, \text{Mo}, \text{W}$) have been extensively studied over the past thirty years.³⁰ Their photochemical behaviour in low molecular weight solvents and inert polymer matrices has been investigated throughout a wide temperature range.^{31,32} The photochemistry of $\text{CpMn}(\text{CO})_3$ ³³ and $(\eta^6\text{-C}_6\text{H}_6)\text{Cr}(\text{CO})_3$ ³⁴ in solution has also been examined thoroughly, but comparatively little work in polymer films has been reported. Several derivatives of the metal carbonyl complexes, such as $M(\text{CO})_{6-x}(\text{CH}_3\text{CN})_x$ ($x = 1-3$),³⁵ $\text{CpMn}(\text{CO})_2(\text{CH}_3\text{CN})$,³⁶ $(\eta^6\text{-C}_6\text{H}_6)\text{Cr}(\text{CO})_2(\text{CH}_3\text{CN})$,³⁷ have been prepared and characterized. Therefore, some simple monomeric carbonyl complexes $M(\text{CO})_6$ ($M = \text{Cr}, \text{Mo}, \text{W}$), $\text{CpMn}(\text{CO})_3$ and $(\eta^6\text{-C}_6\text{H}_6)\text{Cr}(\text{CO})_3$ were chosen to be embedded into PS, PMMA and PSAN films for an initial study. The FT-IR and ATR-FT-IR spectra of these films and the behaviour of several of them under UV irradiation were examined. The three objectives of this research were. (1) to characterize the environments imposed on the metal carbonyl complexes by the three different plastics; and (2) to probe the surface properties of the complex-embedded films;

30. Brateman, P.S. *Metal Carbonyl Spectra*, Academic Press, New York, 1975 and references therein.

31. (a) Boxhoorn, G. *Matrix Isolation and Photochemistry of Transition Metal Carbonyl Complexes* Krips Repro Meppel, 1980. (b) Martin, M.; Ozin, G.A. *Cryochemistry*, John Wiley & Sons, Toronto, 1976.

32. Hooper, R.H.; Rest, A.J. *J. Organomet. Chem.* 1983, 249, 137.

33. Creaven, B.S.; Dixon, A.J.; Kelly, J.M.; Long, C.; Poliakoff, M. *Organometallics*, 1987, 6, 2600.

34. Domogalskaya, E.A.; Sketkina, V.N.; Baranetskaya, N.K.; Trembovler, V.N.; Yavorskii, B.M.; Shteinshneider, A.Y.; Petrovskii, P.V. *J. Organomet. Chem.* 1983, 248, 161.

35. Kilner, M. *Adv. Organomet. Chem.* 1972, 10, 115.

36. Haas, H.; Sheline, R.K. *J. Chem. Phys.* 1967, 47, 2996.

37. Knoll, L.; Reiss, K.; Schafer, J. Kluffers, P. *J. Organomet. Chem.* 1980, 193, C40.

(3) to compare the photochemistry of the complexes in donor (PSAN) and non-donor (PS) polymer matrices.

2.2 Experimental

Materials. Organometallic compounds $M(\text{CO})_6$ ($M = \text{Cr}, \text{Mo}, \text{W}$), $\text{CpMn}(\text{CO})_3$ and $(\eta^6\text{-C}_6\text{H}_6)\text{Cr}(\text{CO})_3$ were purchased from Strem chemicals. The PS, PMMA and PSAN (75:25%) polymers were supplied by Polysciences. Spectrograde benzene was used as received.

Preparation of films. The general procedure for preparing polymer films embedded with organometallic compounds was as follows: a mixture of polymer (~ 1 g) and benzene (70 mL) in a 500 mL round-bottomed flask was stirred overnight to ensure that the polymer had completely dissolved. The solution was then degassed by bubbling N_2 through it for 4-5 min. Approximately 0.05-0.1 g of organometallic complex was added to the polymer-benzene mixture under N_2 with vigorous stirring to produce a 2-3 mol% solution. After the complex had dissolved completely, the solution was rapidly frozen by immersing the flask in a liquid- N_2 bath and then quickly connected to a vacuum line which had two traps on it. Benzene was sublimed off over a 24 h period while the flask was placed in an ice bath during this process. The resulting fluffy material was stored in a freezer (-5°C). To make the films, a sample of the fluffy material was compression moulded between two aluminum foil-covered, flat metal plates using a Carver Laboratory Press. The plates were electrically heated at about 120°C and pressed at 3000 psi (21×10^3 kPa) for 30 min. The temperature was monitored by a thermocouple. After turning off the electric heat, the plates were allowed to cool to below 80°C at 3000 psi. The pressure was released and the films were removed after the plates reached ambient temperature. Films produced in this manner are approximately 0.1 mm thick and have IR absorbances below 2.0 in the $\nu(\text{CO})$ region. The

films were stored in N_2 -filled bottles in the freezer. Special samples of PSAN films doped with large amounts of $W(CO)_6$ (weight % = 21, 40) were also prepared for the Raman measurements.

Microscopic examination. The transparency and uniformity of the films were checked visually under a stereomicroscope (Wild M650). A PS film embedded with $W(CO)_6$ was also examined by electron microscopy (Philips EM 400T), the ultrathin sample was prepared by an Ultracut E using a diamond knife.

FT-IR spectra. Most of FT-IR absorption spectra were recorded on a Nicolet model 6000 spectrometer ($4000-400\text{ cm}^{-1}$, KBr beamsplitter) at 1 cm^{-1} resolution and using a liquid- N_2 -cooled mercury-cadmium-telluride (MCT) detector. The band positions were reproducible to within at least $\pm 1\text{ cm}^{-1}$.

ATR-FT-IR spectra. The surfaces of some films were studied by attenuated-total-reflectance (ATR) IR spectroscopy on a Bomem Michelson 100 spectrometer at 4 cm^{-1} resolution and using a deuterium triglycine sulfate (DTGS) detector. The spectra were obtained by placing a film snugly against the surface of a multireflection KRS-5 prism ($10 \times 5 \times 1\text{ mm}$, 45° entrance angle) through which the spectrometer radiation was directed by a beam condenser optic accessory (Spectra-Bench from Spectra-Tech, Inc.). The penetration depth d_p is on the order of one wavelength and can be calculated using the formula:³⁸ $d_p = \lambda / 2\pi n_p (\sin^2\theta - (n_s/n_p)^2)^{1/2}$. In our case, $\lambda = 1/2000\text{ cm}$, $\theta = 45^\circ$, $n_s = 1.6$ (PS), $n_p = 2.4$ (KRS-5), so d_p is around $5 \times 10^{-4}\text{ mm}$, i.e., about 1 % of the film thicknesses.

Raman spectra. The room-temperature, micro-Raman spectra were recorded on an Instruments S.A. Ramanor U-1000 spectrometer with the use of a Spectra-Physics Model 38. Smith, A.L. (ed) *Applied Infrared Spectroscopy*, John Wiley & Sons, Toronto, 1979.

164 5-W argon-ion laser (514.4 nm) line operating at 300 mW power. The films were placed on a microscope slide and laser beam was focused on the area of interest. 180° scattering was employed; the typical slit widths were 300 μm .

Photolysis experiments. The room-temperature photolysis experiments were performed in a closed box (39.6 cm x 65 cm x 60 cm) lined with aluminium foil. A medium-pressure, quartz mercury immersion lamp (Hanovia 100 W) in a water-cooled quartz cell was used as the light source. The films were attached onto an IR sample-holder located about 5 cm from the lamp and N₂ gas acting as a coolant was blown over the surface of the film during the time of irradiation. Irradiation into specific wavelength regions was achieved using filters: H₂NC(S)C(S)NH₂ in ethanol (250-270 nm);³⁹ Pyrex (>310 nm). The photoreactions were monitored by FT-IR spectroscopy on Nicolet and were recorded immediately after irradiation.

The low-temperature photolysis experiments were performed in a home-built variable-temperature, IR sample chamber, which consisted of two round KBr windows (about 5 cm in diameter) and a cold finger. The polymer film was placed between two rectangular KBr windows (1.5 cm x 2.5 cm) which were then incorporated into a frame mounted onto the cold finger inside the sample chamber. Cooling was achieved by pouring liquid N₂ into the cold finger and the temperature was measured by means of a standard thermocouple. The chamber was purged with N₂ gas. A water-cooled medium-pressure mercury lamp (450 W Hanovia) was used as the irradiation source.

39. Robek, J.F. *Experimental Methods in Photochemistry and Photophysics*, John Wiley and Sons, Toronto, 1982, p 891.

2.3 Results and Discussion

2.3.1 Microscopy Studies

Under the stereomicroscope, the films embedded with monomeric metal carbonyl complexes appeared highly transparent and uniform, except for the PSAN films containing large weight percentage of $W(CO)_6$. The latter films showed partial aggregation of $W(CO)_6$ in the PSAN matrix and were translucent. The electron microscopy picture of a transparent PS film embedded with $W(CO)_6$ (about 10%) is shown in Figure 2-1. The fine stripes on the surface are believed to be due to knife vibration while cutting the tough material. No significant aggregation of $W(CO)_6$ was observed in this electronmicrograph.

Above results indicate that polymer films containing highly dispersed organometallics can be produced by the hot pressing technique. However, like low molecular weight solvents, the use of polymers as solid solvents will probably have a solubility limitation as well. Aggregation of the organometallics will occur at high concentration.

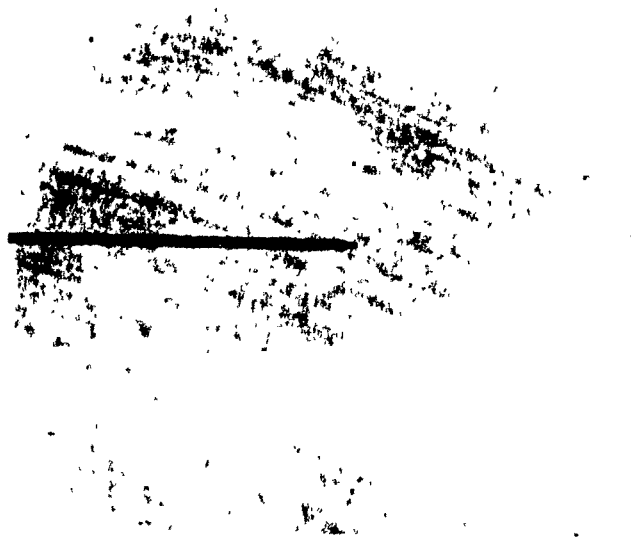


Figure 2-1 Electron micrograph (6000 X) of transparent PS film embedded with $W(CO)_6$ (10%).

2.3.2 Vibrational Spectra

a. IR Spectra

The IR peak positions observed in the $\nu(\text{CO})$ region for the organometallic compounds in some selected solvents and embedded in the polymer matrices are given in Tables 2-1 and 2-2, respectively. There are slight differences in the peak positions and intensities with changes in polymer film. In several cases, there is some evidence of breakdown in the formal IR selection rules.

Table 2-1 Observed carbonyl stretching modes of the monomeric metal carbonyl complexes in various solvents (cm^{-1})

Complex	Solvents			Assignments
	PhMe	MeCO ₂ Et	MeCN	$\nu(\text{CO})$
Cr(CO) ₆		2112vw		a_{1g}
	2020vw	2022w	2024vw	e_g
	1981s	1980s	1979s	t_{1u}
Mo(CO) ₆	2021vw	2022vw	2023vw	e_g
	1982s	1981s	1980s	t_{1u}
W(CO) ₆	2013vw	2017vw		e_g
	1976s	1976s	1974s	t_{1u}

Table 2-2 Observed carbonyl stretching modes of some monomeric metal carbonyl complexes in polymer film matrices (cm^{-1})

Complex	Polymer film			Assignments
	PS	PMMA	PSAN	$\nu(\text{CO})$
$\text{Cr}(\text{CO})_6$	2113vw	2113vw	2113vw	a_{1g}
	2019w	2020w	2021w	e_g
	1980s	1980s	1978s	t_{1u}
$\text{Mo}(\text{CO})_6$		2117vw	2117vw	a_{1g}
	2021w	2022w	2023vw	e_g
	1981s	1982s	1980s	t_{1u}
$\text{W}(\text{CO})_6$	2118w	2118w	2118w	a_{1g}
	2016w	2018w	2016w	e_g
	1977s	1977s	1974s	t_{1u}
$(\eta^6\text{-C}_6\text{H}_6)\text{Cr}(\text{CO})_3$	1970s	1964s	1965s	a_1
	1896s	1902s	1934she	} e
		1887s	1887s	
		1879s		
$\text{CpMn}(\text{CO})_3$	2018s	2016s	2017s	a_1
	1949ms	1945s	1940sh	} e
	1921s	1932s	1929sh	
	1902sh	1919s	1918s	

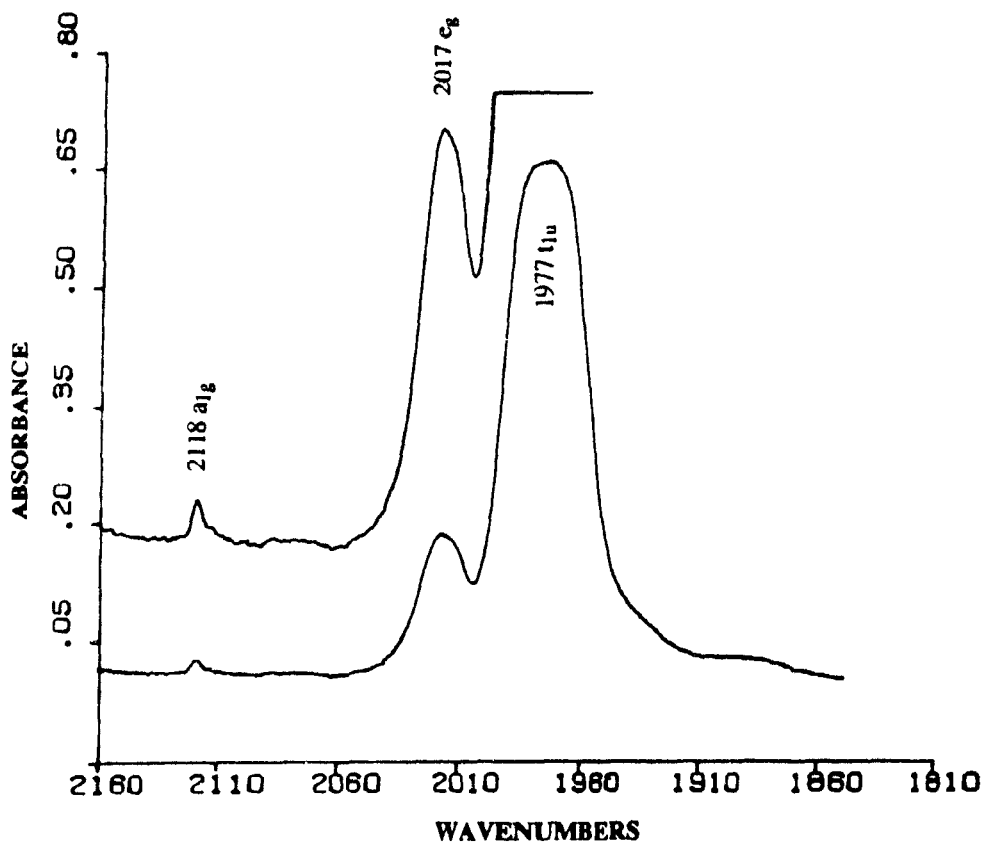


Figure 2-2 The IR spectrum in the $\nu(CO)$ region of $W(CO)_6$ in PMMA film.

$M(CO)_6$. The group VIB $M(CO)_6$ complexes with O_h symmetry have three vibrational $\nu(CO)$ modes ($a_{1g} + e_g + t_{1u}$), for which only the t_{1u} mode is expected to be IR-active.³⁰ In all three polymer matrices, however, there were additional peaks observed. In most cases, there were two extra peaks above the t_{1u} mode [Fig.2-2]. Under O_h selection rules, the a_{1g} and e_g modes are Raman-active only. But, if the $M(CO)_6$ molecules are distorted, the molecular symmetry will be lowered and the a_{1g} and e_g $\nu(CO)$ modes will be able to gain some weak IR activity. Presumably, the hexacarbonyls are slightly distorted by the polymer

matrices leading to the extra IR peaks in the $\nu(\text{CO})$ region. Hooker and Rest³² have noted the same effect for the metal hexacarbonyls in PVC cast films.

The $\nu(\text{CO})$ band positions for the $\text{M}(\text{CO})_6$ complexes in the various polymers are close to those in the structurally related solvents [Tables 2-1 and 2-2]. In a typical case, the IR spectrum of crystalline $\text{W}(\text{CO})_6$ in Nujol mull has a strong peak at 1980 cm^{-1} (t_{1u}) and a very weak band at about 2001 cm^{-1} (e_g). In ethyl acetate and PMMA matrix, the strong t_{1u} peak appears at 1977 cm^{-1} and the e_g mode is shifted to 2017 cm^{-1} . The e_g mode is known to be sensitive to the medium.³⁰ The above IR analysis indicates that $\text{W}(\text{CO})_6$ in solid PMMA film is "dissolved" since its peak positions match closely with those in ethyl acetate. The position of the t_{1u} $\nu(\text{CO})$ mode decreases by about $2\text{-}3 \text{ cm}^{-1}$ on going from PS (Cr, 1980; Mo, 1981; W, 1977 cm^{-1}) to PSAN (Cr, 1978; Mo, 1980; W, 1974 cm^{-1}). These peak positions are close to those for the $\text{M}(\text{CO})_6$ complexes in toluene (Cr, 1981; Mo, 1982; W, 1976 cm^{-1}) and acetonitrile (Cr, 1979; Mo, 1980; W, 1974 cm^{-1}), respectively. In these solvents, the shift on going from toluene to acetonitrile is about 2 cm^{-1} . Similar shifts have been documented previously in studies of the effect of solvents on the positions of $\nu(\text{CO})$ bands in metal carbonyls.^{40,41} The observed shifts for the hexacarbonyls to lower wavenumber in the PSAN matrix reflect the increased polarity of the environment around the metal carbonyl complexes in the PSAN film.

Extra peaks were observed for $\text{M}(\text{CO})_6$ in PSAN films. They were very weak for $\text{M} = \text{Cr}$ ($2074, 1936$ and 1910 cm^{-1}) and weak for $\text{M} = \text{Mo}$ ($2076, 1938$ and 1909 cm^{-1}) and $\text{M} = \text{W}$ ($2075, 1938$ and 1885 cm^{-1}). Since the temperature employed to prepare the films (120°C) is close to that required to prepare derivatives of the type $\text{M}(\text{CO})_{6-x}(\text{CH}_3\text{CN})_x$, where $x = 1\text{-}3$, these extra bands may be due to the monosubstituted species $\text{M}(\text{CO})_5(\text{PSAN})$. This assignment is in accord with the photolysis studies described below. The pressing

40. Brown, D.A.; Hughes, F.J. *J. Chem. Soc. (A)* **1968**, 1519.

41. Parker, D.J.; Stiddard, M.H.B. *J. Chem. Soc. (A)* **1968**, 2263.

temperature is also in the range needed to prepare complexes of the type (arene)Cr(CO)₃. However, no peaks attributable to PSCr(CO)₃ were detected.⁴²

$C_nH_nM(CO)_3$. Complexes of the type of $C_nH_nM(CO)_3$ have C_{3v} symmetry for the $M(CO)_3$ tripod and two strong IR-active $\nu(CO)$ modes (a_1 and e) are expected. Usually, the a_1 band is sharp and the e band is broad. In all three polymer matrices, the e bands are much broader than in solution for both $CpMn(CO)_3$ and $(\eta^6-C_6H_6)Cr(CO)_3$ complexes [Tables 2-1 and 2-2]. Similarly, because of the hot-pressing process, a new peak at 1865 cm^{-1} probably due to $CpMn(CO)_2(PSAN)$ was observed in freshly-prepared PSAN films containing $CpMn(CO)_3$. Another new peak around 1934 cm^{-1} was overlapped. Weak bands due to $Cr(CO)_6$ were observed in the spectra of $(\eta^6-C_6H_6)Cr(CO)_3$ embedded in PMMA and PSAN.

b. ATR-FT-IR Spectra

Several of the metal carbonyl complexes embedded in polymer films were examined by ATR-FT-IR spectroscopy. The relative intensities of the $\nu(CO)$ bands and the nearby peaks due to polymer matrices were measured. The data were compared with those from the corresponding transmission IR spectra. The penetration depth (d_p) of radiation into a polymer film is proportional to the wavelength.³⁸ Therefore, the intensities of the ATR-IR peaks increase on going from the near-IR to the far-IR region. In the $\nu(CO)$ region, d_p is approximately 5×10^{-4} mm, that is about 1% of film thickness.

Fig.2-3(a) shows the transmission IR and ATR-IR spectra of $Cr(CO)_6$ in PS film. With reference to the PS band at $1950\text{-}1850\text{ cm}^{-1}$, the absorption of $Cr(CO)_6$ at 1980 cm^{-1} (t_{1u}) shows no difference in intensity in the IR and ATR-IR spectra. This observation indicates that the metal hexacarbonyl has a similar concentration at the surface as it does inside the

42. Pittman, C.U.Jr.; Grube, P.L.; Ayers, O.E.; McManus, S.P.; Rausch, M.D.; Moser, G.A. *J. Polym. Sci., Polym. Chem. Ed.* **1972**, *10*, 379.

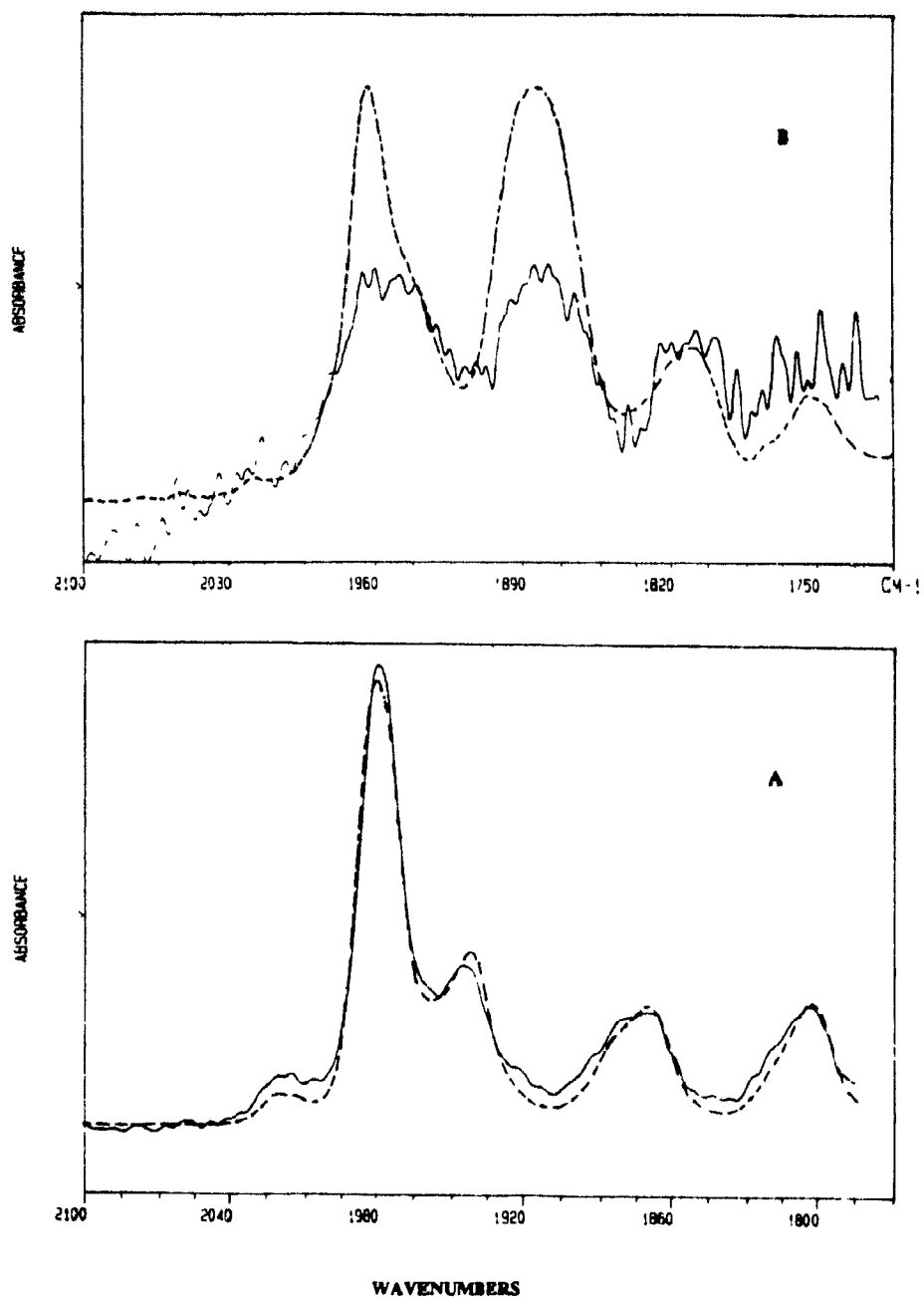


Figure 2-3 Transmission IR (---) and ATR-IR (—) spectra in the $\nu(\text{CO})$ region of (a) $\text{Cr}(\text{CO})_6$ in PS film and (b) $\eta^6\text{-C}_6\text{H}_6\text{Cr}(\text{CO})_3$ in PSAN film.

were no apparent intensity differences in the carbonyl region. However, for the PSAN film embedded with $(\eta^6\text{-C}_6\text{H}_6)\text{Cr}(\text{CO})_3$, there were some significant intensity differences in the $\nu(\text{CO})$ region in the IR and ATR-IR spectra [Fig.2-3(b)]. The absorptions of $(\eta^6\text{-C}_6\text{H}_6)\text{Cr}(\text{CO})_3$ at 1970 and 1896 cm^{-1} are much more intense in the transmission IR than in the ATR-IR. This complex is sensitive to air. The result indicates that $(\eta^6\text{-C}_6\text{H}_6)\text{Cr}(\text{CO})_3$ is more easily decomposed on the surface of the film than in the interior.

c. Raman Spectra

Several of the polymer films, as described earlier, containing metal carbonyls were examined by Raman spectroscopy. Unfortunately, no peaks were observed in the carbonyl region for any of the transparent films. In the case of PSAN films containing a large weight percentage of $\text{W}(\text{CO})_6$, carbonyl peaks were observed, but only if the laser beam was focused onto areas of aggregation. Fig.2-4 shows the Raman spectra of crystalline $\text{W}(\text{CO})_6$, $\text{W}(\text{CO})_6(21\%)\text{-PSAN}$ film, $\text{W}(\text{CO})_6(40\%)\text{-PSAN}$ film and pure PSAN film. Two Raman-active peaks (a_{1g} at 2114 and e_g at 1996 cm^{-1}) were observed in addition to other weaker peaks (1956 cm^{-1} , $\text{W}(\text{CO})_5^{13}\text{CO}$; 2016 cm^{-1} , $t_{1u} + \nu_n$ combination). The Raman spectra of $\text{W}(\text{CO})_6$ have been extensively studied for both the crystalline form and in solution.⁴³ For the crystal, the a_{1g} peak is at 2115 cm^{-1} and e_g at 1998-1996 cm^{-1} . In solution, the a_{1g} band appears around 2120-2117 cm^{-1} and the e_g peak moves to 2012-2010 cm^{-1} . As mentioned earlier, the e_g mode is sensitive to the medium. For $\text{W}(\text{CO})_6$ embedded in PSAN (21 and 40%), the e_g peak appears at 1996 cm^{-1} which is close to that of the crystal. This observation provides further evidence of aggregation of $\text{W}(\text{CO})_6$ in PSAN at high concentrations and supports the contention that $\text{W}(\text{CO})_6$ is "dissolved" at low concentrations.

43. Jones, L. H.; McDowell, R.S.; Goldblatt, M. *Inorg. Chem.* **1969**, *8*, 2349.

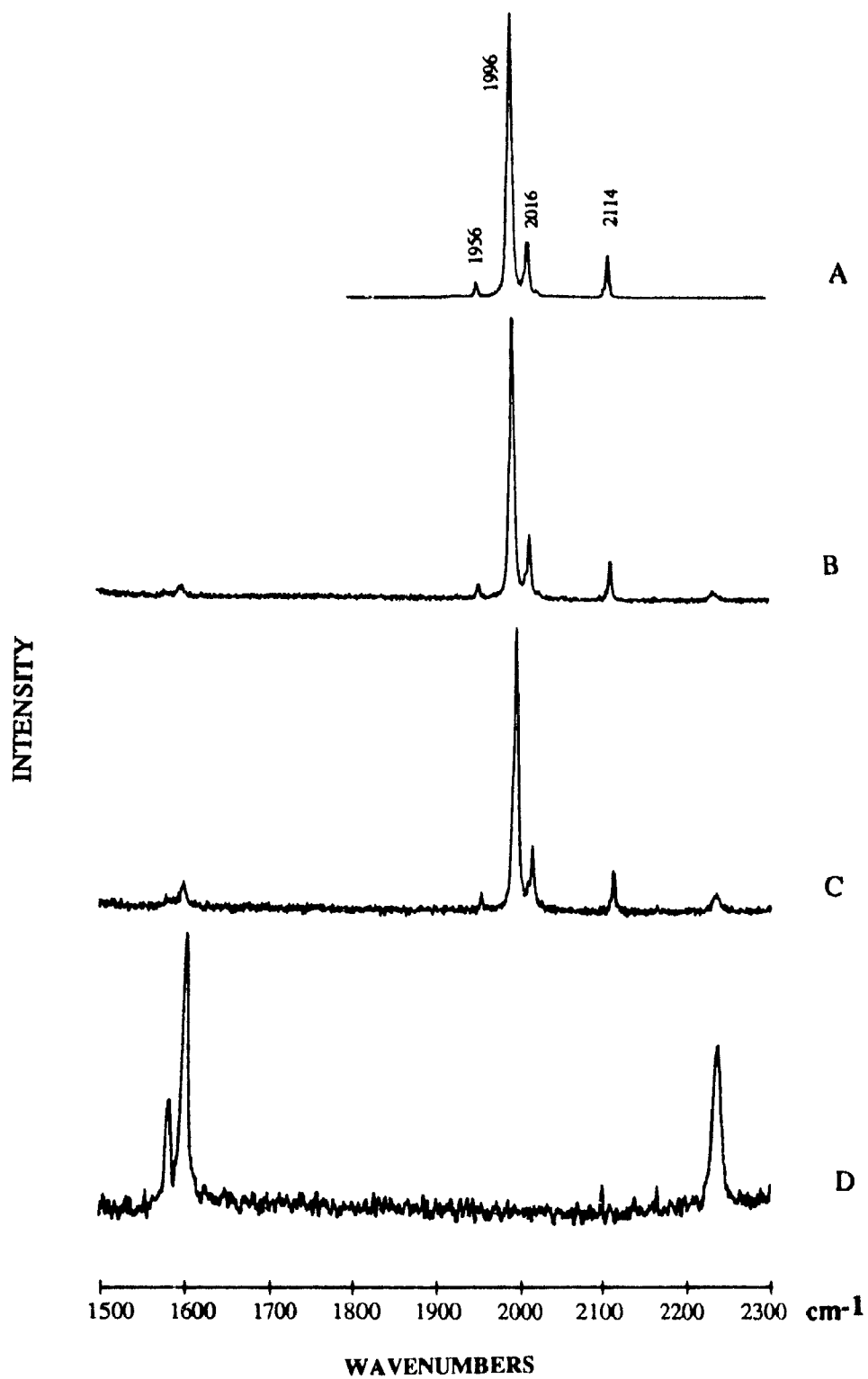


Figure 2-4 The Raman spectra in the $\nu(\text{CO})$ region of (a) crystalline $\text{W}(\text{CO})_6$; (b) $\text{W}(\text{CO})_6(21\%)$ -PSAN film; (c) $\text{W}(\text{CO})_6(40\%)$ -PSAN film and (d) pure PSAN film.

2.3.3 Photolysis Experiments

a. Room-Temperature Photolysis

There was no significant absorption above 300 nm for all three pure polymer films in their UV spectra. The IR spectra of the pure PSAN film was unchanged following UV irradiation (Pyrex filter) for 30 min

M(CO)₆ in PS, PMMA and PSAN (250-270 nm). The $M(CO)_6$ ($M = Cr, Mo, W$) complexes embedded in PS, PMMA and PSAN were irradiated with UV light in the 250-270 nm region ($H_2NC(S)C(S)NH_2$ -ethanol solution as filter). In the case of the PS films, the $\nu(CO)$ bands due to the metal hexacarbonyls decreased dramatically in intensity for all three complexes. No new peaks were observed for $M = Cr$ and Mo , and very weak new peaks appeared around 1930 and 1897 cm^{-1} for $M = W$. The latter disappeared rapidly after placing the film in the dark. No peak attributable to $(\eta^6\text{-phenyl})M(CO)_3$ was detected.

Irradiation of $M(CO)_6$ in PMMA films showed similar behaviour to that observed by Massey and Orgel¹¹ although they reported no actual data. The parent hexacarbonyl $\nu(CO)$ bands decreased in intensity and two new peaks appeared in the spectra at lower wavenumbers together with one very weak peak at higher wavenumber [Table 2-3]. These new peaks are very close in position to those of the intermediate $M(CO)_5(THF)$ reported by Hooker and Rest³². An oxygen atom of PMMA may act as a ligand in coordinating the $M(CO)_5$ species. This supports the proposal that the product of room-temperature irradiation of the metal hexacarbonyl in PMMA is $M(CO)_5(PMMA)$. The relative intensities of the $\nu(CO)$ bands due to the $M(CO)_5(PMMA)$ species and the corresponding starting hexacarbonyls recorded immediately after irradiation were: strong for $M = W$, moderate for $M = Mo$ and weak for $M = Cr$. These observations are consistent with the stability of the appropriate $M(CO)_5$ species. The longer-lived $W(CO)_5$ species is more likely to be trapped

by a pendant group from PMMA than the shorter-lived Cr and Mo analogs. All of the $M(\text{CO})_5(\text{PMMA})$ species disappeared with time upon storage of the irradiated films in the dark.

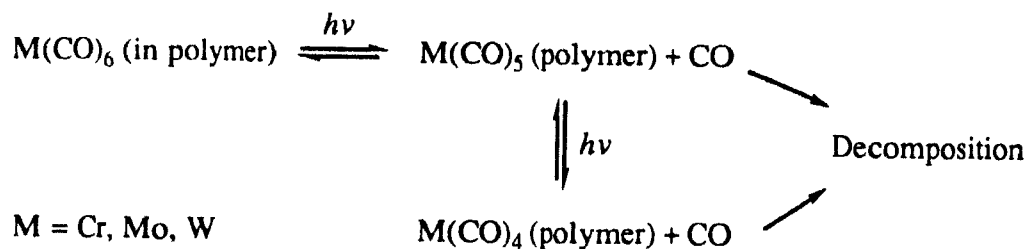
In the case of the PSAN films, several new bands appeared upon irradiation together with a decrease in intensity of the $\nu(\text{CO})$ bands of the metal hexacarbonyls [Table 2-3]. At the beginning, the new peaks were very close to those reported for the complexes $M(\text{CO})_5(\text{NCMe})$ ⁴⁴. As the irradiation continued, additional bands appeared which were assigned to the disubstituted complexes *cis*- $M(\text{CO})_4(\text{NCMe})_2$.⁴⁴ The intensities of the bands due to $M(\text{CO})_4(\text{PSAN})_2$ were less intense than those of the monosubstituted species, but were strong for $M = \text{W}$, moderate for $M = \text{Mo}$ and weak for $M = \text{Cr}$. After irradiation of the PSAN film containing $\text{W}(\text{CO})_6$, the film was no longer soluble in toluene, presumably because *cis*- $\text{W}(\text{CO})_4(\text{PSAN})_2$ functions as a crosslinking agent. For $M = \text{Mo}$, the irradiated film dissolved in toluene with some difficulty, possibly because $\text{Mo}(\text{CO})_4(\text{PSAN})_2$ is less stable and decomposed in solution. Addition of a large excess of methanol to this toluene solution caused the polymer to precipitate. The precipitate was washed with methanol and dried. The IR spectrum of this material showed only strong $\nu(\text{CO})$ bands due to $\text{Mo}(\text{CO})_5(\text{PSAN})$. No peaks due to the disubstituted species or the starting $\text{Mo}(\text{CO})_6$ complex were detected. This observation confirms the attachment of the complex to the polymer chain to form an organometallic polymer.

W(CO)₆ in PS, PMMA and PSAN (no filter). Films containing $\text{W}(\text{CO})_6$ in PS, PMMA and PSAN were also irradiated at room temperature through quartz with no filter. The $\nu(\text{CO})$ bands due to $\text{W}(\text{CO})_6$ decreased in intensity much more rapidly than when a filter was used. In PS [Fig.2-5], weak new peaks at 2074, 1931 and 1897 cm^{-1} , assigned to $\text{W}(\text{CO})_5(\text{PS})$ [Table 2-3], were detected by measuring the IR spectrum immediately after irradiation.

44. (a) Dobson, G.R.; El-Sayed, M.F.A.; Stolz, I.W.; Sheline, R.K. *Inorg. Chem.* **1962**, *1*, 526. (b) Stolz, I.W.; Dobson, G.R.; Sheline, R.K. *Inorg. Chem.* **1963**, *2*, 323. (c) Ross, B.L.; Grasselli, J.Y.; Ritchey, W.M.; Kaesz, H.D. *Inorg. Chem.* **1963**, *2*, 1023.

These new peaks rapidly decreased in intensity upon standing (20 min) with a slight increase in the intensities of the bands due to $W(CO)_6$. The positions of these new weak bands do not correspond to those of "naked" $W(CO)_5$.³² In PMMA, strong new bands due to $W(CO)_5(PMMA)$ appeared initially which gradually decreased in intensity on standing (8h), and the bands due to $W(CO)_6$ were substantially regenerated [Fig.2-6], which is similar to that observed by Massey and Orgel¹¹. The CO ligands needed are presumably produced by decomposition of $W(CO)_5(PMMA)$; free CO was not detected in the matrix at room temperature.⁴⁵ Irradiation of $W(CO)_6$ in PMMA at $-150^\circ C$, however, did afford evidence of free CO (at 2133 cm^{-1}). In PSAN, bands due to $W(CO)_5(PSAN)$ and *cis*- $W(CO)_4(PSAN)_2$ soon appeared while those of the parent complex completely disappeared [Fig.2-7]. Upon standing in dark (8 h), the peaks due to the monosubstituted species continued to intensify at the expense of the disubstituted species.

The photochemical behaviour of $M(CO)_6$ in polymer matrices is summarized in Eq.2-1. The relative concentrations of the major products are dependent on M and the polymer matrix concerned.



Eq. 2-1

45. Hooker, R.H.; Rest, A.J. *J. Chem. Phys.* **1985**, *82*, 3871.

Table 2-3 Assignment of the CO stretching modes of the species generated by UV irradiation of the monomeric metal carbonyl complexes embedded in polymer matrices (cm⁻¹)

Species	Local symmetry	$\nu(\text{CO})(\text{cm}^{-1})$		
Cr(CO) ₅ (PMMA)	C _{4v}		1932sh(e)	1884w(a ₁)
Cr(CO) ₅ (PSAN)	C _{4v}	2074vw(a ₁)	1936s(e)	1914sh(a ₁)
Mo(CO) ₅ (PMMA)	C _{4v}		1932sh(e)	1884w(a ₁)
Mo(CO) ₅ (PSAN)	C _{4v}	2076mw(a ₁)	1941s(e)	1903mw(a ₁)
<i>cis</i> -Mo(CO) ₄ (PSAN) ₂	C _{2v}	2020mw(a ₁)	1918s(a ₁)	1911s(b ₁) 1850m(b ₂)
W(CO) ₅ ¹	C _{4v}	2080w(a ₁)	1946s(e)	1910w(a ₁)
W(CO) ₅ ²	C _{4v}	2079w(a ₁)	1940s(e)	1910w(a ₁)
W(CO) ₅ (PS)	C _{4v}	2074w(a ₁)	1931s(e)	1897m(a ₁)
W(CO) ₅ (PMMA)	C _{4v}	2074w(a ₁)	1930s(e)	1884m(a ₁)
W(CO) ₅ (PSAN)	C _{4v}	2075vw(a ₁)	1938s(e)	? ³ (a ₁)
<i>cis</i> -W(CO) ₄ (PSAN) ₂	C _{2v}	2015mw(a ₁)	1901s(a ₁)	1885s(b ₁) 1851m(b ₂)
η^6 -C ₆ H ₆ Cr(CO) ₂ (PSAN)	C _s	1891s(a')	1835s(a'')	
CpMn(CO) ₂ (In PS)	C _{2v}	1953s(a ₁)	1896s(b ₂)	
CpMn(CO) ₂ (PSAN)	C _s	1934s(a')	1864s(a'')	

¹In PS film at -145°C. ²In PMMA film at -150°C. ³Overlapped with *cis*-W(CO)₄(PSAN)₂ bands.

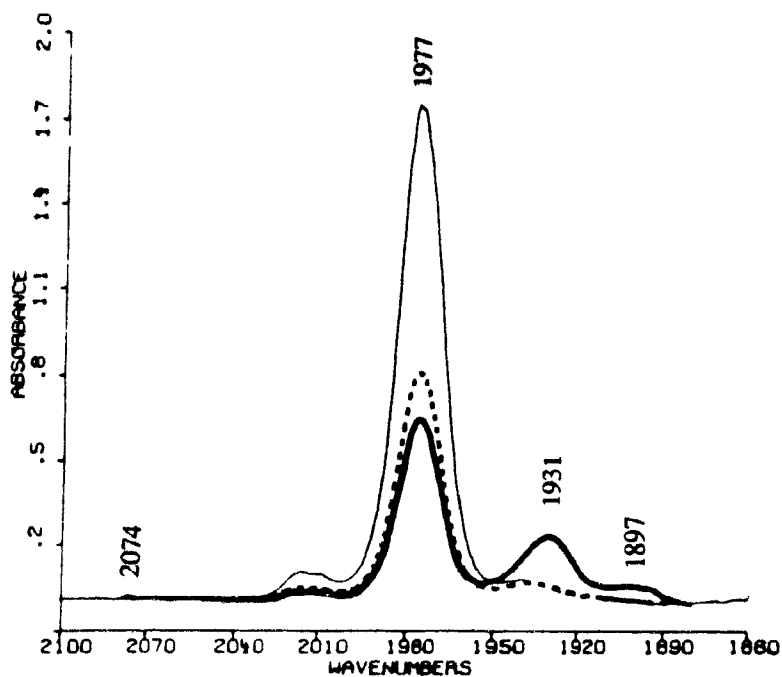


Figure 2-5 The IR spectra in the $\nu(\text{CO})$ region of $\text{W}(\text{CO})_6$ in PS film (—) before irradiation, (---) after irradiation for 10 min and (····) after allowing the latter sample to stand for 20 min.

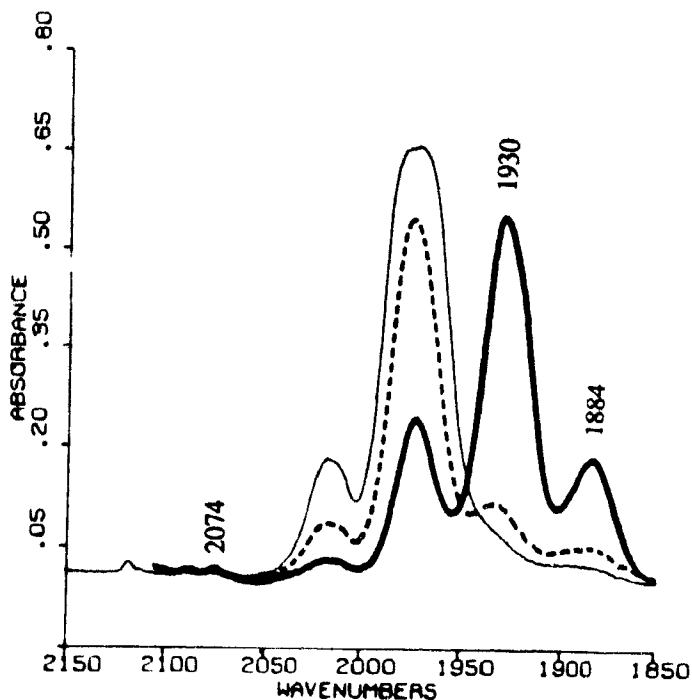


Figure 2-6 The IR spectra in the $\nu(\text{CO})$ region of $\text{W}(\text{CO})_6$ in PMMA film (—) before irradiation, (---) after irradiation for 10 min and (····) after allowing the latter sample to stand for 8 h.

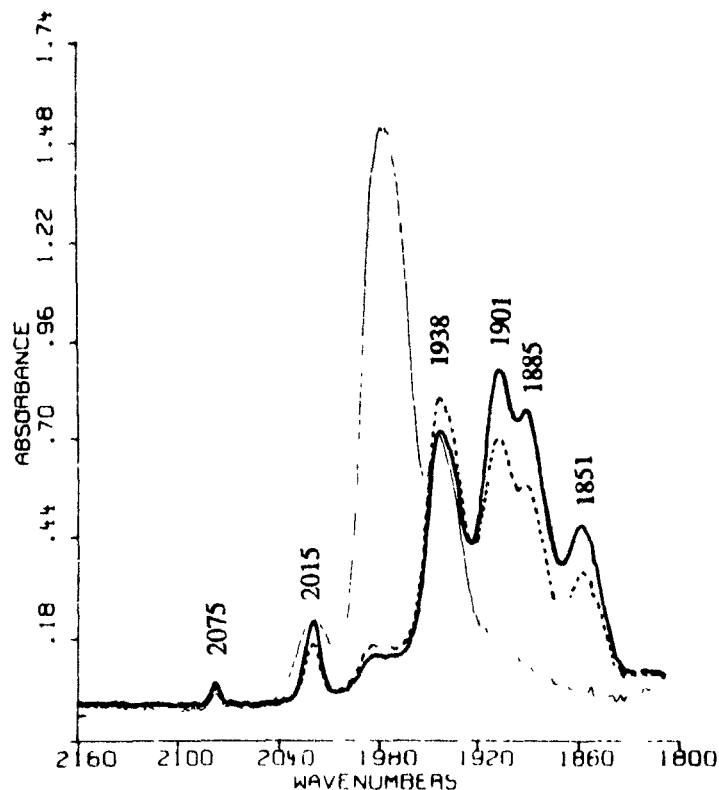


Figure 2-7 The IR spectra in the $\nu(\text{CO})$ region of $\text{W}(\text{CO})_6$ in PSAN film (—) before irradiation, (---) after irradiation for 10 min and (····) after allowing the latter sample to stand for 8 h.

$(\eta^6\text{-C}_6\text{H}_6)\text{Cr}(\text{CO})_3$ ($>310\text{ nm}$). Room-temperature irradiation of $(\eta^6\text{-C}_6\text{H}_6)\text{Cr}(\text{CO})_3$ in PS, PMMA or PSAN using a Pyrex filter ($>310\text{ nm}$) led to the parent $\nu(\text{CO})$ bands decreasing in intensity. In PS and PMMA, new bands due to $\text{Cr}(\text{CO})_6$ appeared, consistent with earlier studies. It has been reported that, while the initial product of photolysis at low temperature in an inert matrix is $(\eta^6\text{-C}_6\text{H}_6)\text{Cr}(\text{CO})_2$,⁴⁶ the final product at room temperature in methyl methacrylate⁴⁷ and in other solvents⁴⁸ is $\text{Cr}(\text{CO})_6$. In addition, new

46. Rest, A.J.; Sodeau, J.R.; Taylor, D.J. *J. Chem. Soc., Dalton Trans.* **1978**, 651.

47. Bamford, C.H.; Al-Femei, K.Y.; Konstantinov, C.J. *J. Chem. Soc., Faraday Trans* **1977**, *1*, 1406.

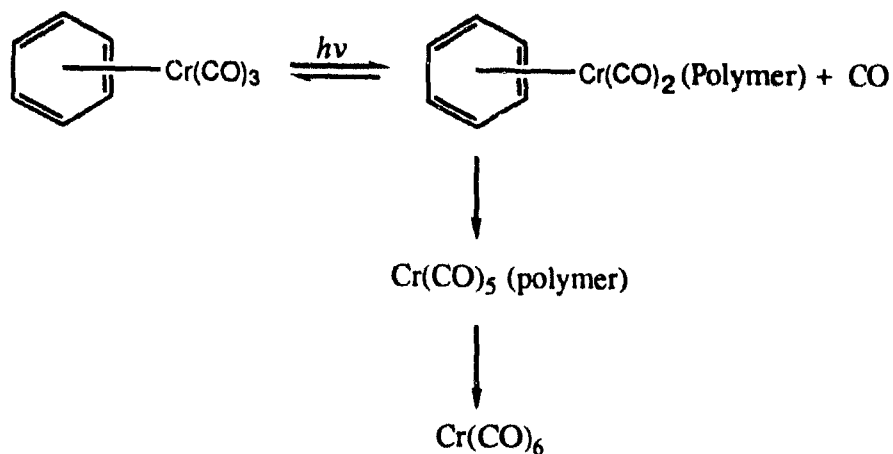
48. Trembovler, V.N.; Baranetskaya, N.K.; Fok, N.V.; Zaslavskaya, G.B.; Yavorskii, B.M.; Setkina, V.N. *J. Organomet. Chem.* **1976**, *117*, 339.

bands at 2062 and 1930 cm^{-1} were also observed in PMMA. Their frequencies are similar to those of the $\text{Cr}(\text{CO})_5\text{X}$ species observed earlier during the irradiation of $\text{Cr}(\text{CO})_6$ in polymer films and are not in the range appropriate to those expected for $(\eta^6\text{-C}_6\text{H}_6)\text{Cr}(\text{CO})_2(\text{PMMA})$.^{47,49} New bands due to $\text{Cr}(\text{CO})_6\text{X}$ disappeared upon standing (one day) with a slight increase in intensity of the band due to $\text{Cr}(\text{CO})_6$. It is worth noting that the proposed mechanism for the photo-production of $\text{Cr}(\text{CO})_6$ from $(\eta^6\text{-C}_6\text{H}_6)\text{Cr}(\text{CO})_3$ in solution involves aggregation of two or more chromium species.^{34,47} However, non-volatile metal complexes, at the concentrations used here, are assumed to be well isolated in polymer films⁵⁰ and unable to aggregate. Therefore, it is reasonable to assume that $\text{Cr}(\text{CO})_6$ results from the scavenging of CO molecules generated by decomposition of $(\eta^6\text{-C}_6\text{H}_6)\text{Cr}(\text{CO})_2$.

In PSAN, new bands of a major product appeared at 1891 and 1835 cm^{-1} , but $\text{Cr}(\text{CO})_6$ was not detected. In addition, weak bands due to $\text{Cr}(\text{CO})_5(\text{PSAN})$ were observed. The bands due to the major product largely decreased in intensity upon standing for a few days with little increase in the intensities of the other bands. The unstable complex $(\eta^6\text{-C}_6\text{H}_6)\text{Cr}(\text{CO})_2(\text{NCMe})$ displays $\nu(\text{CO})$ bands in the IR in hexane solvent at 1915 and 1814 cm^{-1} .³⁷ The new bands appearing in PSAN film are in the appropriate range and are tentatively assigned to $(\eta^6\text{-C}_6\text{H}_6)\text{Cr}(\text{CO})_2(\text{PSAN})$. The photochemical behaviour of $(\eta^6\text{-C}_6\text{H}_6)\text{Cr}(\text{CO})_3$ in polymer matrices is summarized in Eq.2-2, the relative concentration of the major products is dependent on the polymer properties.

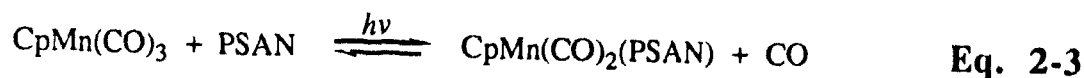
49. Black, J.D.; Boylan, M.J.; Baranerman, P.S. *J. Chem. Soc., Dalton Trans.* **1981**, 674.

50. Mascetti, J. Rest, A.J. *J. Chem. Soc., Chem. Commun.* **1987**, 221.



Eq. 2-2

CpMn(CO)₃. Irradiation of CpMn(CO)₃ in PS, PMMA and PSAN at room temperature through Pyrex led to a decrease in the intensities of the parent bands. In PS, two new $\nu(\text{CO})$ bands appeared at 1953 and 1896 cm^{-1} . These bands were also detected, although with lower relative intensities, in PMMA. The new bands were stable upon standing, even for several days. Their positions are in agreement with those reported^{46,49} for CpMn(CO)₂ and are assigned accordingly. In PSAN, the parent bands disappeared after only 30 min irradiation and were replaced by two new strong bands (1934s and 1864s cm^{-1}) attributable to CpMn(CO)₂(PSAN)³⁶ [Fig.2-8] [Eq.2-3].



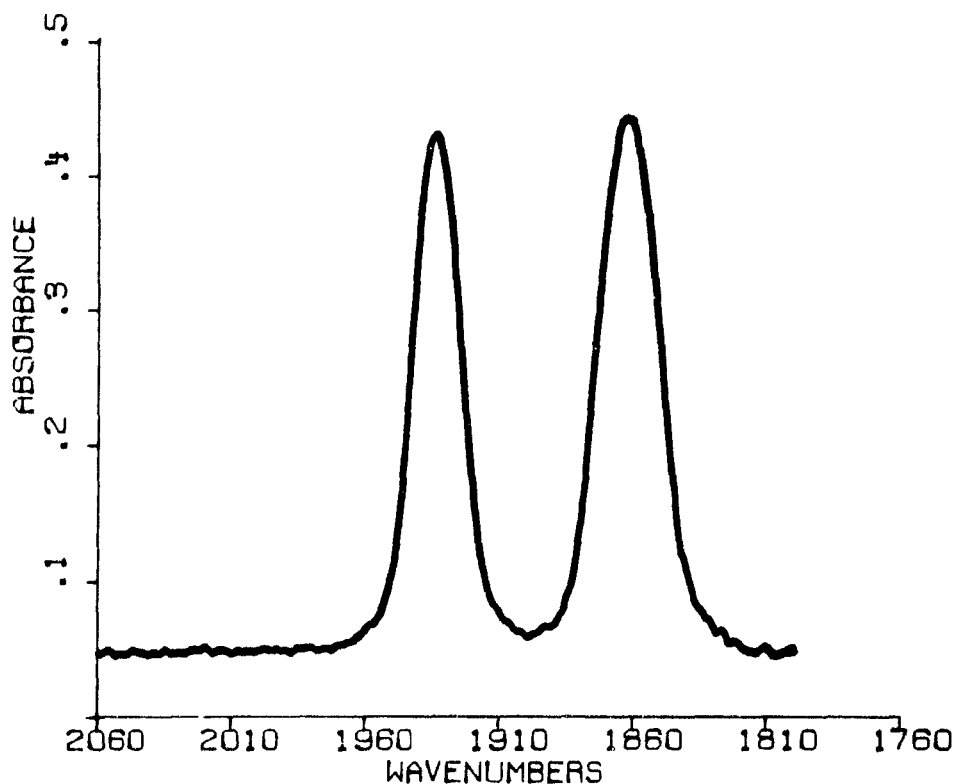


Figure 2-8 The IR spectrum in the $\nu(\text{CO})$ region of $\text{CpMn}(\text{CO})_2(\text{PSAN})$ produced by UV irradiation (Pyrex filter) of $\text{CpMn}(\text{CO})_3$ in PSAN for 30 min.

b. Low-Temperature Photolysis

On lowering the temperature of the polymer films embedded with $\text{W}(\text{CO})_6$, the IR spectra of the hexacarbonyl became slightly less smooth than the spectra taken at room temperature. No significant shifts in band positions were observed. Following irradiation of $\text{W}(\text{CO})_6$ in a PS matrix at -145°C for 30 min, the film turned yellow. New peaks appeared at 2080 (w, sharp), 1946 (s, br) and 1910 (w, br) cm^{-1} , together with a broad, weak band due to free CO at 2133 cm^{-1} . The parent band at 1977 cm^{-1} had almost totally vanished [Fig.2-9]. These three new bands are shifted to higher wavenumbers compared to the peaks assigned to

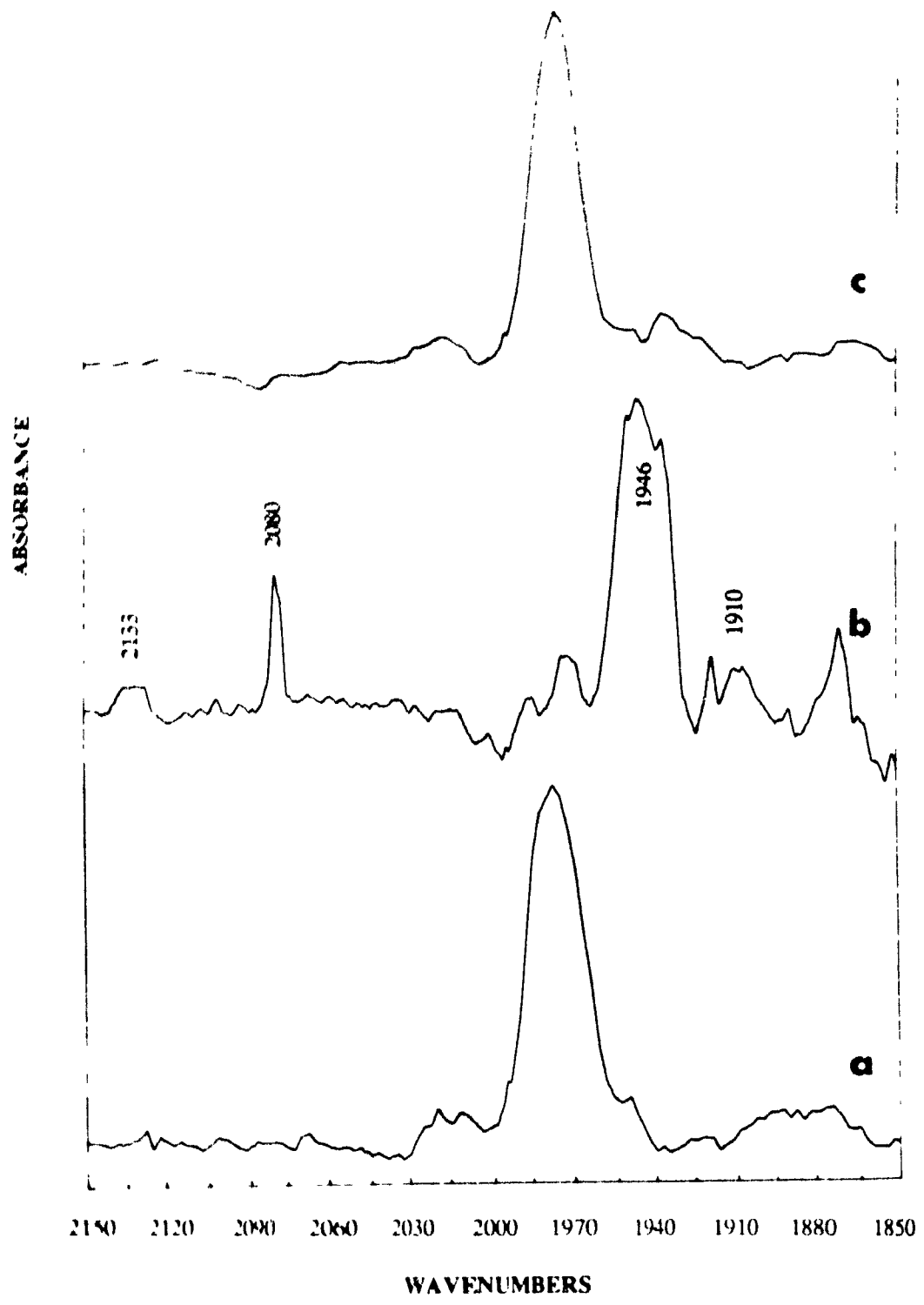


Figure 2-9 The IR spectra in the $\nu(\text{CO})$ region of $\text{W}(\text{CO})_6$ in PS film (a) at -145°C before irradiation, (b) after irradiation for 30 min at -145°C and (c) after allowing the latter sample to warm up to room temperature.

$W(CO)_5(PS)$ photogenerated at room temperature. Unlike the analogous system at room temperature, the 'naked' $W(CO)_5$ is believed to be present here. On slowly warming the film, the strong band due to $W(CO)_6$ was regenerated rapidly together with the total disappearance of the three new bands and the free CO peak.

A $W(CO)_6$ -embedded PMMA film showed similar behaviour upon irradiation at $-150^\circ C$ for 30 min. The film turned yellow and three new peaks grew at 2079 (w, sharp), 1940 (s, br), 1910 (w, br, sh) cm^{-1} , together with a free CO peak at 2135 (w, br) cm^{-1} and a decrease in intensity of the parent hexacarbonyl $\nu(CO)$ bands. As in the previous case, the three new peaks are assigned to $W(CO)_5$ species. But, the thermal regeneration of $W(CO)_6$ in PMMA occurs much slower than it does in PS. On slowly warming the film, a very weak, sharp peak appeared at 2075 cm^{-1} with a concomitant decrease in intensity of the peak at 2079 cm^{-1} . The peaks at 1940 and 1910 cm^{-1} shifted to 1930 and 1890 cm^{-1} , respectively. The three new bands (2075, 1930 and 1890 cm^{-1}), which are very close to the peaks generated by irradiation of $W(CO)_6$ in PMMA at room temperature, are assigned to $W(CO)_5PMMA$. As the film is being warmed up, the C=O ligand from the PMMA chain interacts with the $W(CO)_5$ species to form $W(CO)_5(PMMA)$. The latter then gradually decomposes upon standing at room temperature with the regeneration of $W(CO)_6$.

2.4 Conclusions

The hot-pressing technique employed in our work for embedding organometallic complexes into polymers is very flexible, quite general and reasonably non-destructive. The films generated are transparent and the organometallics are highly dispersed in the solid polymer matrices at a reasonable concentration. The polymers PS, PMMA and PSAN approximate the solvents toluene, ethyl acetate and acetonitrile, respectively, in their influence on the shapes and positions of the IR bands of metal carbonyls. A comparison of

the ATR-IR spectra of the films with their transmission IR spectra indicates that there are no significant differences between the interior and surfaces of the films in the case of relatively stable complexes. The photochemical result indicates simple decomposition of monomeric complexes in PS, which suggests that PS functions as an inert matrix. PMMA has weakly coordinating C=O groups on the chain that can stabilize coordinatively-unsaturated intermediates such as $W(CO)_5$ to form $W(CO)_5PMMA$. PSAN contains donor nitrile ligands that can form fairly stable organometallic polymers upon irradiation of organometallics in the solid PSAN matrix.

CHAPTER 3. Vibrational Spectra, Photochemistry and Iodine Oxidation Reactions of Dimeric Metal Carbonyl Complexes in Polymer Matrices

3.1 Introduction

In the previous chapter, a general method for preparing polymer films containing organometallic complexes was described. The transmission IR and ATR-IR spectra of several monomeric metal carbonyl complexes embedded in PS, PMMA and PSAN films were investigated, as well as their photochemistry. The results indicate that the IR peak positions of metal carbonyl complexes in the $\nu(\text{CO})$ region are affected by the properties of the polymers. The band shifts are similar to those in structurally-related low molecular weight solvents. Dimeric organometallic complexes, such as $[\text{CpFe}(\text{CO})_2]_2$, are good solutes for studying solvent properties, since the positions of their IR absorptions are sensitive to the solvent polarity.⁵¹ Presented in this chapter are the IR spectra of the dimeric metal carbonyl complexes $[\text{CpFe}(\text{CO})_2]_2$, $[\text{CpMo}(\text{CO})_3]_2$ and $\text{Mn}_2(\text{CO})_{10}$ embedded in PS, PMMA and PSAN matrices, and their photochemical behaviour. In the addition, the oxidation reactions of the dimers in different polymer films with I_2 vapour have been examined and compared. The polarized IR spectra of $\text{Mn}_2(\text{CO})_{10}$ soaked in polyethylene (PE) film before and after stretching have also been investigated. The overall objectives of the research work were: (1) to extend our efforts to characterize the environments in different polymer matrices imposed on the metal carbonyls; (2) to develop "room temperature matrices" for the study of solid-state chemical reactions of organometallic complexes; (3) to investigate the orientational behaviour of a linear metal carbonyl dimer in an orientable polymer matrix.

51. Manning, A.R. *J. Chem. Soc. (A)*, **1968**, 1319.

3.2 Experimental

Materials. The starting materials $[\text{CpFe}(\text{CO})_2]_2$, $[\text{CpMo}(\text{CO})_3]_2$ and $\text{Mn}_2(\text{CO})_{10}$ were purchased from Strem Chemicals, while the polymers were supplied by Polysciences. Low-density polyethylene (0.9142 g/cm^3 , m.p. = 106°C) was employed for the polarized IR measurements. The *trans* stereochemistry of the iron complex was confirmed by its IR spectrum in a KBr disk.⁵¹ Films containing the embedded dimers were prepared as described in the previous chapter. Most of the FT-IR spectra were recorded on a Nicolet model 6000 spectrometer.

Iodine oxidation reactions. These reactions were performed at ambient temperature on thin films of comparable thickness (usually about 0.05 mm); thick films (0.11 mm) were also used for the iron dimer. The films were attached to plastic IR mounts by means of "Scotch" tape and then placed in screwtop jars (280 cm^3 capacity) containing 4.6g of pulverized crystalline iodine. The pure polymer films and those containing the dimers were exposed to I_2 vapour in the sealed jars over a period of 10 days. The oxidation reactions were monitored by FT-IR spectroscopy. No significant changes in the IR spectra of the pure polymer films were observed.

Photolysis. The room-temperature photochemical studies were conducted using a water-cooled, medium-pressure quartz mercury immersion lamp (Hanovia 450 W) following a similar procedure to that described earlier. Irradiation with wavelengths above 310 nm was achieved using a Pyrex filter. The photolysis of the metal carbonyl dimers embedded in polymer films was monitored by FT-IR spectroscopy.

Polarized FT-IR study. A PE film containing $\text{Mn}_2(\text{CO})_{10}$ was prepared by soaking the PE film in a $\text{Mn}_2(\text{CO})_{10}/\text{CH}_2\text{Cl}_2$ solution (about 1 g /100 mL) for 10 h, washing it with

acetone and then drying under vacuum. The dimer was aligned by stretching the film to about 5 times its original length. Polarization of the IR beam was achieved with a rotatable AgBr wire-grid polarizer (Perkin-Elmer Corp.) The dichroic spectra (A_{\parallel} - A_{\perp}) were obtained by direct subtraction of the perpendicular spectra A_{\perp} (recorded with the electric vector of the IR beam rotated 90° with respect to the direction in which the film had been stretched) from the parallel spectra A_{\parallel} (recorded with the electric vector parallel to the direction of stretching). The spectra were measured on a Bomem Michelson 100 spectrometer operating at 4 cm^{-1} resolution and using a DTGS detector. The spectra of the films were recorded both before and after stretching.

3.3 Results and Discussion

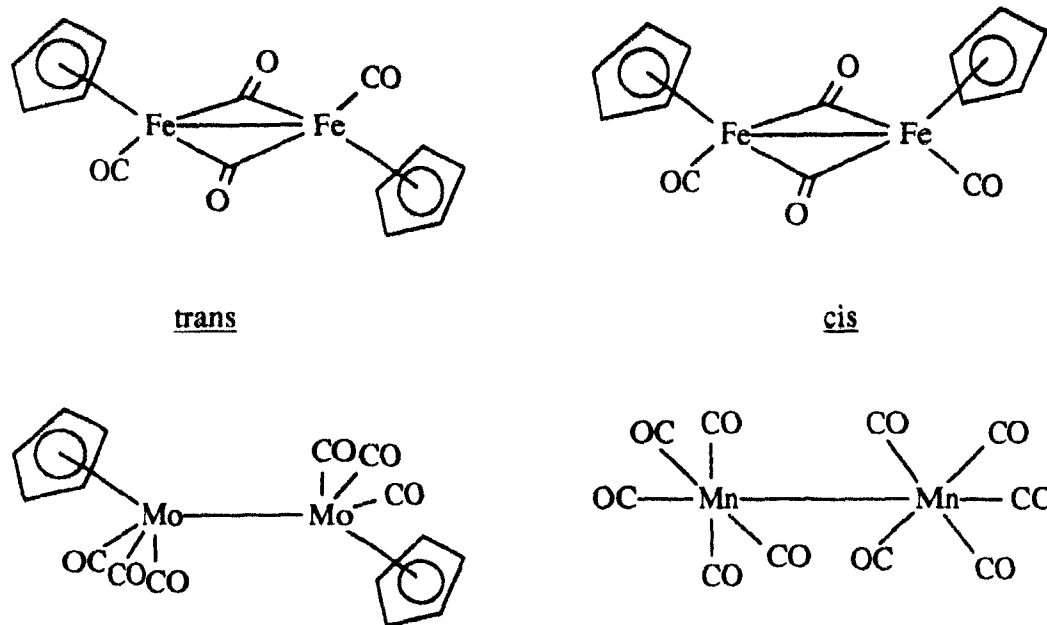
3.3.1 IR Spectra

As mentioned in the earlier chapter, the polymers employed have an IR-window in the metal carbonyl stretching region; even the strong PMMA band centered at $1750\text{-}1720\text{ cm}^{-1}$ did not interfere with the bands due to the bridging CO ligands in $[\text{CpFe}(\text{CO})_2]_2$. Table 3-1 lists the $\nu(\text{CO})$ peak positions for the dimeric metal carbonyls embedded in the three polymers as well as in the three organic solvents which have similar structural features to each of the polymers.

Table 3-1 Observed carbonyl stretching modes of $[\text{CpFe}(\text{CO})_2]_2$, $[\text{CpMo}(\text{CO})_3]_2$ and $\text{Mn}_2(\text{CO})_{10}$ in different media (cm^{-1})

Complexes	PS	PMMA	PSAN	Assignment
$[\text{CpFe}(\text{CO})_2]_2$	1996s	1993s	1992s	a_1 (<i>cis</i>)
	1953m	1952s	1950m	b_u (<i>trans</i>)
	1782vs	1782vs	1777s	a_u, b_1 (bridg)
$[\text{CpMo}(\text{CO})_3]_2$	2013vw	2011m	2010m	I ^a
	1955s	1956s	1957s	II ^a
	1903s	1911s	1910s	} III ^a
	1888s			
$\text{Mn}_2(\text{CO})_{10}$	2044s	2043s	2044m	b_2
	2008s,br	2010sh	2008s,br	e_1
	1981m	2000s,br	1983w	b_2
	Toluene	Ethyl acetate	Acetonitrile	
$[\text{CpFe}(\text{CO})_2]_2$	1997s	1995s	1992s	a_1 (<i>cis</i>)
	1953s	1954m	1952w	b_u (<i>trans</i>)
	1783vs	1783s	1775s	a_u, b_1 (bridg)
$[\text{CpMo}(\text{CO})_3]_2$	2015vw	2013w	2011m	I ^a
	1956s	1958s	1957s	II ^a
	1912s	1914s	1911s	III ^a
$\text{Mn}_2(\text{CO})_{10}$	2046m	2047m	2047m	b_2
	2010s	2011s	2011s	e_1
	1981w	1982w	1981w	b_2

^aNo vibrational assignments have been proposed for these peaks.



Scheme 3-1

$[\text{CpFe}(\text{CO})_2]_2$. The complex $[\text{CpFe}(\text{CO})_2]_2$ exists in solution at room temperature as an equilibrium mixture of *cis* (C_{2v}) and *trans* (C_{2h}) isomers⁵¹ [Scheme 3-1]. Each isomer contains two terminal and two bridging CO groups. The barrier to interconversion is approximately 40 kJ mol^{-1} .⁵² The *cis/trans* ratio increases as the solvent polarity increases. The starting material had *trans* stereochemistry as confirmed by its IR spectrum in KBr which showed two broad bands at 1950 and 1770 cm^{-1} , both split into doublets. The IR spectra in the polymers exhibit two terminal $\nu(\text{CO})$ bands: one around 1990 cm^{-1} due to the a_1 mode of the *cis* isomer and the other around 1950 cm^{-1} belonging to the b_u mode of the

52. Bullitt, J.G.; Cotton, F.A.; Marks, T.J. *Inorg. Chem.* **1972**, *11*, 671 and references therein.

trans isomer, together with a bridging $\nu(\text{CO})$ band at 1774 cm^{-1} [Table 3-1, Fig 3-1]. Obviously, this indicates the existence of both the *cis* and *trans* isomers in polymer matrices. Fig.3-1 also shows that the *cis/trans* ratio increases with increasing polarity of the polymer film. As in solution, the most polar polymer PSAN, gives a *cis*-rich distribution.

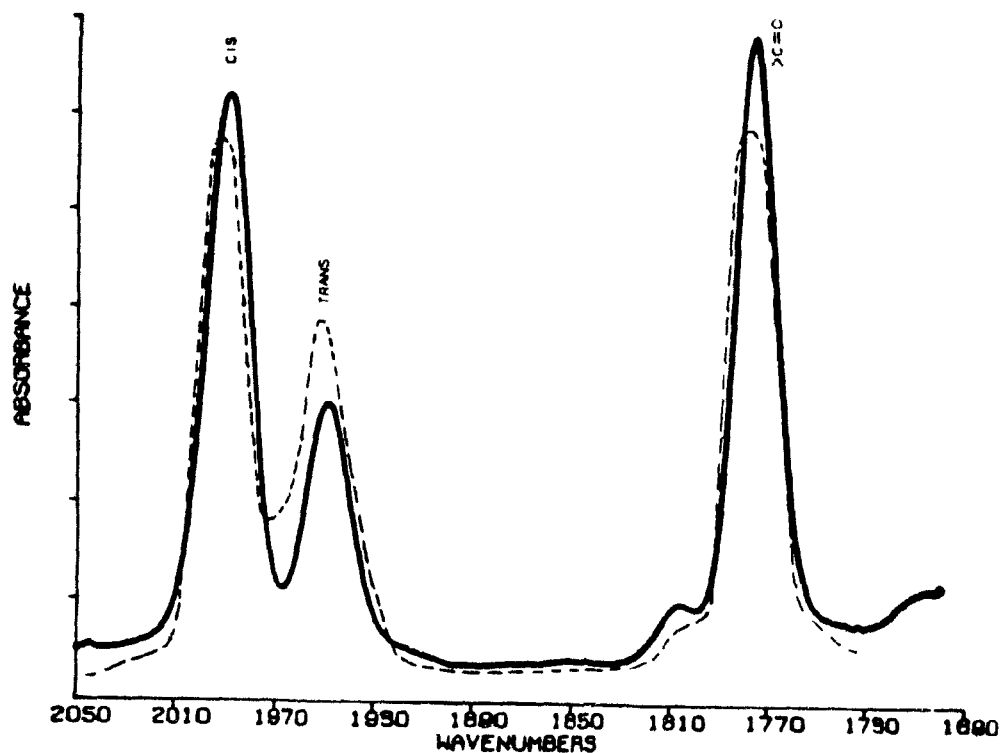


Figure 3-1 The IR spectra in the $\nu(\text{CO})$ region of $[\text{CpFe}(\text{CO})_2]_2$ in PS (---) and PSAN (—) showing the effect of the polymer on the relative amounts of the *cis* and *trans* isomers.

$[\text{CpMo}(\text{CO})_3]_2$. Unlike the iron dimer, $[\text{CpMo}(\text{CO})_3]_2$ has no bridging CO groups and the two $\text{CpMo}(\text{CO})_3$ fragments are held together by a single Mo-Mo bond. The molecule has C_{2h} symmetry (staggered *trans*, Scheme 3-1) for which three IR-active $\nu(\text{CO})$ modes ($a_u +$

$2b_u$) are predicted.⁵³ Usually, however, only two bands (II, III) are observed in solution with the lower-energy band (III) being broad and split into two components in hydrocarbon solvents and in Nujol mull. There is an additional peak (I) observed at higher energy in polar solvents, which has been attributed to the presence of non-centrosymmetric rotamers.⁵⁴ Table 3-1 lists the IR peak positions of this dimer embedded in the three polymers. Two strong bands (II,III) are observed, together with band I. Band III is broad in PMMA and PSAN, and split into a doublet in PS. The intensity of the highest energy band (I) decreases as the polarity of the polymer decreases in the following order: PSAN > PMMA > PS, consistent with the solution studies.

$Mn_2(CO)_{10}$. There is a single Mn-Mn bond between the two $Mn(CO)_5$ moieties which are staggered with respect to one another. The molecular symmetry of $Mn_2(CO)_{10}$ is D_{4d} ⁵⁵ [Scheme 3-1] and three IR-active $\nu(CO)$ modes ($2b_2 + e_1$) are expected in the terminal carbonyl region [Table 3-1]. The IR spectra in the three polymer films and in the organic solvents show little variation in shape and peak position, except for the band at 2010-2000 cm^{-1} in PMMA which was broader.

3.3.2 Photochemistry

The photochemistry of the iron,⁵⁶ molybdenum⁵⁷ and manganese⁵⁸ carbonyl dimers has been studied intensively in solution. Several papers concerning photolysis of the dimers in

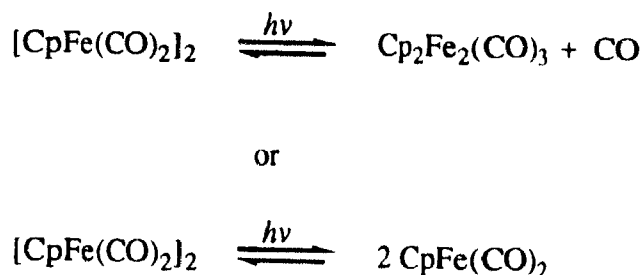
53. Fischer, R.D., Noack, K. *J. Organomet Chem* **1969**, *16*, 125.

54. In ref. 30, p 85.

55. Parker, D.J., Studdard, M.H.B. *J. Chem. Soc. (A)*, **1966**, 695.

56. (a) Goldman, A.S.; Tyler, D.R. *Inorg Chem*. **1987**, *26*, 253. (b) Blaha, J.P.; Bursten, B.E.; Dewan, J.C.; Frankel, R.B.; Randolph, C.L.; Wilson, B.A.; Wrighton, M.S. *J. Am. Chem Soc.* **1985**, *107*, 4561. (c) Tyler, D.R.; Schmidt, M.A.; Gray, H.B. *J. Am. Chem. Soc.* **1983**, *105*, 6018. (d) Caspar, J.V.; Meyer, T.J. *J. Am. Chem. Soc.* **1980**, *102*, 7794. (e)

low-temperature, rigid media have also been reported.^{59,60} There are two primary photoproducts: one is a binuclear intermediate formed by reversible CO dissociation, e.g., $\text{Cp}_2\text{Fe}_2(\text{CO})_3$ and $\text{Mn}_2(\text{CO})_9$; while the other is a 17-electron fragment such as $\text{CpFe}(\text{CO})_2$ and $\text{Mn}(\text{CO})_5$ formed by reversible homolytic metal-metal bond scission [Scheme 3-2].



Scheme 3-2

The final products depend on the media and the possibility of ligand involvement. Fluid solution favours the homolytic cleavage of metal-metal bond. Irradiation in the presence of nucleophilic ligands (such as PR_3) favours the formation monosubstituted binuclear

Abrahamson, H.B.; Palazzolito, M.C.; Reichel, C.L.; Wrighton, M.S. *J. Am. Chem. Soc.* **1979**, *101*, 4123.

57. (a) Philbin, C.E.; Goldmand, A.S.; Tyler, D.R. *Inorg. Chem.* **1986**, *25*, 4434. (b) Hooker, R.H.; Mahmoud, K.A.; Resat, A.J. *J. Organomet. Chem.* **1983**, *254*, C25 (c) Wrighton, M.S.; Ginley, D.S. *J. Am. Chem. Soc.* **1975**, *97*, 4246.

58. (a) Hepp, A.F.; Wrighton, M.S. *J. Am. Chem. Soc.* **1983**, *105*, 5934. (b) Rothberg, L.J.; Cooper, N.J.; Peters, K.S.; Vaida, V. *J. Am. Chem. Soc.* **1982**, *104*, 3536. (c) Wegman, R.W.; Olsen, R.J.; Gard, D.R.; Faulkner, L.R.; Brown, T.L. *J. Am. Chem. Soc.* **1981**, *103*, 6089. (d) Fox, A.; Poe, A. *J. Am. Chem. Soc.* **1980**, *102*, 2497. (e) Wrighton, M.S.; Ginley, D.S. *J. Am. Chem. Soc.* **1975**, *97*, 2065.

59. Hepp, A.F.; Blaha, J.P.; Lewis, C.; Wrighton, M.S. *Organometallics* **1984**, *3*, 174.

60. Hooker, R.H.; Mahmoud, K.A.; Rest, A.J. *J. Chem. Soc., Chem Commun* **1983**, 1022.

complexes. The complexes $\text{CpFe}(\text{CO})_2\text{X}$ and $\text{Mn}(\text{CO})_5\text{X}$ are the dominant products when the dimers are photolyzed in the presence of halocarbons (CCl_4 for example).

In PS and PMMA films. Irradiation of the three dimers embedded in PS and PMMA at room temperature does not result in any new bands being detected in the $\nu(\text{CO})$ region, only decomposition occurs.

The rate of decrease in intensity of the bands in the carbonyl region upon irradiation was much slower in PMMA than in PS for all three dimers [Table 3-2]. As discussed in Chapter 2, photogenerated CO easily diffuses out of polystyrene. Any coordinatively-unsaturated intermediates that are formed are expected to be unstable under the reaction conditions (room temperature, continued irradiation) and in the absence of any stabilizing donor ligand. Therefore, further decomposition leads to the rapid decrease in intensity. The C=O groups of PMMA can partially stabilize photogenerated intermediates and this may decrease the rate of further decomposition. PMMA is also much less permeable⁶¹ than PS and photogenerated free CO should escape less easily from PMMA film than from PS film. This would increase the possibility of reversing the reaction in PMMA. Thus, the relatively slow photodecomposition of the dimers embedded in PMMA is quite reasonable.

In the case of $[\text{CpFe}(\text{CO})_2]_2$, the terminal $\nu(\text{CO})$ bands due to the *cis* and *trans* isomers, and the associated bridging carbonyl band all decrease in intensity at approximately the same rate. It has been reported that the *cis* and *trans* isomers differ dramatically in photosensitivity at low temperature in inert media.⁶⁰ In CH_4 (12K) and PVC (12-77K), only the *trans* derivative undergoes photoreaction and the *cis* one remains unchanged. Presumably, the *cis* isomer undergoes CO loss too, but, because of lack of movement of the Cp ring at low temperature, the reaction is rapidly reversed. By embedding in the rigid polymer film, the complexes are unable to diffuse transversely inside the media as they can

61. (a) Lee, W.M. *Organic Coatings and Plastics Chemistry, ACS Adv. Chem. Ser.* **1978**, 39, 341. (b) Salame, M. *Polymer Prepr. (Am. Chem. Soc. Div. Polym. Chem.)*, **1967**, 8, 137.

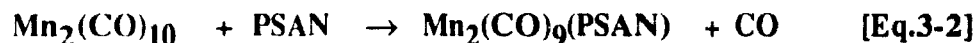
in fluid solutions. However, unlike in the low-temperature matrices, the dimers and the photogenerated intermediates can still rotate rapidly at room temperature in the polymer cage and free CO can diffuse out of the film. Therefore, the *cis* and *trans* isomers may be expected to photodecompose in a similar manner under such conditions.

Table 3-2 Consumption of metal carbonyl starting material (as a percentage) by photoreaction (30 min) as a function of polymer and film thickness (mm)

Complex	Polymer	Thickness (mm)	Reaction (%)
[CpFe(CO) ₂] ₂	PS	0.06	70
		0.11	25-35
	PMMA	0.06	10
	PSAN	0.10	10
[CpMo(CO) ₃] ₂	PS	0.06	25
	PMMA	0.06	0-5
	PSAN	0.06	30
Mn ₂ (CO) ₁₀	PS	0.06	100
	PMMA	0.06	5-10
	PSAN	0.07	70-80

In PSAN films. Upon irradiation, new $\nu(\text{CO})$ peaks were observed in the IR spectra for both $[\text{CpFe}(\text{CO})_2]_2$ and $\text{Mn}_2(\text{CO})_{10}$ in PSAN [Figs.3-2 and 3-3, respectively].

In the case of the iron dimer, the new peaks appeared in both the terminal (1935 cm^{-1}) and bridging (1745 cm^{-1}) $\nu(\text{CO})$ regions. A parallel experiment in CH_3CN showed similar spectral changes. The new peaks in PSAN are consistent with the formation of the monosubstituted dimer,⁶² $\text{Cp}_2\text{Fe}_2(\text{CO})_3\text{PSAN}$ [Eq.3-1] with one terminal and two bridging carbonyl groups. Attempts to isolate this particular polymer-supported species by dissolving the irradiated film in toluene and adding ethanol failed because of its instability. A polymer was precipitated which displayed no $\nu(\text{CO})$ band.



On dissolving the irradiated PSAN film containing $\text{Mn}_2(\text{CO})_{10}$ in toluene and adding ethanol, a polymer was precipitated which displayed $\nu(\text{CO})$ bands in the IR at $2090(\text{w})$, $2023(\text{s})$, $1990\text{-}1981(\text{s,br})$ and $1957\text{-}1944(\text{s,br})\text{ cm}^{-1}$. [Fig.3-3]. These new peaks indicate that the polymer is free of the parent $\text{Mn}_2(\text{CO})_{10}$ complex and they agree reasonably well with those reported⁶³ for $\text{eq-Mn}_2(\text{CO})_9(\text{NCCH}_3)$ [Eq.3-2] and are thus assigned to its PSAN analog.

62. Haines, R.J.; DuPreez, A.L. *Inorg. Chem.* **1969**, *8*, 1459.

63. (a) Ziegler, M.L.; Hass, H.; Sheline, R.K. *J. Inorg. Nucl. Chem.* **1962**, *24*, 1172. (b) Koelle, U. *J. Organomet. Chem.* **1978**, *155*, 53.

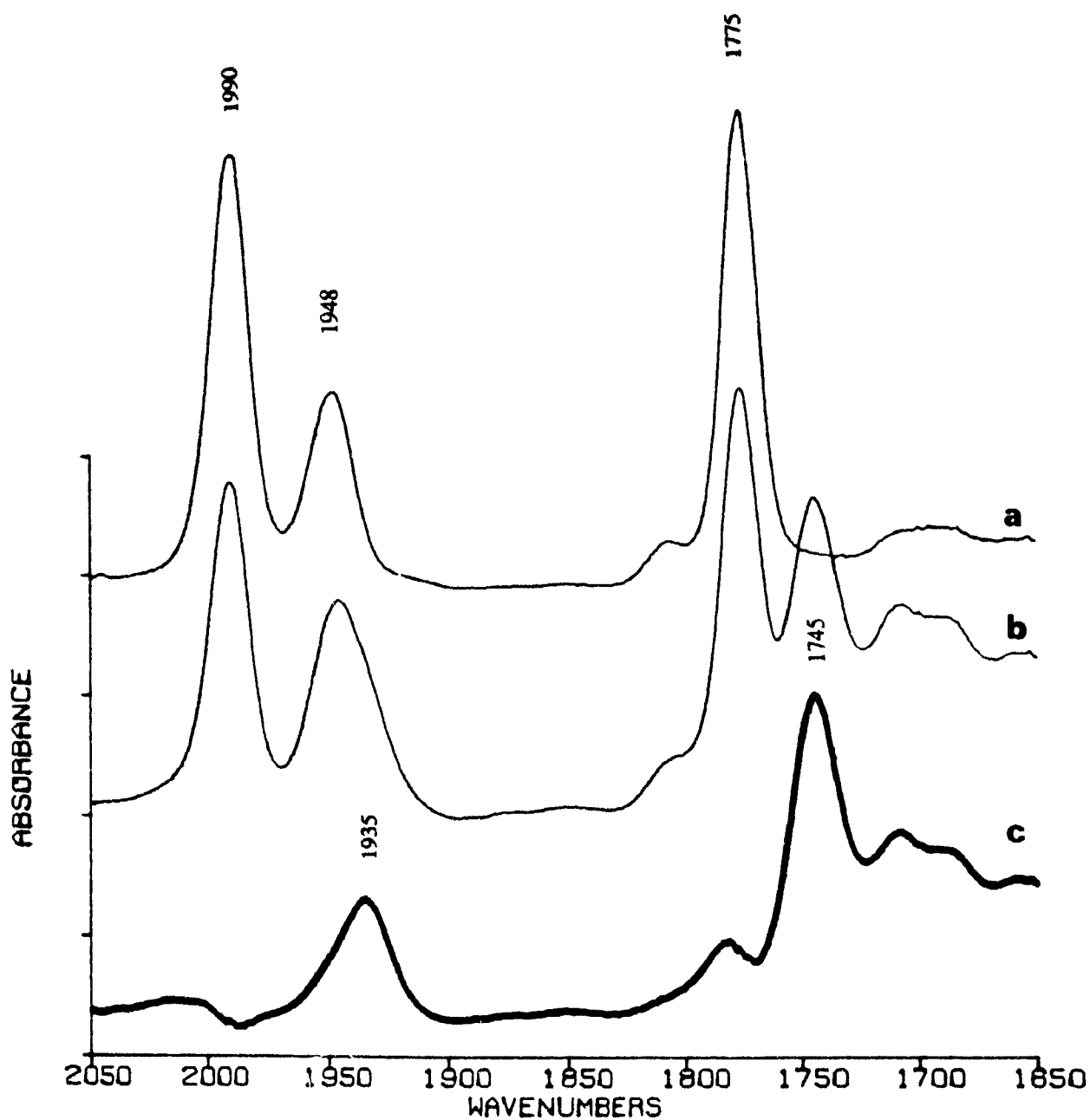


Figure 3-2 The IR spectra in the $\nu(\text{CO})$ region of $[\text{CpFe}(\text{CO})_2]_2$ in PSAN: (a) before irradiation; (b) irradiation for 4 h and (c) spectrum a subtracted from spectrum b.

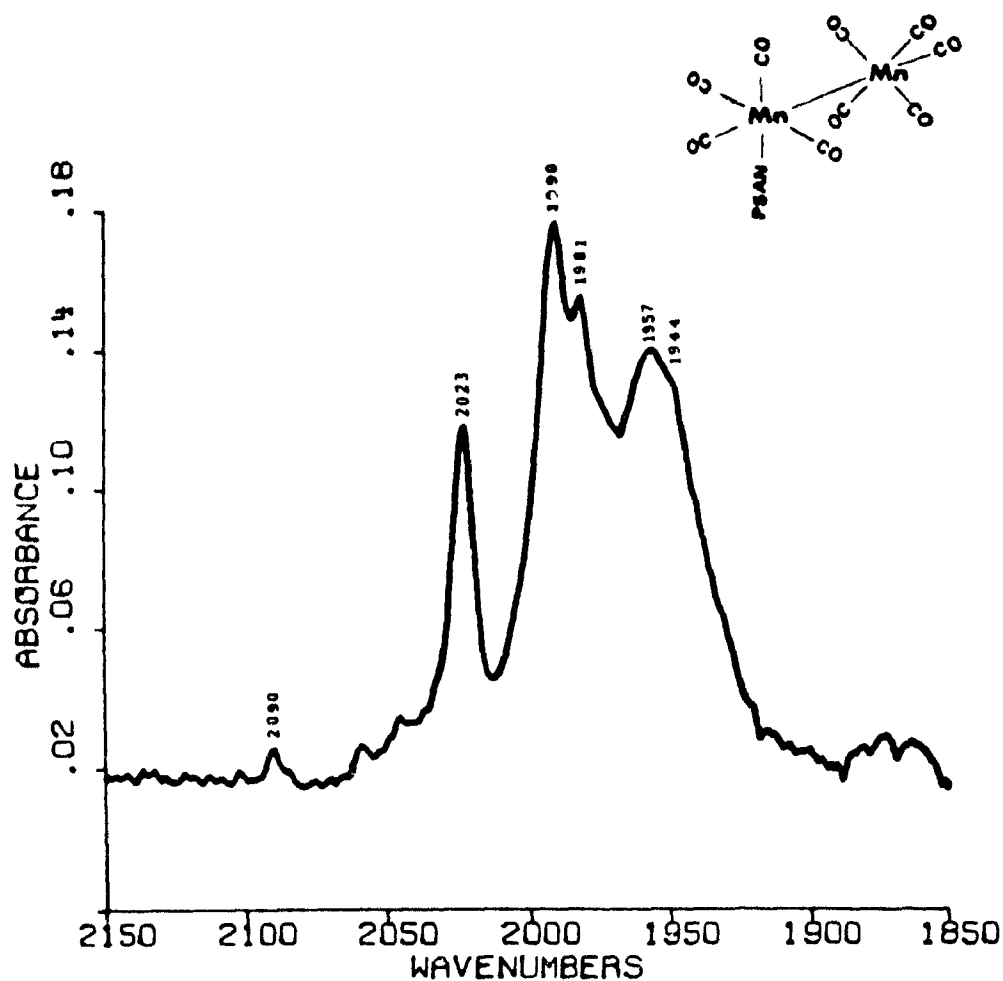


Figure 3-3 The IR spectrum in the $\nu(\text{CO})$ region of $\text{eq-Mn}_2(\text{CO})_9(\text{PSAN})$ in PSAN.

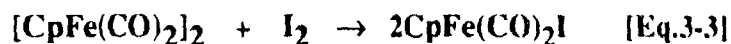
Reactions involving binuclear intermediate pathways are proposed for both cases here. The dimers apparently lose one terminal CO upon irradiation which is then replaced by a pendant nitrile ligand from the PSAN copolymer. This result further suggests that polymers containing potential ligands can scavenge photogenerated intermediates leading to the formation of polymer-supported complexes in the solid polymer matrices.

The peaks due to $[\text{CpMo}(\text{CO})_3]_2$ in PSAN gradually diminished and no significant new peaks appeared during the irradiation. The failure to detect analogous products for

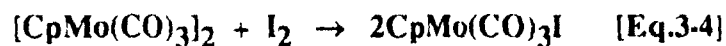
molybdenum is of interest in view of the photochemical preparation of complexes such as $\text{Cp}_2\text{Mo}_2(\text{CO})_5[\text{P}(\text{C}_6\text{H}_5)_3]$. The photochemistry of $[\text{CpMo}(\text{CO})_3]_2$ is, however, very sensitive to reaction conditions.^{57(a)}

3.3.3 Iodine Oxidation Reactions

$[\text{CpFe}(\text{CO})_2]_2$ in PS. The iron carbonyl dimer is oxidized rapidly in PS film by I_2 vapour at room temperature, as evidenced by the appearance after only one day of a new $\nu(\text{CO})$ band at 2040 cm^{-1} and an increase in intensity of the band at 1996 cm^{-1} , concomitant with a decrease in the intensities of the other parent bands [Fig 3-4]. The film turned deep brown after 10 days and only two strong bands at 2044 and 2003 cm^{-1} were detected, which are in agreement with those for the oxidation product $\text{CpFe}(\text{CO})_2\text{I}^{64}$ [Eq.3-3].



$[\text{CpMo}(\text{CO})_3]_2$ in PS. Iodine oxidation of the molybdenum dimer in PS film leads similar behaviour to that above, except the oxidation product is less stable. After one day's exposure to I_2 vapour, a new peak appeared at 2038 cm^{-1} which reached its maximum intensity after five days. At the same time, the parent peaks greatly diminished revealing additional new peaks at 1961 and 1939 cm^{-1} . The product with three peaks at 2038 , 1961 and 1939 cm^{-1} was identified as $\text{CpMo}(\text{CO})_3\text{I}^{64}$ [Eq 3-4]. After extended oxidation (10 days), no $\nu(\text{CO})$ peaks were detected, which indicates that further decomposition occurred to give products containing no CO ligands.



64. Sloan, T.E.; Wojcicki, A. *Inorg. Chem.* **1968**, 7, 1268.

$Mn_2(CO)_{10}$ in PS. On exposure of the PS film embedded with $Mn_2(CO)_{10}$ to I_2 vapour, new peaks gradually appeared at 2045 and 2028 cm^{-1} , while the peaks at 2008 and 1982 cm^{-1} slowly decreased in intensity. The final bands observed after exposure for 10 days at 2128, 2045 and 2008 cm^{-1} are consistent with the formation of $Mn(CO)_5I$ ⁶⁵ [Eq.3-5].

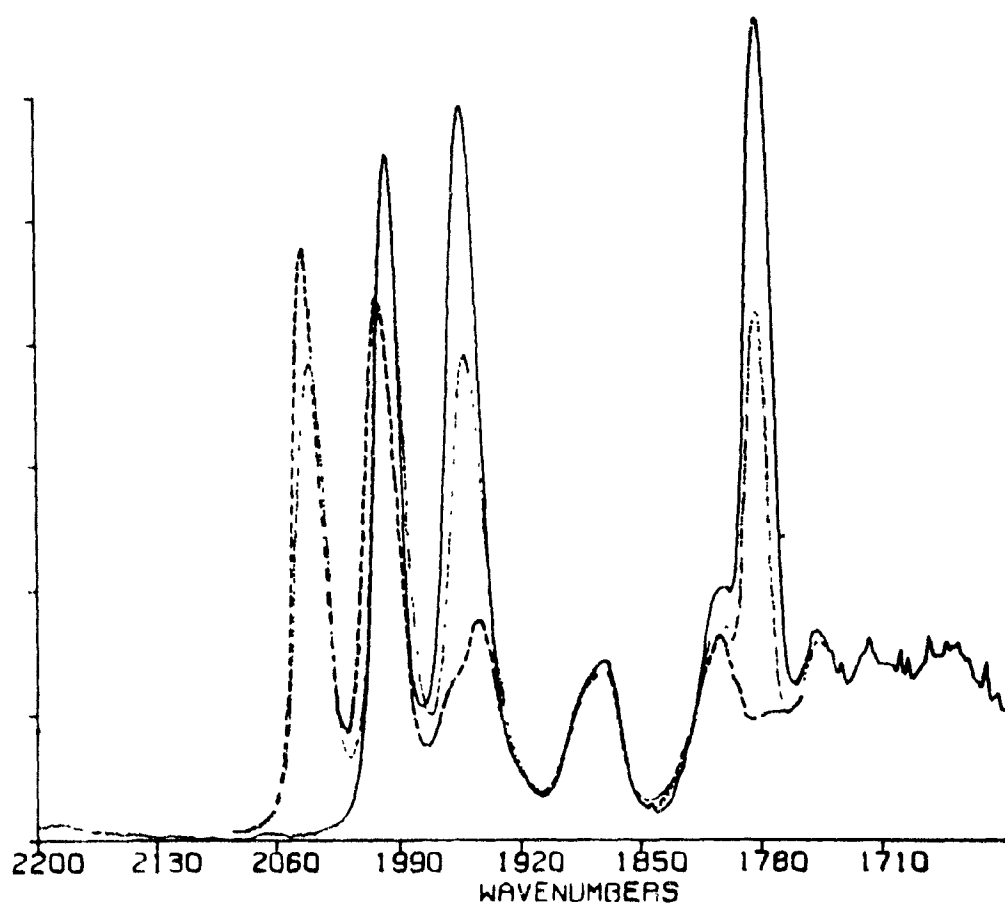


Figure 3-4 The IR spectra in the $\nu(CO)$ region of $[CpFe(CO)_2]_2$ in PS : (—) before exposure to I_2 ; (···) after exposure to I_2 for 1 day and (---) 10 days.

65. Kaesz, H.D.; Bau, R.; Hendrickson, D.; Smith, J.M. *J. Am. Chem. Soc.* **1967**, *89*, 2844.

In PMMA, PSAN and thick PS films. Similar oxidation reactions were performed for all three dimers in PMMA, PSAN and PS films. Table 3-3 lists the extent of oxidation of the three dimers in different films. The oxidations took place more slowly in thick PS films than in thin PS ones, and they were also slower in PSAN. However, virtually no oxidation occurred in the PMMA films during the 10-day exposure period. The differences in oxidation rates among these three type of films illustrate that the polymer microstructures play an important role in the reactions of the organometallics with I₂ in solid polymer matrices. Presumably these differences depend on the rates of I₂ diffusion into the films, which are believed to be related to the relative gas permeabilities of the polymers. This suggestion is consistent with the results since PMMA has the lowest permeability.⁶¹

Table 3-3 Consumption of metal carbonyl starting material (as percentage) by iodine oxidation (10 days) as a function of polymer and film thickness (mm)

Complex	Polymer	Thickness (mm)	Reaction (%)
[CpFe(CO) ₂] ₂	PS	0.05	100
		0.11	20-30
	PMMA	0.05	0-5
		PSAN	0.09
[CpMo(CO) ₃] ₂	PS	0.05	90-95
	PMMA	0.05	0-5
	PSAN	0.08	20-30
Mn ₂ (CO) ₁₀	PS	0.05	50-60
	PMMA	0.05	0-5
	PSAN	0.06	20-30

3.3.4 Polarized FT-IR Studies

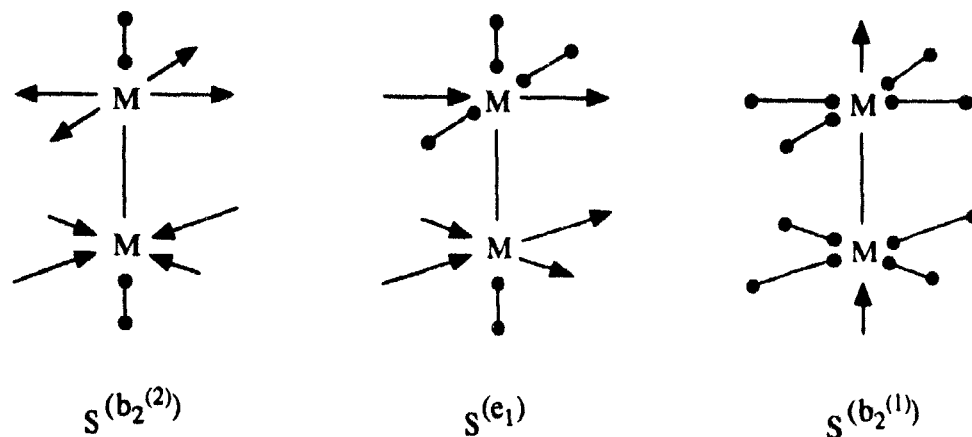
The intensity of an IR absorption band is proportional to the square of the transition moment (or change in dipole moment) of the molecular vibration causing the band. In the case of polarized IR radiation, the intensity also depends on the relative directions of the transition moment and the electric field vector of the incident radiation. The square of the component of the transition moment in the direction of the electric field vector is proportional to the absorbance.⁶⁶ Therefore, polarized IR spectroscopy measurements can be used to reveal some information about the molecular orientation in the solid if the band assignments are known. To do these measurements, it is necessary to cut thin, transparent wafers from single crystals of the material of interest. An alternative approach is to orient the compound in a nematic liquid crystal solvent, a procedure that has been successfully used in studying the polarized IR spectra of transition metal carbonyl complexes.⁶⁷ Liquid crystal solvents are somewhat limited in their use because of the complexity of their IR spectra.

Upon stretching a polymer film containing an embedded material, partial orientation of the material can occur.⁶⁸ PE has a very simple IR absorption, which makes it convenient for studying the polarizations of embedded metal carbonyls. As mentioned earlier, under the established D_{4d} symmetry of $Mn_2(CO)_{10}$, only two b_2 modes (at 1981 and 2043 cm^{-1}) and one e_1 mode (at 2012 cm^{-1}) are IR active [Fig.3-5(a)], with z- and x,y-polarizations,

66. Colthup, N. B.; Daly, L.H.; Wiberley, S. E. *Introduction to Infrared and Raman Spectroscopy* Academic Press, New York, 1975, p 105.

67. (a) Butler, I.S.; Sedman, J. *Appl. Spectrosc* 1988, 42, 497. (b) Levenson, R.A.; Gray, H.B.; Caesar, G.P. *J Am. Chem. Soc.* 1970, 92, 3653.

68. (a) Hoshi, T., Ota, K.; Yoshino, J.; Murofushi, K.; Tanizaki, Y. *Chem. Lett.* 1977, 357. (b) Frackowiak, D., Gantt, E.; Hotchandani, S.; Lipschultz, C. A.; Leblanc, R. M. *Photochem. Photobiol* 1986, 43, 335.



Scheme 3-3

respectively [Scheme 3-3].⁶⁷ Therefore, two (b_2) bands with the same polarization and another one (e_1) with opposite polarization are expected in the polarized IR spectra of oriented $\text{Mn}_2(\text{CO})_{10}$ in the carbonyl region. Such a pattern was observed in the dichroic IR spectrum of $\text{Mn}_2(\text{CO})_{10}$ soaked in PE film after stretching [Fig.3-5(b)]. The intensity of the peak at 2012 cm^{-1} (e_1 , x,y-polarization) measured perpendicular to the direction of stretching (A_{\perp}) is greater than that measured parallel (A_{\parallel}) and so ($A_{\parallel}-A_{\perp}$) is negative. While A_{\parallel} is greater than A_{\perp} for other the two bands at 1981 and 2043 cm^{-1} (b_2 , z-polarization), which have positive ($A_{\parallel}-A_{\perp}$) values. The degree of orientation of this dimer S_{zz} is about 0.1. Dichroic IR spectra of unstretched sample showed no peak in the $\nu(\text{CO})$ region ($A_{\parallel}-A_{\perp}$ is zero).

Fig.3-6 depicts the parallel (—) and perpendicular (---) polarized IR spectra in the low-frequency region of $\text{Mn}_2(\text{CO})_{10}$ in PE after stretching. There are two bands, the one at 649 cm^{-1} has been assigned to an e_1 $\delta(\text{MnCO})$ mode with x, y polarization and the other at 643

cm^{-1} due to a b_2 $\delta(\text{MnCO})$ mode with z polarization.⁶⁹ The spectra show clearly that the two bands have opposite polarizations: A_{\parallel} is greater than A_{\perp} for the peak at 643 cm^{-1} and A_{\parallel} is smaller than A_{\perp} for the band at 649 cm^{-1} . The polarizations of the peaks at 649 and 643 cm^{-1} are in agreement with their assignment as e_1 and b_2 $\delta(\text{MnCO})$ modes, respectively. The weak peak around 670 cm^{-1} exhibits parallel polarization suggesting b_2 symmetry. On symmetry grounds, however, there should only be one b_2 mode observed in the $\delta(\text{MnCO})$ region.⁶⁹ The additional peak is best attributed to a B_2 symmetry combination, e.g., $643 (b_2) + 39 \text{ cm}^{-1} (a_1, \text{lattice mode})$ ⁶⁹.

The above results indicate that $\text{Mn}_2(\text{CO})_{10}$ is partially oriented in polyethylene matrix after stretching. The polarized IR data show that the $\text{Mn}_2(\text{CO})_{10}$ molecule tends to align with its long axis (z-axis) parallel to the direction in which the polymer is being stretched. The measurements of the polarized IR spectra of oriented metal carbonyls in PE can provide useful information on band assignments and their polarization characteristics. The method employed here is very simple and the matrix used has a wide IR window. Since earlier results have demonstrated that polymer films are useful media for chemically transforming organometallic complexes in the solid plastics, it would be interesting to study solid-state chemical reactions of oriented metal carbonyls in polymer matrices.

69. D.M.Adams and I.D.Taylor, *J.C.S., Faraday Trans II* **1982**, 78, 1065.

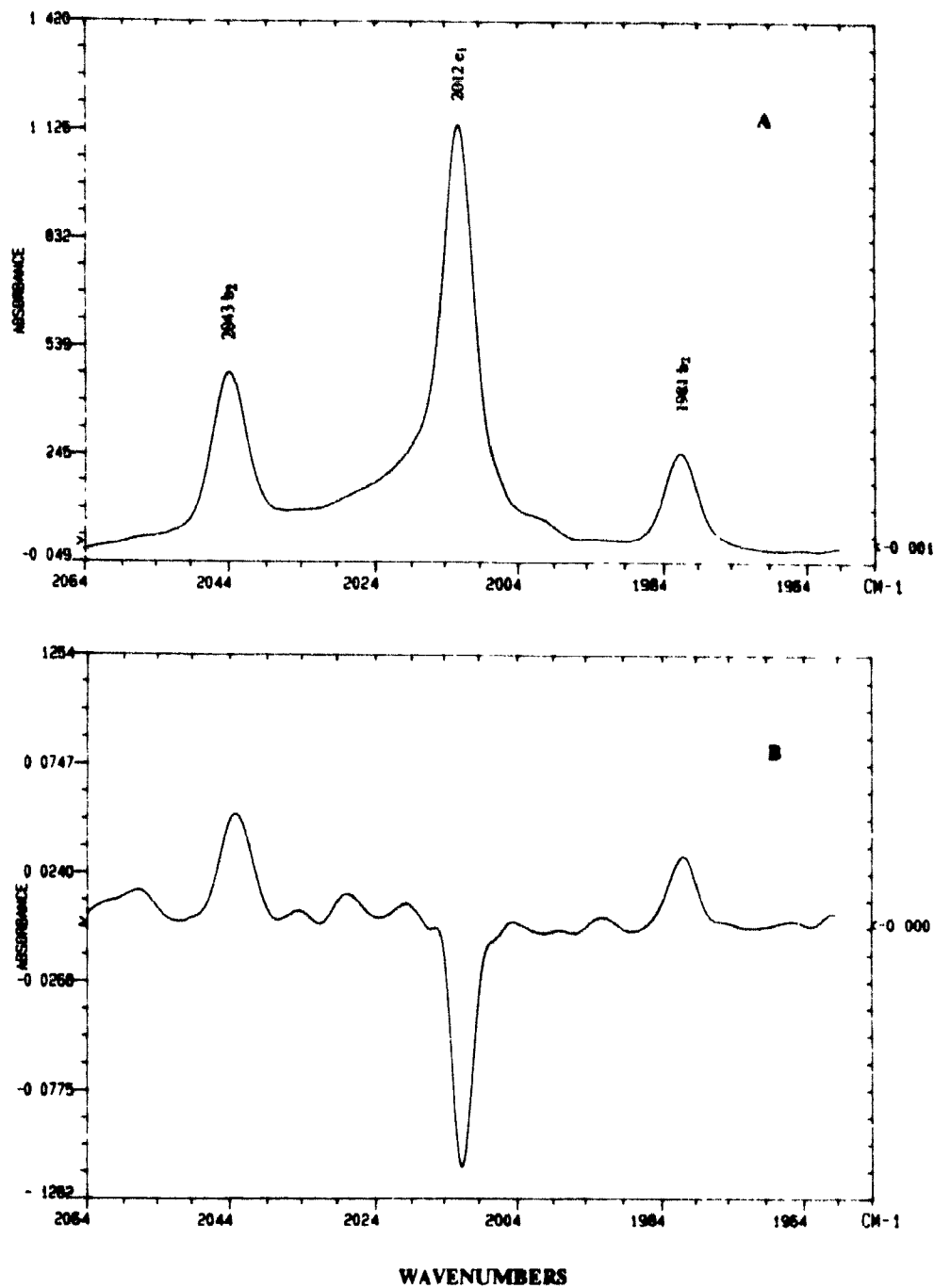


Figure 3-6 (a) The parallel polarized IR spectrum in the $\nu(\text{CO})$ region of $\text{Mn}_2(\text{CO})_{10}$ soaked in PE film after stretching; (b) dichroic IR spectra (A_{\parallel} - A_{\perp}) of $\text{Mn}_2(\text{CO})_{10}$ in PE after stretching.

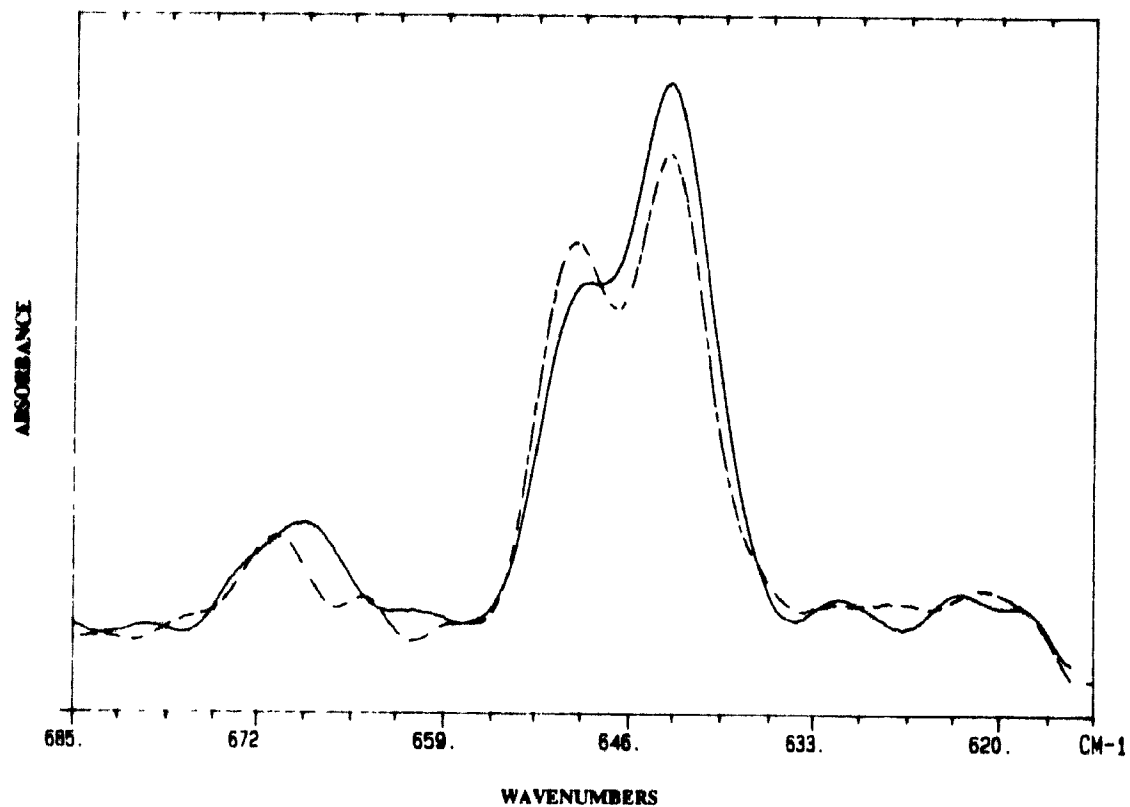


Figure 3-7 The parallel (—) and perpendicular (---) polarized IR spectra in the low-frequency region of $Mn_2(CO)_{10}$ in PE film after stretching.

3.4 Conclusions

The three polymer matrices examined afford chemical environments similar to those in structurally-related organic solvents with respect to the relative intensities and shapes of the IR bands in the $\nu(\text{CO})$ region of the three metal carbonyl dimers. PSAN polymer is capable of stabilizing photogenerated binuclear intermediates by coordination of pendant nitrile groups and thus acts as both the matrix and reactant. The I_2 oxidation reactions in PS film show the ability of small molecules diffusing into polymer matrices to undergo reaction with embedded complexes. The photolysis and oxidation results demonstrate additional methods of transforming organometallic complexes embedded in solid polymers. Since these useful plastics can be pressed into any desired shape, it should be possible to transform embedded complexes after fabrication. These are useful for the synthesis of organometallic polymers and unstable complexes in solid state. The photochemical and oxidation reactions in different polymers indicate that PMMA offers a more protective environment for the metal carbonyl dimers than PS does. This illustrates that the chemical reactivities of embedded organometallics are strongly affected by the polymer microstructures. Finally, the polarized IR spectral study indicates that $\text{Mn}_2(\text{CO})_{10}$ can be partially oriented in PE film by stretching.

CHAPTER 4. Reactions of Organometallics Embedded in Polystyrene Matrices With Gases

4.1 Introduction

Investigations of the chemical reactions occurring at gas-solid interfaces are important from both the practical⁷⁰ and theoretical⁷¹ standpoint. For instance, there is considerable interest with respect to gas separation^{70(a)} and the study of reaction mechanisms^{71(a,b)}. The knowledge obtained from such studies may also provide valuable information in connection with photosynthesis and other biochemical reactions, which occur in rigid environments. An analogy between the environment surrounding a metal complex in a metal-protein and that of a complex embedded in a polymer has long been recognized. For example, heme and 1-(2-phenylethyl) imidazole embedded in PS reversibly binds O₂ in the presence of water.⁴ Recently, Kenneth et al. have synthesized a series of copper(I) complexes containing ligands that are covalently attached to cross-linked polystyrene and investigated the reversible binding of CO gas to these complexes.^{70(a)} This ability shows considerable potential for applications in membrane or pressure-swing recovery of CO from gas streams. Finally, polymer-trapped micro particles of PbS possessing unusual band gaps have been prepared by treatment of lead acetate embedded in ethylene-15% methacrylic acid copolymer with H₂S.⁷²

In addition to our investigations of the FT-IR spectra of organometallic carbonyl complexes embedded in various polymer films (PS, PMMA and PSAN) and their

70. (a) Balkus, K.J.Jr.; Kortz, A.; Drago, R.S. *Inorg. Chem.* **1988**, 2, 9. (b) Hirai, H.; Hara, S.; Komiyama, M. *Bull. Chem. Soc. Jpn.* **1986**, 59, 109. (c) *ibid.* **1986**, 59, 1051. (d) Hirai, H.; Woda, K.; Komiyama, M. *Bull. Chem. Soc. Jpn.* **1986**, 1043.

71. (a) Sedlacek, A.J.; Mansueto, E.S.; Wight, C.A. *J. Am. Chem. Soc.* **1987**, 109, 6223. (b) Sedlacek, A.J.; Wight, C.A. *J. Phys. Chem.* **1988**, 92, 2821. (c) Burdett, J.K.; Downs, A.J.; Gaskill, G.P.; Graham, M.A.; Turner, J.J.; Turner, R.F. *Inorg. Chem.* **1978**, 17, 523.

72. Mahler, W. *Inorg. Chem.* **1988**, 27, 435.

photochemical reactivities, some of these films embedded with metal carbonyl dimers have also been exposed to I_2 vapour. The oxidation rates are dependent on the polymer with the reaction in polystyrene being the fastest and PMMA the slowest. These observations have prompted further studies of the reactions of gases with organometallics in solid polymer matrices. Reported here is the chemistry of $CpRu(COD)Cl$ (COD = cycloocta-1,5-diene) and Vaska's compound *trans*- $Ir(CO)Cl(PPh_3)_2$ embedded in PS with the gases H_2 , O_2 , I_2 , CO , ^{13}CO and SO_2 .

4.2 Experimental

The complex *trans*- $Ir(CO)Cl(PPh_3)_2$ was purchased from Strem Chemical Inc. and was used without further purification. $CpRu(COD)Cl$ was kindly provided by Dr. Eric Singleton and was purified by recrystallization from CH_2Cl_2 /hexanes. Polystyrene (M W = 125,000-250,000) was obtained from Polysciences. The gases SO_2 (99.98%, Matheson), H_2 , O_2 , CO (Linde) and ^{13}CO (Icon) were used as received. The films containing organometallics (wt% = 5, 0.06-0.08 mm thickness) were prepared as described previously and kept under N_2 prior to use. The FT-IR absorption spectra were recorded on a Bomem Michelson 100 spectrometer at 4 cm^{-1} resolution using a DTGS detector. Spectra were recorded both before and after gas treatment. The relative intensities of the individual reactant and product bands, as well as those of nearby polystyrene bands were used to determine the extent of reaction and its reversibility.

I₂-Oxidation. The iodine oxidation reactions were performed as described in Chapter 3. The oxidation reactions were monitored by FT-IR spectroscopy over a period of months.

Other gas reactions. The other gas reactions were carried out at room temperature in Carius tubes. The following experimental procedure was employed. A film was placed in a Carius

tube under N_2 and the vessel was quickly connected to a vacuum (about torr 0.2 mmHg) for a few minutes. Then, the tube was closed off, removed from the vacuum line and subjected to the desired gas at about 2 atm pressure controlled by a regulator. The tube was closed and kept at room temperature in the dark for a certain period of time. The gas pressure was released and the FT-IR spectrum of the film was recorded immediately. For the reversibility studies, the gas-treated films were kept either under vacuum or in air at room temperature in the dark. The degassing reactions were monitored by IR spectroscopy.

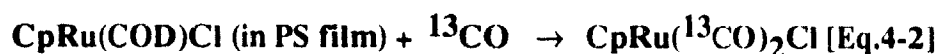
The films containing *trans*-Ir(^{13}CO)Cl(PPh $_3$) $_2$ were obtained by keeping *trans*-Ir(CO)Cl(PPh $_3$) $_2$ -embedded films under a ^{13}CO atmosphere for long periods of time (one day) and then placing them under vacuum. The CO addition and CO exchange reactions of *trans*-Ir(^{13}CO)Cl(PPh $_3$) $_2$ in PS were performed in a specially designed IR gas-flow-through cell, since the reaction rates were very fast. The cell consisted of a stainless-steel holder equipped with two stainless-steel valves and two NaCl windows mounted by screws within the holder. Good vacuum or pressure was achieved by placing rubber gaskets between the windows and the steel holder. The films containing *trans*-Ir(^{13}CO)Cl(PPh $_3$) $_2$ were placed inside the cell under N_2 and then the cell was connected to a vacuum line. After closing the vacuum valve, the cell was filled with CO gas at about 1 atm. The IR spectra were recorded immediately after filling the cell with CO and the reactions were monitored with time. The cell was eventually reconnected to the vacuum line in order to check the reversibility of the reactions.

ATR-FT-IR. The surface properties of some of the gas treated films at different stages were examined by ATR-IR spectroscopy. The spectra were obtained by using the multireflection KRS-5 crystal ($10 \times 5 \times 1 \text{ mm}^3$, 45° entrance angle) and the beam-condenser optical accessory described in Chapter 2. The penetration depth d_p was about 1% of the film thicknesses ($5 \times 10^{-4} \text{ mm}$). Transmission IR absorption spectra of the same films were also measured.

4.3 Results and Discussion

4.3.1 Substitution Reactions of CpRu(COD)Cl in PS Films

CpRu(COD)Cl contains an easily displaced cyclooctadiene ligand and has been shown to be a versatile and highly reactive precursor to a wide range of ruthenium compounds.^{73(a)} Ligands, such as CO, PPh₃ and CN(CH₂)₆NC, substitute the COD ligand in solution to give neutral products of the type CpRuL₂Cl in high yields.^{73(a)} PS films embedded with CpRu(COD)Cl are brown-orange and transparent. After treating such a film with CO gas for two days, there is no significant difference in colour, but there is a dramatic change in the IR spectrum in the $\nu(\text{CO})$ region [Fig 4-1(a)] This observation suggests that CO ligand substitution has occurred. Two strong peaks appeared at 2050 and 1998 cm^{-1} [Table 4-1]; these are in excellent agreement for those of CpRu(CO)₂Cl⁷³ [Eq.4-1].



A similar reaction took place upon placing a CpRu(COD)Cl-embedded film in the ¹³CO-filled Carius tube. In the IR spectrum, two new bands in the $\nu(\text{CO})$ region (2003 and 1955 cm^{-1}) [Table 4-1, Fig.4-1(b)] were detected, which are consistent with the formation of CpRu(¹³CO)₂Cl [Eq.4-2]. The intensities of the carbonyl peaks showed little change when

73. (a) Albers, M.O.; Robinson, D.J.; Shaver, A.; Singleton, E. *Organometallics* **1986**, *5*, 2199. (b) Blackmore, T.; Cotton, J.D.; Bruce, M.I.; Stone, F.G.A. *J. Chem. Soc. (A)* **1968**, 2931.

the treated films were left in the air at room temperature for months. The above results demonstrate that labile ligands on organometallic complexes embedded in solid polymer matrices can be substituted by stronger ligands in gas diffusion reactions.

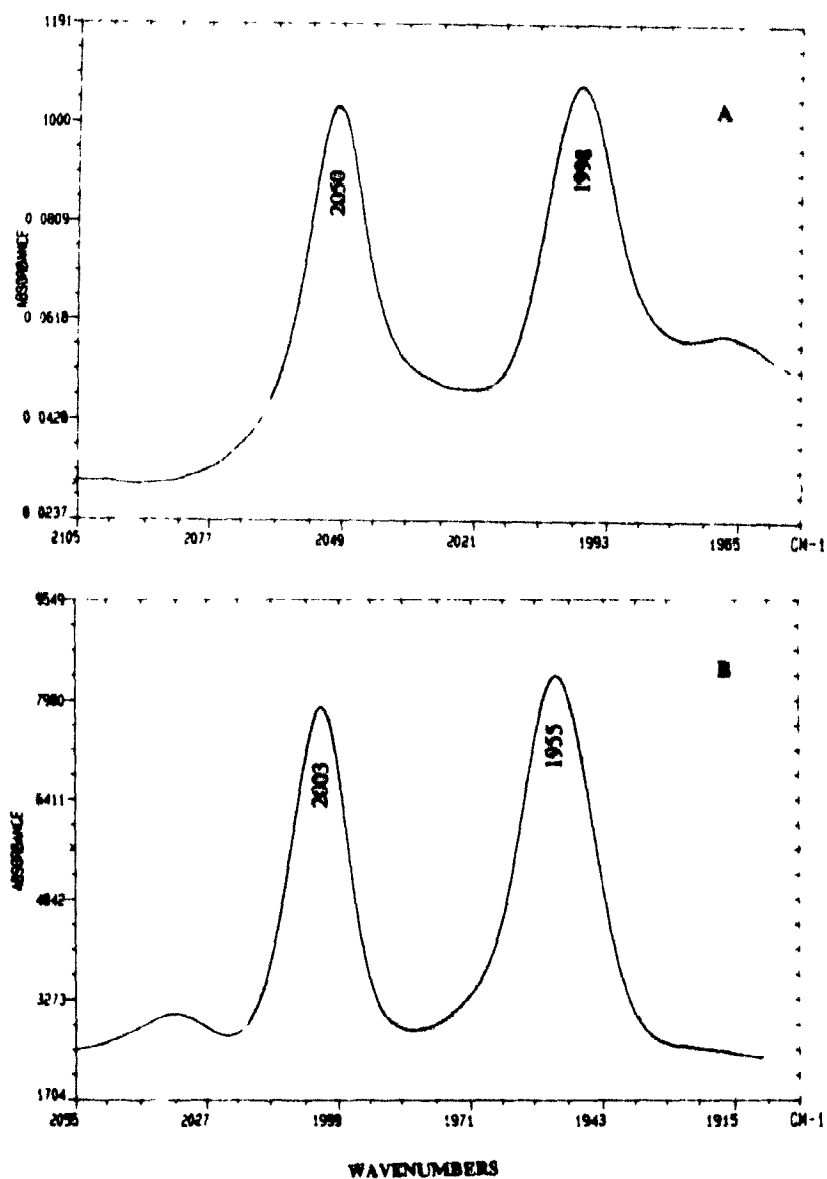


Figure 4-1 The IR spectra in the $\nu(\text{CO})$ region of (a) $\text{CpRu}(\text{CO})_2\text{Cl}$ and (b) $\text{CpRu}^{13}\text{CO}_2\text{Cl}$.

Table 4-1 The carbonyl stretching frequencies of *trans*-Ir(CO)Cl(PPh₃)₂ and selected adducts and of CpRu(CO)₂Cl in PS and other media (cm⁻¹)

Complexes	Medium	$\nu(\text{CO})$
Ir(CO)Cl(PPh ₃) ₂	PS	1964
	toluene	1967
	Nujol	1952
Ir(¹³ CO)Cl(PPh ₃) ₂	PS	1917
Ir(CO) ₂ Cl(PPh ₃) ₂	PS	1964, 1928
Ir(¹³ CO) ₂ Cl(PPh ₃) ₂	PS	1917, 1884
Ir(CO)(¹³ CO)Cl(PPh ₃) ₂	PS	1950, 1905
Ir(CO)(H ₂)Cl(PPh ₃) ₂	PS ^a	1990
	benzene ^b	1983
	Nujol ^c	1970
Ir(CO)(O ₂)Cl(PPh ₃) ₂	PS	2006
Ir(CO)(SO ₂)Cl(PPh ₃) ₂	PS	2019
Ir(CO)(SO ₄)Cl(PPh ₃) ₂	PS	2049
Ir(CO)(I ₂)Cl(PPh ₃) ₂	PS	2066
CpRu(CO) ₂ Cl	PS	2050, 1998
CpRu(¹³ CO) ₂ Cl	PS	2003, 1955

a) $\nu(\text{Ir-H})$: 2202, 2092 cm⁻¹

b) $\nu(\text{Ir-H})$: 2220, 2095 cm⁻¹; Ref.75

c) $\nu(\text{Ir-H})$: 2190, 2100 cm⁻¹; Ref.75

4.3.2 Addition Reactions of $\text{Ir}(\text{CO})\text{Cl}(\text{PPh}_3)_2$ in PS Films

Vaska's compound $\text{trans-Ir}(\text{CO})\text{Cl}(\text{PPh}_3)_2$ is a d^8 -system with square-planar geometry and two *trans* PPh_3 ligands. It can readily undergo addition reactions in solution with many neutral gases, such as O_2 , H_2 , CO , I_2 , SO_2 and these reactions are reversible in some cases.⁷⁴ The reaction mechanisms have been extensively investigated and most of the adducts have been fully characterized. The IR spectrum of $\text{trans-Ir}(\text{CO})\text{Cl}(\text{PPh}_3)_2$ in Nujol mull has a strong $\nu(\text{CO})$ peak at 1952cm^{-1} , while $\text{trans-Ir}(\text{CO})\text{Cl}(\text{PPh}_3)_2$ embedded in PS film shows a strong absorption at 1964cm^{-1} [Table 4-1], close to that observed in toluene solution.

a. H_2 addition

The yellow colour of the film became lighter upon treatment with H_2 (~2 atm) in a Carius tube for 1 h, but it did not fade further over a period of 5 days. Two new $\nu(\text{Ir-H})$ bands at 2202w and 2092vs cm^{-1} and a new $\nu(\text{CO})$ peak at 1990s cm^{-1} were observed in the IR spectrum, together with a concomitant decrease in intensity of the band due to the parent complex [Fig.4-2]. These new bands are consistent with *cis* addition to give the dihydride product which has an octahedral structure shown below:⁷⁵ [Eq.4-3].



74. (a) Vaska, L. *Acc Chem. Res.* **1968**, *1*, 335. (b) Collman, J.P. *Acc. Chem. Res.* **1968**, *1*, 136.

75. (a) Vaska, L., DiLuzio, J.W.; *J. Am. Chem. Soc.* **1962**, *84*, 679. (b) Vaska, L.; *J. Am. Chem. Soc.* **1966**, *88*, 4100. (c) Chock, P. B.; Halpern, J. *J. Am. Chem. Soc.* **1966**, *88*, 3511.

The IR peak positions of the dihydride in the PS matrix are closer to those in benzene than to those in Nujol mull [Table 4-1], consistent with earlier proposals concerning the environment provided by PS.

It has been reported that the dihydride remains unchanged in the solid state even when kept under vacuum at 25°C for 16 hr but it loses H₂ in solution.⁷⁵ When the H₂-treated film was kept under vacuum for 3 days, the IR bands due to the dihydride diminished significantly with strong recovery of the peak due to Vaska's compound. This indicates the reversibility of the H₂ addition reaction in PS film [Fig.4-2]. The dehydrogenation reaction in PS also takes place when H₂-treated film was left standing in air. There was some *trans*-Ir(CO)Cl(PPh₃)₂ regeneration (1964 cm⁻¹) and O₂-adduct (2006 cm⁻¹) formation [Fig.4-2].

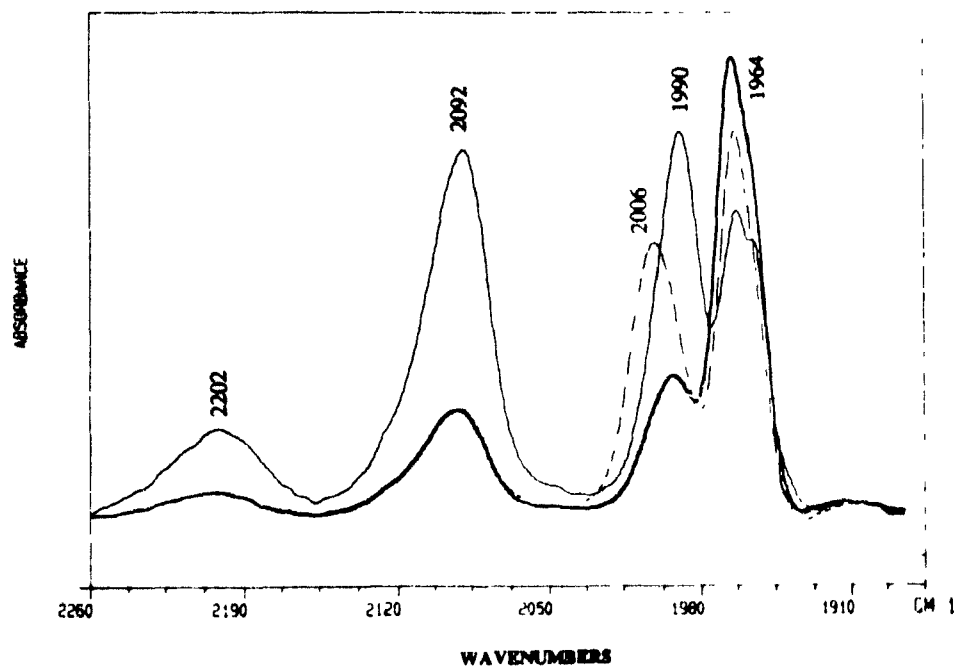


Figure 4-2 The IR spectra in the $\nu(\text{CO})$ region of Ir/PS upon treatment with H₂ (—) for 5 days; (—) followed by exposure to vacuum for 3 days and (---) followed by exposure to air for 3 days.

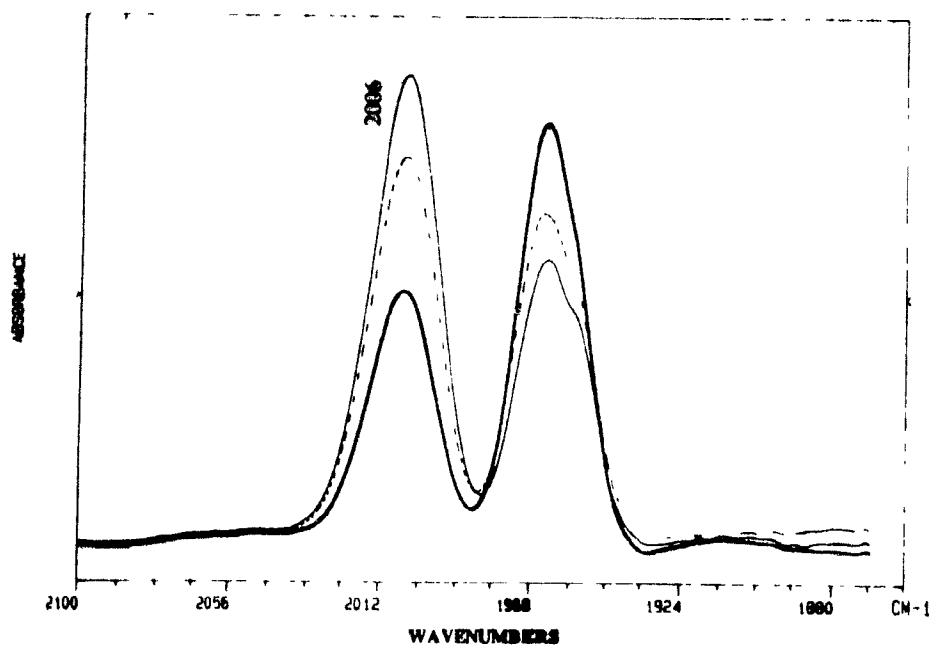


Figure 4-3 The IR spectra in the $\nu(\text{CO})$ region of Ir/PS upon treatment with O_2 (—) for 5 days; (—) followed by exposure to vacuum for 3 days and (···) followed by exposure to air for 3 days.

b. O_2 addition

After Ir/PS was placed in an O_2 -filled tube for 5 days, the O_2 -adduct was produced⁷⁶ with the appearance of a new peak at 2006 cm^{-1} and the decrease of the original peak at 1964 cm^{-1} in the IR spectrum [Fig.4-3, Eq.4-4].

76. (a) Vaska, L. *Science* **1963**, *140*, 809. (b) Reed, C.A.; Roper, W.R. *J. Chem. Soc., Dalton Trans.* **1973**, 1370. (c) McGinnety, J.A.; Payne, N.C.; Ibers, J.A. *J. Am. Chem. Soc.* **1969**, *91*, 6301.

The complex $\text{Ir}(\text{CO})(\text{O}_2)\text{Cl}(\text{PPh}_3)_2$ has a structure similar to that of the H_2 -adduct with a distorted octahedral configuration. The IR band in the $\nu(\text{CO})$ region due to the O_2 -adduct decreased gradually upon standing in air, but rapidly in *vacuo*. The deoxygenation reaction takes place much faster in *vacuo* than in air [Fig.4-3].



c. SO_2 addition

Exposure of Vaska's compound embedded in PS film to SO_2 in a Carius tube quickly led to a colour change from yellow to green-yellow. The IR absorption due to *trans*- $\text{Ir}(\text{CO})\text{Cl}(\text{PPh}_3)_2$ vanished and a new strong peak at 2019 cm^{-1} appeared [Table 4-1], which is assigned⁷⁷ to $\text{IrCl}(\text{CO})(\text{SO}_2)(\text{PPh}_3)_2$, [Eq 4-5, Fig.4-4]. The molecular structure of this complex determined that the SO_2 is bonded to the metal *via* the sulfur atom and the coordination geometry around the Ir is that of a tetragonal pyramid as shown below. It was reported that the SO_2 adduct in the crystalline state releases SO_2 upon heating above 150°C and reverts to the starting material in boiling benzene.^{77(a)} At ambient conditions in vacuum, SO_2 dissociated from the SO_2 -adduct in PS film quite quickly with regeneration of the starting material [Fig.4-4].

Upon exposure of the O_2 -adduct to SO_2 , the sulfate compound $\text{Ir}(\text{CO})(\text{SO}_4)\text{Cl}(\text{PPh}_3)_2$ was produced [Eq.4-6] as evidenced by the IR peak at 2049 cm^{-1} , which is in agreement

77. (a) Vaska, L; Bath, S.S. *J. Am. Chem. Soc.* **1966**, 88, 1333. (b) La Placa, S.J.; Ibers, J.A. *Inorg. Chem.* **1966**, 5, 405.

with that reported⁷⁸ [Table 4-1]. The band due to the iridium sulfate complex remained unchanged when the film was kept under vacuum for hours or in air over the period of a month.

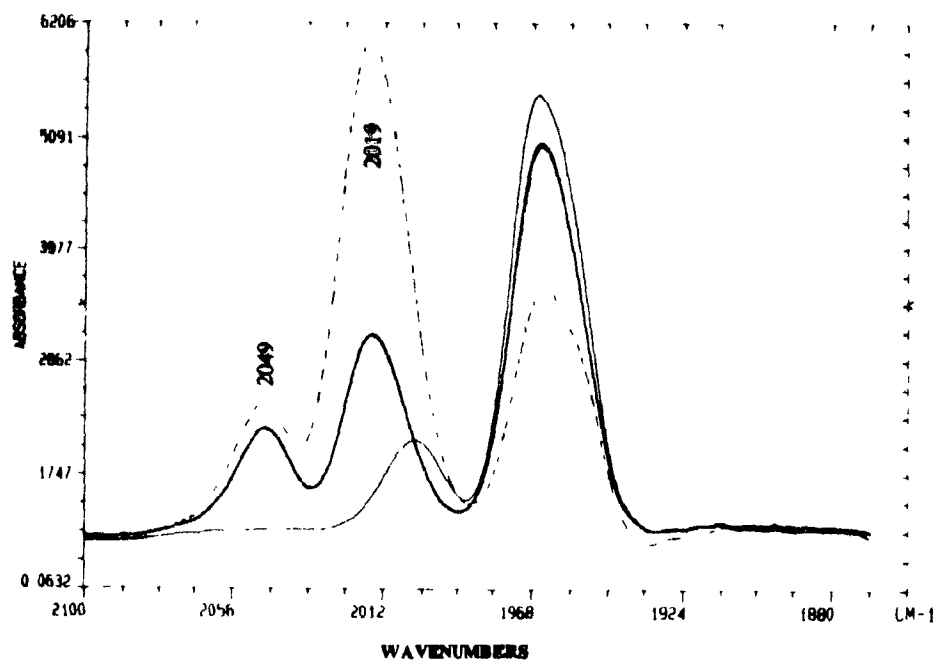
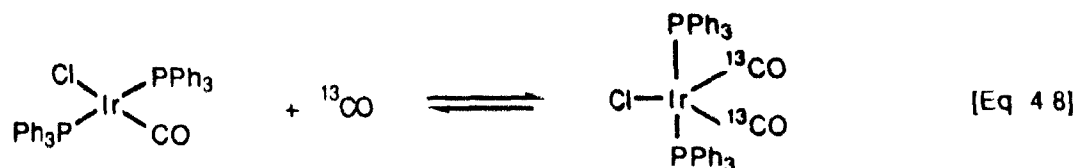
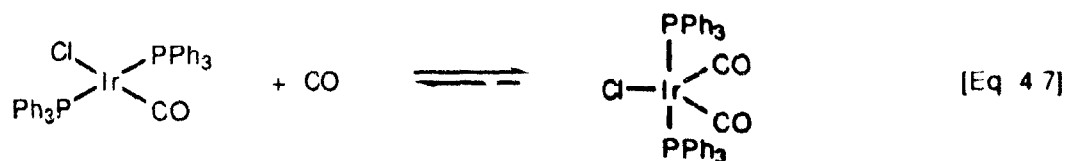


Figure 4-4 The IR spectra in the $\nu(\text{CO})$ region of Ir/PS upon treatment with SO_2 (—) before treatment, (---) treatment for 3 h and (—) followed by exposure to vacuum for 15 h.

78. (a) Valentine, J.; Valentine, D. Jr.; Collman, J.P. *Inorg. Chem.* **1971**, *10*, 219. (b) Horn, R.W.; Weissberger, E.; Colman, J.P. *Inorg. Chem.* **1970**, *9*, 2367.

d. CO addition

As in solution,⁷⁹ the CO addition reaction of Vaska's compound in PS film was very rapid and reversible. Treatment of the films with gaseous CO or ¹³CO gave two pair of peaks at 1964 and 1929 cm⁻¹ and at 1916 and 1884 cm⁻¹, respectively, consistent with the formation of Ir(CO)₂Cl(PPh₃)₂ and the ¹³CO analogue. The structure of the CO-adduct was proposed to be trigonal bipyramid and the two PPh₃ were in the axial positions, [Eq 4 7,4-8] Exposure of Ir(CO)₂Cl(PPh₃)₂ or the ¹³CO analogue in PS to vacuum resulted in quick dissociation of a carbonyl. The bands due to the starting materials *trans*-Ir(CO)Cl(PPh₃)₂ (1964 cm⁻¹) and Ir(¹³CO)Cl(PPh₃)₂ (1917 cm⁻¹) were observed, respectively.



When *trans*-Ir(¹³CO)Cl(PPh₃)₂ in PS was treated with CO gas in a gas-flow-through IR cell, the IR spectrum of the film changed markedly in a few minutes with several new peaks appearing [Fig.4-5]: one strong band appeared at 1964 cm⁻¹ which overlapped with a band around 1950 cm⁻¹; another strong band at 1917 cm⁻¹ had shoulders at each side, around 1928 cm⁻¹ and 1905 cm⁻¹, together with a weak shoulder at 1884 cm⁻¹. After the film was placed in a vacuum for 30 min, all the shoulders disappeared with only two strong bands left, one at 1964 cm⁻¹ assigned to *trans*-Ir(CO)Cl(PPh₃)₂ and the other at 1917 cm⁻¹ due to Ir(¹³CO)Cl(PPh₃)₂. There are five possible complexes produced during the time the film was exposed to the CO gas [Eq.4-9] [Table 4-1, Fig.4-5].

79. (a) Vaska, L. *Science* **1966**, *152*, 769; (b) Payne, N.C.; Ibers, J.A. *Inorg. Chem.* **1969**, *8*, 2714.

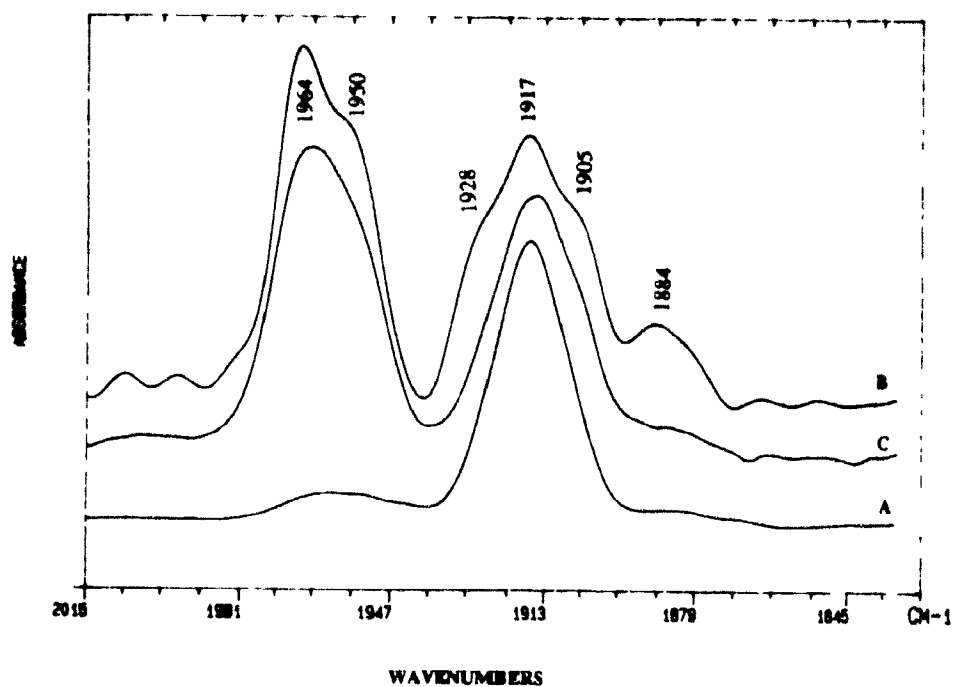
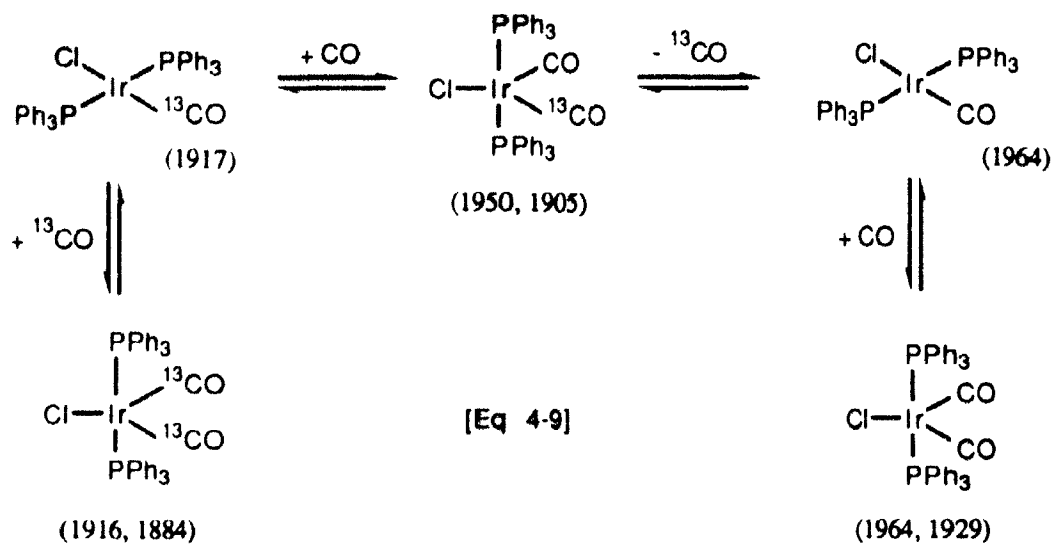
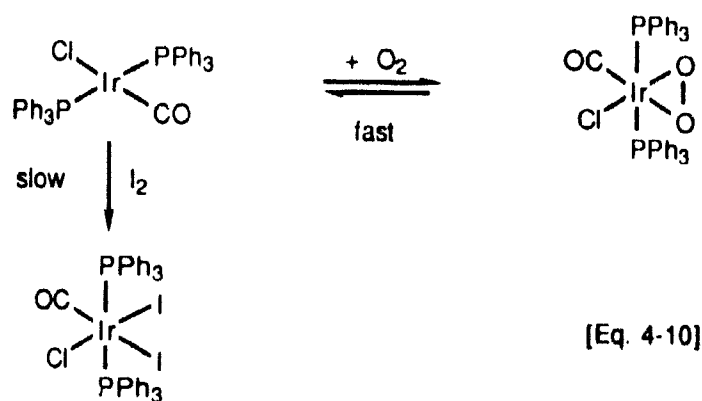


Figure 4-5 The IR spectra in the $\nu(\text{CO})$ region of $\text{Ir}^{13}\text{CO/PS}$ upon treatment with CO (a) before treatment; (b) after treatment for 20 min and (c) followed by exposure to vacuum for 30 min.

e. I₂ addition

Reaction of Vaska's compound in PS film with I₂ occurs more slowly than with other gases. Exposure of the film embedded with Ir(CO)Cl(PPh₃)₂ to I₂ vapour at ambient conditions over a 3-day period led to the gradual growth of a new peak at 2066 cm⁻¹ due to the I₂-adduct⁸⁰, together with a strong band at 2006 cm⁻¹ belonging to the O₂-adduct and a peak due to the original compound. After two months in the I₂ jar, the band due to the I₂-adduct was the only one remaining. Clearly, Vaska's compound in PS film is oxidized quickly by O₂ in air and the slowly by I₂. However, because of the reversibility of the O₂ addition, the final product is eventually the I₂-adduct [Eq.4-10]



4.3.3 ATR-IR Studies

Exposure of *trans*-Ir(CO)Cl(PPh₃)₂ embedded in PS film to I₂ for 3 h affords a low yield of the I₂-adduct since only a very weak peak at 2066 cm⁻¹ was detected in the transmission IR absorption spectrum, together with a moderate peak at 2006 cm⁻¹ due to the O₂ adduct and a strong band due to the starting material. An ATR-IR spectrum of this same film in the ν(CO) region, however, showed a very strong I₂-adduct absorption with a weak O₂-adduct

80. Bennett, M.A.; Clark, R.J.H.; Milner, D.L. *Inorg. Chem.* **1967**, *6*, 1647.

band [Fig.4-6]. No band due to the original complex was detected. This result indicates that most of the compound on the film surface has been oxidized by I_2 during the short exposure time. After exposure of the film to I_2 for two months, no significant difference was observed between the IR and ATR-IR spectra of this film.

For the O_2 -treated film containing a small amount of the O_2 -adduct, no difference was observed between the transmission IR and ATR-IR spectra. Similar results were obtained for the ATR-IR and IR spectra of films embedded with $CpRu(COD)Cl$ which had been treated with CO gas

These results indicate that I_2 with its relatively large molecular size has a low diffusion rate into PS films. This probably results in the observation that the Vaska's compound on the film surface is more easily oxidized by I_2 than that in the interior of the film. Conversely, the smaller O_2 and CO molecules can readily diffuse into PS films and therefore no differences are observed between the transmission IR and ATR-IR spectra.

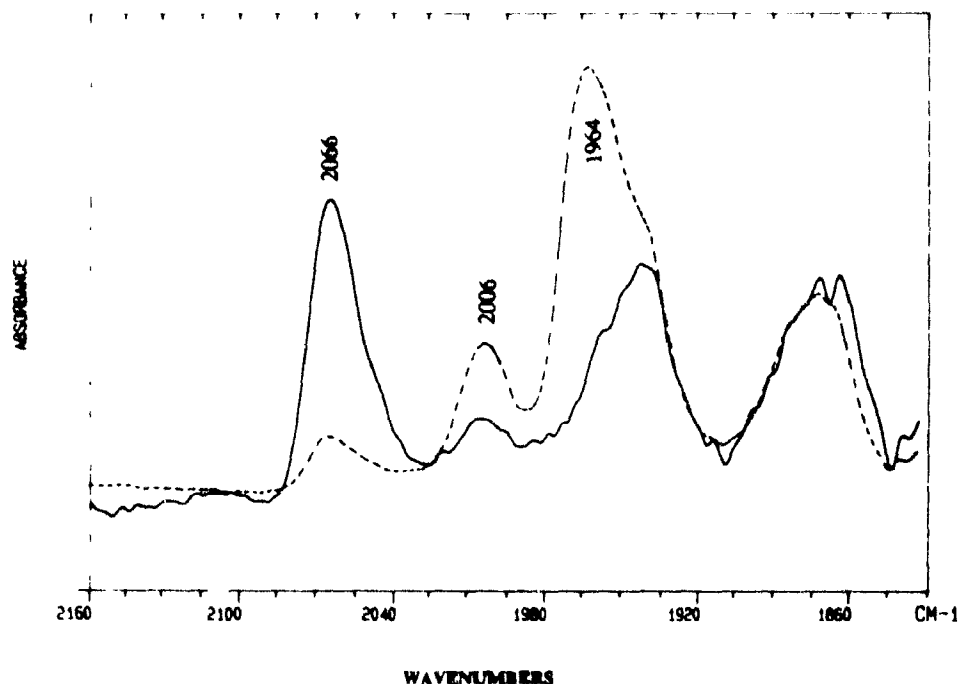


Figure 4-6 The IR (---) and ATR-IR (—) spectra in the $\nu(CO)$ region of Ir/PS upon treatment with I_2 for 3 h.

4.4 Conclusions

The IR peak positions in the $\nu(\text{CO})$ region of Vaska's complex and its adducts in PS matrices are close to those found in benzene. The complexes are apparently embedded in PS such that they are highly dispersed and the environment surrounding them is similar to that in solution. Addition and substitution reactions of the complexes with gaseous reagents, as well as the reverse reactions, are easily performed in PS films. This demonstrates that polymers are useful media for "solid-state" syntheses. ATR-IR and IR studies suggest that the PS matrix may modify the relative rates of reactions by hindering the diffusion of large gaseous molecules in the plastic. This observation provides an extra element of selectivity not possible with normal solvents. These types of materials are potentially useful in gas separation, as gas sensors and indicators of gas permeability since they are easily prepared and the reactions can be monitored by IR spectroscopy.

PART II.
THE PREPARATION AND CHARACTERIZATION OF AN
ELECTRICALLY CONDUCTING POLY(3-ALKYLTHIOPHENE)-
IRON(II) COMPLEX

CHAPTER 5. General Introduction

5.1 Conducting Polymers

The term "polymer" has long been associated with compounds having insulating properties. The low conductivities (σ) of polymers range from $10^{10} \Omega^{-1} \text{ cm}^{-1}$ for polyvinylchloride to $10^{-18} \Omega^{-1} \text{ cm}^{-1}$ for polytetrafluoroethylene, these values are many orders of magnitude below those for metals and inorganic semiconductors [Scheme 5-1].^{81,82,83} The insulating properties result from electrons in the polymer framework being localized in individual bonding molecular orbitals and the large band gaps existing between the valence and conduction bands.

The idea of making semiconducting or even metal-like conducting polymers, whereby the electrical properties of metals and the advantages of plastics can be combined has been a stimulus for polymer science for more than 20 years.⁸⁴ The first conducting polymers were mostly refractory pyropolymers resembling graphites, such as heat-treated polyacrylonitrile (PAN) [Scheme 5-2].^{85,86} In the early 70's, single crystals of highly-conjugated inorganic poly(sulphur nitride) $-(S=N)_n$ were found to be metallic conductors⁸⁷ and even superconductors at very low temperature⁸⁸. The intrinsic conductivity arises from the

81. Bowden, M.J.(ed.); Turner, S.R.(ed.) *Electronic and Photonic Applications of Polymers* American Chemical Society: Washington, D C., **1988**.

82. Potember, R.S.; Hoffman, R.C., Hu, H.S.; Cocchiaro, J E , Viands, C A., Murphy, R.A.; Poehler, T.O. *Polymer* **1987**, *28*, 574.

83. Bryce, M.R , *Chem. Br.* **1988**, 781.

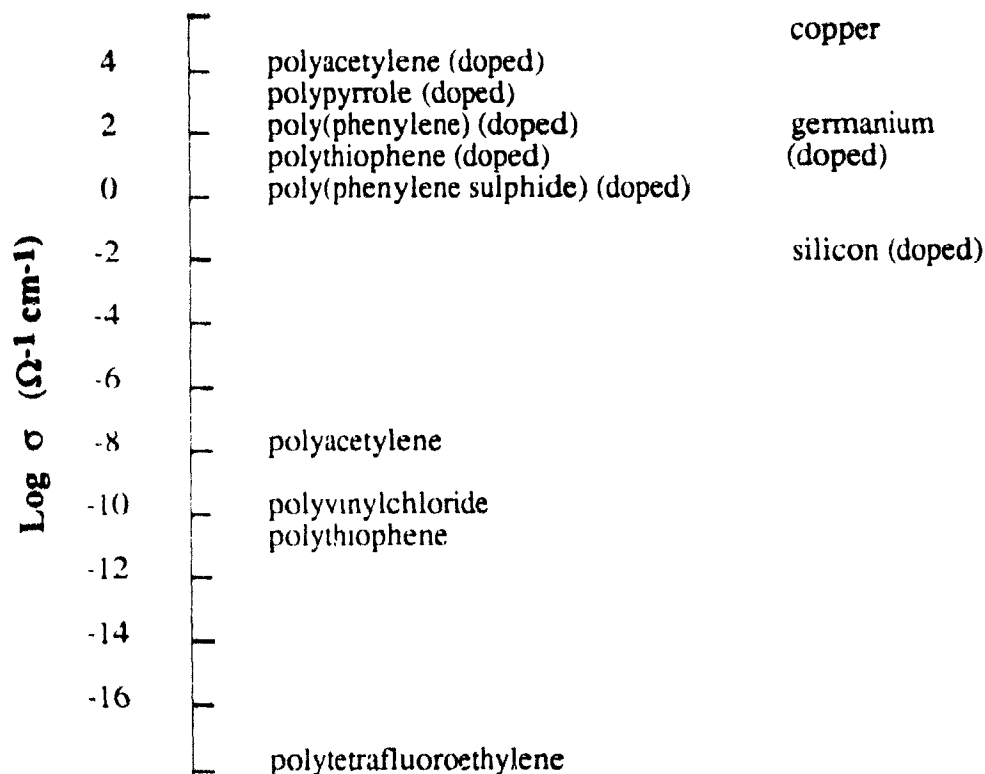
84. Goodings, E P. *Chem Soc Rev.* **1976**, *5*, 95.

85. Topchiev, A.V. *J Polym Sci. Part A* **1963**, *1*, 591.

86. Suzuki, M.; Takahashi, K , Mitani, S. *Japan. J. Appl. Phys.* **1975**, *14*, 741.

87. Hsu, C.H.; Labes, M M. *J. Chim. Phys.* **1974**, *61*, 4640.

88. Greene, R.L.; Street, G.B.; Suter, L.J *Phys Rev Letters* **1975**, *34*, 577.



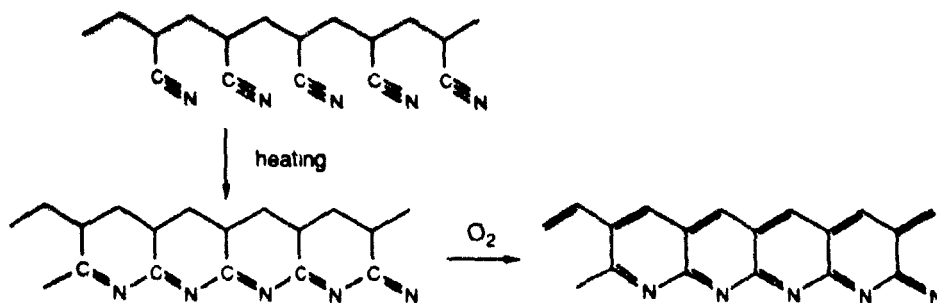
Scheme 5-1

presence of one unpaired electron associated with each sulfur-nitrogen unit which can move under the effect of an applied electric field.⁸⁹ It was also found that introduction of mixed valence states into polymer chains, such as polypyridine containing pendent osmium(II/III) groups,⁹⁰ can induce semiconductivity through redox behaviour. While the ferrocene(Fe^{II}) polymer is practically an insulator, the mixed-valence ferrocene-ferricinium($\text{Fe}^{\text{II}}/\text{Fe}^{\text{III}}$) polymer has a conductivity of 10^{-6} - $10^{-3} \Omega^{-1} \text{ cm}^{-1}$ upon partial oxidation [Scheme 5-3].⁹¹ Polymeric stacked, planar metal complexes, such as $[\text{Pt}(\text{CN})_4]^{2-}$, can also be partially

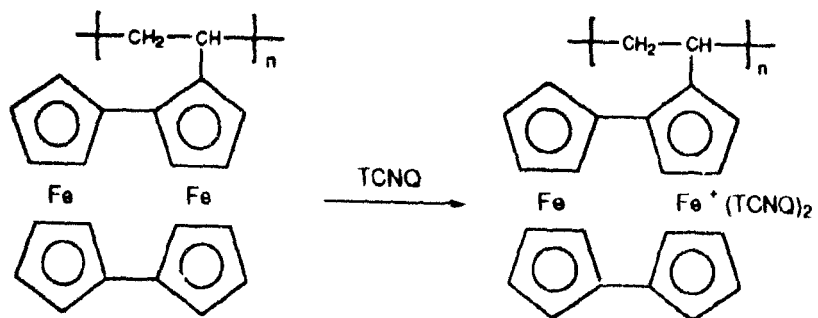
89. Greene, R.L. Street, G B. *Science* **1984**, *226*, 651.

90. Jernigan, J.C.; Murray, R.W. *J. Phys. Chem.* **1987**, *91*, 2030.

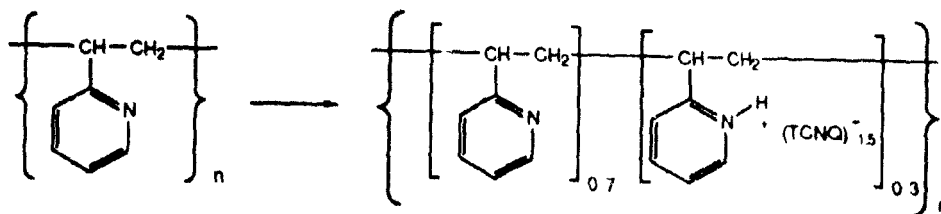
91. Pittman, C.U.Jr.; Suryanarayanan, B. *J. Am. Chem. Soc.* **1974**, *96*, 7916.



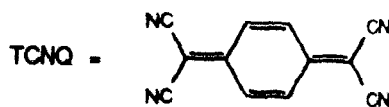
Scheme 5-2



Scheme 5-3



Scheme 5-4



oxidized to give one dimensional, mixed-valence type crystals with high conductivity along its stacking directions.⁹² Some highly-crystalline, charge-transfer (CT) complexes and ion radical salts are known to be anisotropic organic conductors.^{83,89,93} Several of them have been incorporated into polymer chains, e.g., the TCNQ-poly(2-vinylpyridine) complex ($\sigma = 1.2 \times 10^{-2} \Omega^{-1} \text{cm}^{-1}$) [Scheme 5-4].⁹⁴ Although the conductivities are sometimes lower than those of the monomeric complexes, the rigid stacks are plasticized by the flexible, σ -bonded polymer backbone

Conducting polymers, however, became an extremely active area about 10 years ago.^{95,96} when MacDiarmid, Heeger and coworkers discovered that polyacetylene $-(\text{CH}=\text{CH})_n$ becomes highly conductive upon oxidation or reduction. Since then, many chemists, physicists and material scientists have been attempting to synthesize new types of conducting polymers and to develop theories to explain the conduction mechanisms. A few conferences have been held on this specific topic, there are also several books and a vast number of papers.^{81,97,98}

Considerable effort has been made in search of new types of conducting polymers following the development of a number of conjugated organic polymer systems which exhibit similar electrical properties. Several approaches have been developed to synthesize stable, processible, and highly conducting polymers. More than ten different types of

92. Schultz, A. J.; Williams, J. M., Brown, R. K. in ref.1(c), p313.

93. Ferraris, J. *J. Am. Chem. Soc.* **1973**, *95*, 948.

94. Goodings, E. P. *Discuss. Faraday Soc.* **1971**, *51*, 157.

95. Shirakawa, H., Louis, E.J.; MacDiarmid, A.G.; Chiang, C.K.; Heeger, A.J. *J. Chem. Soc. Chem. Commun.* **1977**, 578.

96. Chiang, C.K.; Druy, M.A., Gau, S.C., Heeger, A.J.; Louis, E.J.; MacDiarmid, A.G.; Park, Y. W., Shirakawa, H. *J. Am. Chem. Soc.* **1978**, *100*, 1013.

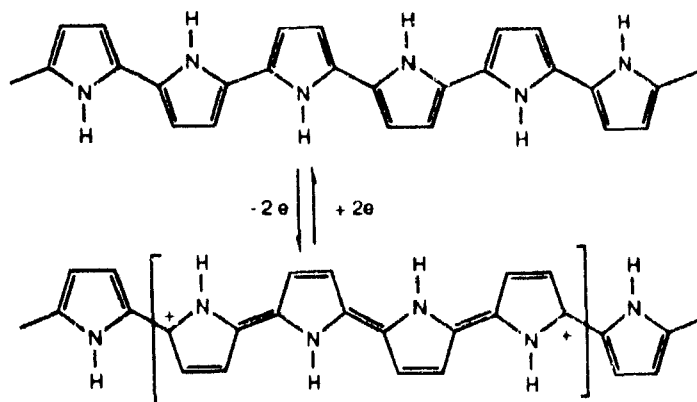
97. Skotheim, T.A. (ed.) *Handbook of Conducting Polymers* Vol. 1 and 2, Marcel Dekker, New York, **1986**.

98. Kuzmany, H., Mehring, M.; Roth, S. (eds) *Electronic Properties of Conjugated Polymers* Springer Ser. Solid-State Sci. 76, New York, **1987**.

conjugated polymers have been shown to be conducting [Scheme 5-1]. Among them, polypyrrole (PP), polythiophene (PT), poly(*p*-phenylene) (PPP), poly(*p*-phenylene sulphide) (PPS), and their copolymers have received a great deal of attention.

Polyacetylene is still considered the prototype for conducting polymers and is the most extensively studied. Recently, a stable, copperlike conducting polyacetylene has been synthesized by BASF scientists with a conductivity of $1.5 \times 10^5 \Omega^{-1} \text{ cm}^{-1}$, a significant improvement compared to the value of $200 \Omega^{-1} \text{ cm}^{-1}$ for the first iodine-doped polyacetylene 10 years ago. This new type of $-(\text{CH})_n$ polymer has fewer $-\text{CH}_2-$ defects and a much higher degree of order than those made previously.

The first conducting polyheterocycle, **polypyrrole**, dates back 20 years, when a black powder called "pyrrole black" with a conductivity of $8 \Omega^{-1} \text{ cm}^{-1}$ was made by Dall'Olio and coworkers by the oxidation of pyrrole in sulfuric acid.⁹⁹ Ten years later, this work was considerably extended by Street and his colleagues, who made films of the polymer in a one-step electrochemical polymerization.¹⁰⁰ The films can be cycled electrochemically between a conducting (doped) state and an insulating (undoped) state [Scheme 5-5].



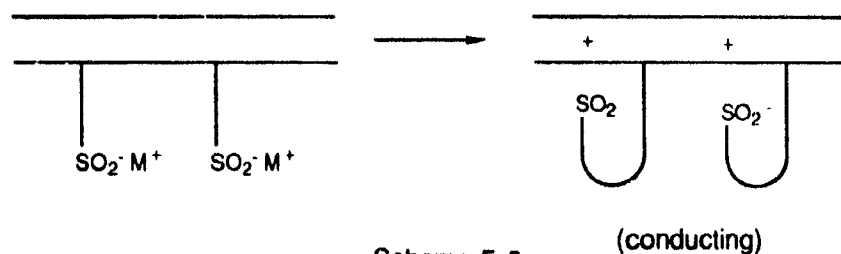
Scheme 5-5

99. Dall'Olio, A.; Dascola, Y.; Varacco, V.; Bocchi, C.R. *C. R. Seances Acad. Sci., Ser C* **1968**, 267, 43.

100. Kanazawa, K.K.; Diaz, A.F.; Geiss, R.H.; Gill, W.D.; Kwak, J.F.; Logan, J.A.; Rabolt, J.F.; Street, G.B. *J. Chem. Soc., Chem. Commun.* **1979**, 854.

Polythiophene and its derivatives afford another class of technologically important conducting polyheterocycles. They can be synthesized chemically^{101,102} or electrochemically^{103,104}. The most interesting aspect of this class of heterocyclic polymer is the case of 3-substitution. Several 3-substituted polymers have been prepared with high conductivities and stabilities.¹⁰³ Substitution renders them soluble in many organic solvents and sometimes even in water.

3-Alkyl sulfonate-substituted thiophene and N-alkyl sulfonate-substituted pyrrole polymers can form "self-doped" systems in which the counter anion is covalently bound to the conjugated polymer chain [Scheme 5-6].^{105,106} These types of polymer have generated considerable theoretical interest and have opened up new avenues of possible applications.



101. Adel, A.; Zimmer, H.; Mulligan, K.J.; Mark, H.B.Jr.; Pons, S.; McAleer, J.F. *J. polym. Sci. Polm. Lett. Ed.* **1984**, *22*, 77.

102. Jen, K.Y.; Miller, G.G.; Elsenbaumer, R.L. *J. Chem. Soc., Chem. Commun.* **1986**, 1346.

103. Hotta, S.; Rughooputh, S.D.D.V.; Heeger, A.J.; Wudl, F. *Macromolecules* **1987**, *20*, 212.

104. Roncali, J.; Garreau, R.; Yassar, A.; Marque, P.; Garnier, F.; Lemaire, M. *J. Phys. Chem.* **1987**, *91*, 6706.

105. Audebert, P.; Bidan, G.; Lapkowski, M.; Limosin, D. in ref.98, p366.

106. Reynolds, J. R. *CHEMTECH*, **1988**, July, 440.

Poly(*p*-phenylene) has been known for many years and can be synthesized in various ways, including reaction of benzene with $\text{AlCl}_3\text{-CuCl}_2$ ¹⁰⁷ or Grignard coupling of dihalobenzenes using nickel salts as catalysts.¹⁰⁸ The product is a non-melting, insoluble brown or yellow powder with high heat-resistance and electrical insulation. Very strong oxidizing or reducing agents (AsF_5 , K) are required to produce highly conducting materials ($50\text{-}500 \text{ } \Omega^{-1} \text{ cm}^{-1}$).¹⁰⁹ Lately, electropolymerization of benzene leading to the direct formation of conducting polymer films has been reported.¹¹⁰ The reactions take place in solvents such as HF, SO_2 and nitrobenzene, because benzene is oxidized at a very positive potential (+2.4 V vs. Ag/AgCl).

Poly(phenylene sulphide) is one of the commercial polymers that can be oxidized to form conducting species. Strong oxidizing agents such as AsF_5 are necessary to achieve highly conducting PPS. A stable conducting polymer solution with an AC conductivity of $2 \times 10^{-2} \text{ } \Omega^{-1} \text{ cm}^{-1}$ has been produced when a dispersion of PPS powder in liquid AsF_3 was exposed to gaseous AsF_5 vapour.¹⁰⁹ The solution conducts electricity both ionically and electronically, while films of the oxidized polymer have pure electronic conductivities.¹⁰⁶

The development of useful conducting polymers must confront special problems, such as low stability and poor processibility, which put limits on their potential application. Many efforts directed towards the synthesis of environmentally stable and tractable conducting polymers have been made recently. Techniques, such as encapsulation, the use of barrier resins, coating with sacrificial layers, and addition of antioxidants have been used to

107. Speight, J.G.; Kovacic, P.; Koch, F.W. *J. Macromol. Sci.* **1971**, C5, 298.

108. Yamamoto, T.; Yamamoto, A. *Chem. Lett.* **1977**, 353.

109. Frommer, J.E.; ElsenBaumer, R.L.; Chance, R.R. In *Polymers in Electronics* Davidson, T. (ed.), ACS Symposium Series 242, American Chemical Society: Washington, D. C., **1984**, 447.

110. Dietrich, M.; Mortensen, J.; Heinze, J. *J. Chem. Soc. Chem. Commun.* **1986**, 1131. and references therein.

stabilize conducting polymers.¹¹¹ For example, conducting polyacetylene shows much better stability when it is coated with poly(*p*-xylylene). Pure polyacetylene, which is very sensitive to O₂, can be stabilized by the addition of antioxidants, such as hindered amines (e.g., N-bromosuccinimide NBS) which act as free radical traps. A NBS-treated polyacetylene exhibits a higher conductivity than an untreated one after doping with I₂.

In term of tractability, several approaches have been explored.¹¹¹ Conducting-insulating polymer alloys, such as polypyrrole-polyvinylchloride¹¹² and polythiophene-polystyrene,¹¹³ have been prepared and examined. Some of them are highly conducting and flexible. Random, graft and block copolymerization of conjugated polymers with other flexible polymers can also improve the solubilities of intractable polymers. An acetylene-phenylacetylene (26%) random copolymer is soluble in CH₂Cl₂, while the conductivity is lower than that for homopolyacetylene.¹¹¹ The designed synthesis of soluble precursor polymers, which can be easily purified in solution and then go on to yield conducting polymers with the desired shape, could be an innovative and useful process. Polyacetylene¹¹¹, polyphenylene¹¹⁴, and several other poly(arylene vinylene) derivatives¹¹⁵, have been synthesized *via* soluble precursors. 3-Alkylthiophene polymers have been shown to be soluble in many solvents and are highly conducting after being doped.

111. Baker, G. L. in ref. 81, p271 and references therein.

112. Niwa, O.; Kakuchi, M.; Tamamura, T. *Macromolecules* **1987**, *20*, 749.

113. Hotta, S.; Rughooputh, S.D.D.V.; Heeger, A.J. *Synth. Met.* **1987**, *22*, 79.

114. Ballard, D.G.H.; Curtis, A.; Shirley, I.M.; Taylor, S.C. *J. Chem. Soc. Chem. Commun.* **1983**, 954.

115. Murase, I.; Ohnishi, T.; Noguchi, T.; Hirooka, M. *Polym. Commun.* **1984**, *25*, 327.

5.2 Conductivity Mechanisms of Solid Materials^{81,116}

Electrical conduction results from the flow of charged particles through a medium under the influence of an electric field. The conductivity σ is dependent on the number of charge carriers n (cm^{-3}), their charge e and their mobilities μ ($\text{cm}^2 \text{V}^{-1} \text{s}^{-1}$) [Eq.5-1]:

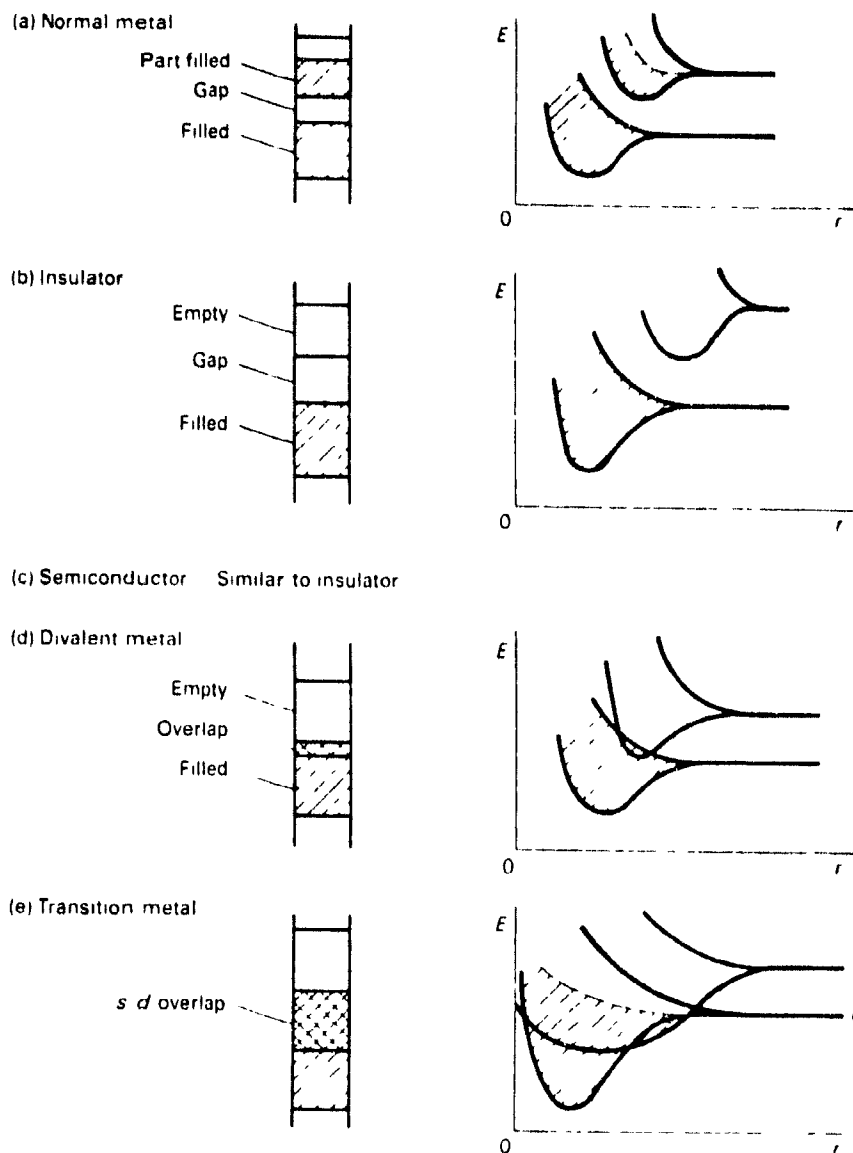
$$\sigma = ne\mu \quad \text{[Eq.5-1]}$$

Usually, in a solid, charge carriers may be electrons or ions, and conduction may therefore be electronic or ionic.

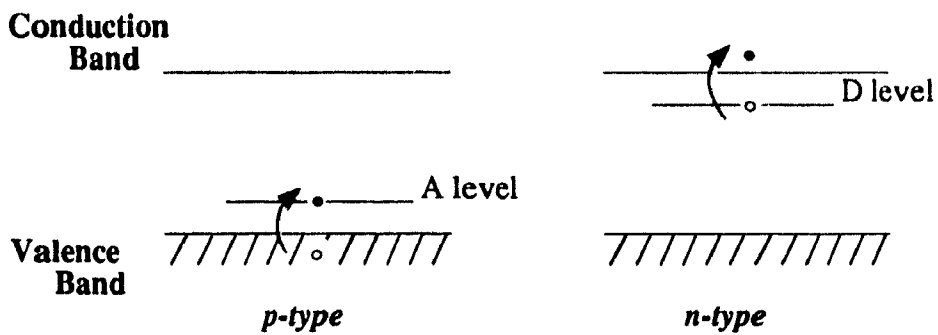
a. Electronic Conductivity

Band conduction. When a large number of atoms are brought together in a crystalline lattice, the valence atomic orbitals can overlap and mix to form bands. Electrons in such a band move essentially independently of the atomic nuclei. A partially or completely occupied band is called the valence band, while an empty band is called the conduction band. Only electrons in a partially-filled valence band or those promoted into a conduction band can conduct electricity. The energy gap separating the two bands is termed the band-gap, and its magnitude determines whether such a material is a metal, semiconductor or an insulator [Scheme 5-7].^{116(a)} The more orbitals that overlap, the wider the bands and thus the gap will be smaller which leads to higher electronic conductivity.

116. (a) Pollock, D. D. *Electrical Conduction in Solids: An Introduction* American Society For Metals, Ohio, 1985. (b) Bolter, H.; Bryskin, V. V. *Hopping Conduction in Solids* VCH Verlagsgesellschaft: Akademie-Verlag, Berlin, 1985. (c) Weller, P. F. (ed), *Solid State Chemistry and Physics* Vol. 1, Marcel Dekker, Inc. New York, 1973.



Scheme 5-7 (Adapted from ref.116(a).)



Scheme 5-8

In the case of **metals**, the valence bands are either only partially-filled [Scheme 5-7(a)] as for the monovalent metals Na and K, or they overlap with the empty conduction bands in energy [Scheme 5-7(d)] as observed for the divalent alkaline-earth metals. For transition metals, both conditions apply [Scheme 5-7(e)]. Thus for metals, there is no gap between the highest occupied and lowest unoccupied levels, and the electrons can readily move upon application of an electric field, giving rise to metallic conductivity.

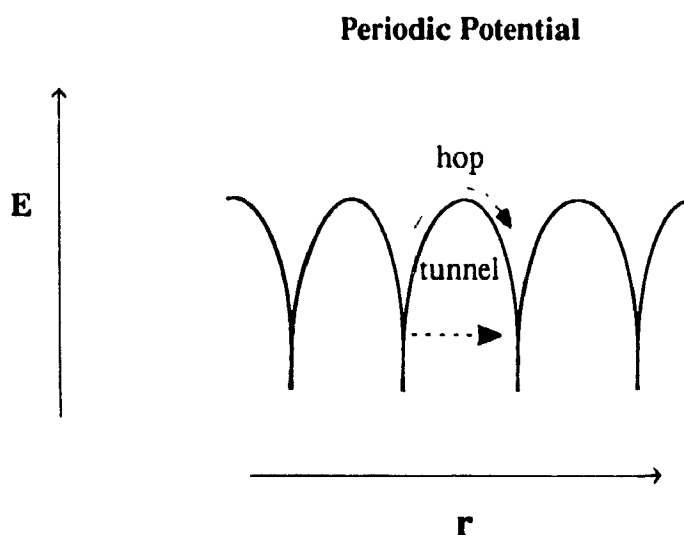
If a material has a full valence band and an empty conduction band separated by an energy gap, energy must be supplied (either thermal or photo) to cause some electrons to jump across the gap into the conduction band (promotion) in order to achieve conductivity. Solids, such as pure silicon and germanium, having energy gaps in the order of 1 eV, are called **intrinsic semiconductors** [Scheme 5-7(c)]. Ordinary energies are sufficient to excite electrons from the valence band to the conduction band. Both the electrons in the conduction band and the resulting holes (absence of electrons) in the previously filled valence band act as charge carriers in the conduction process. They move freely under an applied electric field.

The conductivity properties of semiconductors can be modified by the presence of impurities and such materials are called **extrinsic semiconductors**. For example, doping silicon with a small amount of boron (acceptor) or phosphorus (donor) produces *p*- or *n*-type semiconductors, respectively [Scheme 5-8]. The doping agents are of the appropriate size to fit into the silicon lattice. The boron atoms have only three valence electrons, one less than Si, thus leading to the occurrence of isolated empty energy levels just above the Si valence band. Electrons can be excited from the valence band into these levels, leaving the holes created in the valence band to act as positively charged carriers, ie, *p*-type semiconductors. On the other hand, the phosphorus atoms have one extra electron located in isolated energy levels just below the Si conduction band. These electrons are easily promoted to the conduction band to act as electronic carriers, ie, *n*-type. Such doping gives

rise to unpaired electrons, which can be detected by electron spin resonance (ESR) techniques.

Most organic compounds and polymers have very narrow bands and large energy gaps [Scheme 5-7(b)]. Normal energies cannot promote electrons in filled valence bands to the conduction band. Therefore, no electrical conduction is possible by electrons under these conditions and the materials are termed **insulators**.

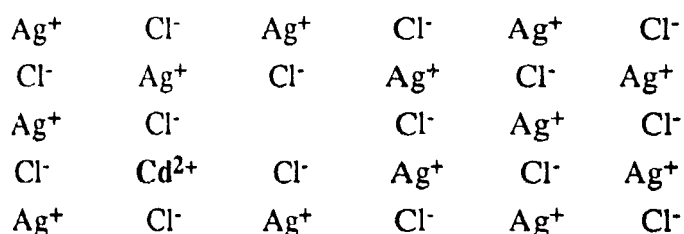
Hopping conduction. When the orbitals on neighboring sites do not overlap appreciably, the valence electrons are strongly affected by the atomic nucleus and become much more localized. In this case, electronic conduction may result from electron hopping. Electrons can hop between adjacent sites by either a thermally-activated jump over a barrier or a phonon-assisted tunnelling through the barrier [Scheme 5-9].^{116(b,c)} Hopping conduction is likely to occur in compounds having the metal in more than one oxidation state. For example, in the mixed-valence compound, $M_xV_2O_5$ ($M = Na, K$), the vanadium ion can be V^{4+} or V^{5+} and an electron can jump between them to produce an effective means of electron transport.



Scheme 5-9

b. Ionic Conductivity

In most ionic crystals, molecular crystals and polymeric solids, the valence electrons are tightly bound to their respective nuclei and there are large energy gaps between the valence and conduction bands. No measurable electronic conductivity occurs in such materials at room temperature. However, electrical conduction in ionic crystals can result from diffusion of ions in an applied electric field. This is called **ionic conduction**. Most crystalline solids contain lattice imperfections, such as vacancies or foreign atom substitutions of higher or lower charge. For example, cation vacancies in AgCl can be created by CdCl₂ doping [Scheme 5-10] ¹¹⁷ The presence of such imperfections could greatly increase the diffusion rate of ions through the lattice. Thus, the vacancies move in the direction opposite to those of the ions. Weakly-bound impurity ions present in molecular crystals and polymeric materials can also act as charge carriers. However, ions are generally about 10⁵ times as large as electrons and their ionic mobilities are therefore much lower. Thus, ionic conductivity is usually lower than electronic conduction. For most dielectric materials, ionic conductivity decays with time. That is, when these solids are subjected to constant voltages at intermediate temperatures, the DC current diminishes after a few seconds or a few minutes to a lower, steady-state value with a corresponding higher residual DC resistance R_T due to the removal of all of the readily available ionic carriers. ^{116(a)}



Scheme 5-10

(Adapted from ref.117.)

117. Butler, I. S.; Harrod, J. F. *Inorganic Chemistry: Principle and Applications* The Benjamin/Cummings Publishing Company, Inc. Redwood City, California, 1989.

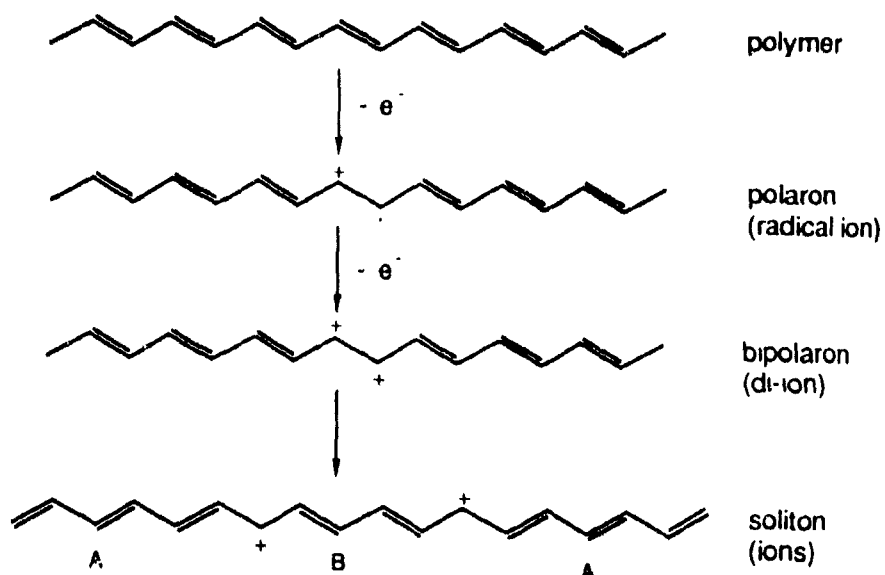
c. Conducting Polymers

The metallic behaviour of some polymers, such as graphite polymers and $-(S=N)-n$, arises from the overlapping of the valence and conduction bands or is due to the presence of a partially-filled valence band.^{84,117} The conductivity of the mixed-valence polymer $[Pt(CN)_4]$ (II/IV) occurs by the formation of a partially-filled valence band along the stacked direction.⁹² Electron hopping dominates the conductivity of ferrocene-ferricenium (II/III) polymers.⁸⁴ In the case of conjugated polymers doped with oxidizing or reducing agents, the origin of the conductivity is a source of controversy. Initially, the conductivity was explained by drawing an analogy with the doping of inorganic semiconductors such as silicon doped with B or P atoms. It was assumed that removing electrons from the valence band (oxidation) or adding electrons to the conduction band (reduction) led to conduction.⁸³ However, this was an oversimplification since the conductivity is far greater than that can be accounted for on the basis of free spin alone. To account for the phenomenon of spinless conductivity, physicists have introduced the concept of transport *via* structural defects in the polymer chain. It is believed that the situation is very different from the generation of charge carriers by doping as understood for inorganic semiconductors. Doping of polymers is more appropriately seen as a chemical modification. The dopant perturbs the polymer chain extensively, not only because of its large size, but also because of the extensive charge transfer taking place between the polymer chain and the dopant. This causes the polymer to become ionic and leads to changes in the geometry of the chain. The charge carriers are believed to be related to charge transfer-induced geometric modifications of the polymer chains. This leads to the formation of polarons, bipolarons or solitons, or in chemical terminology, radical ions, di-ions and ions.⁸¹

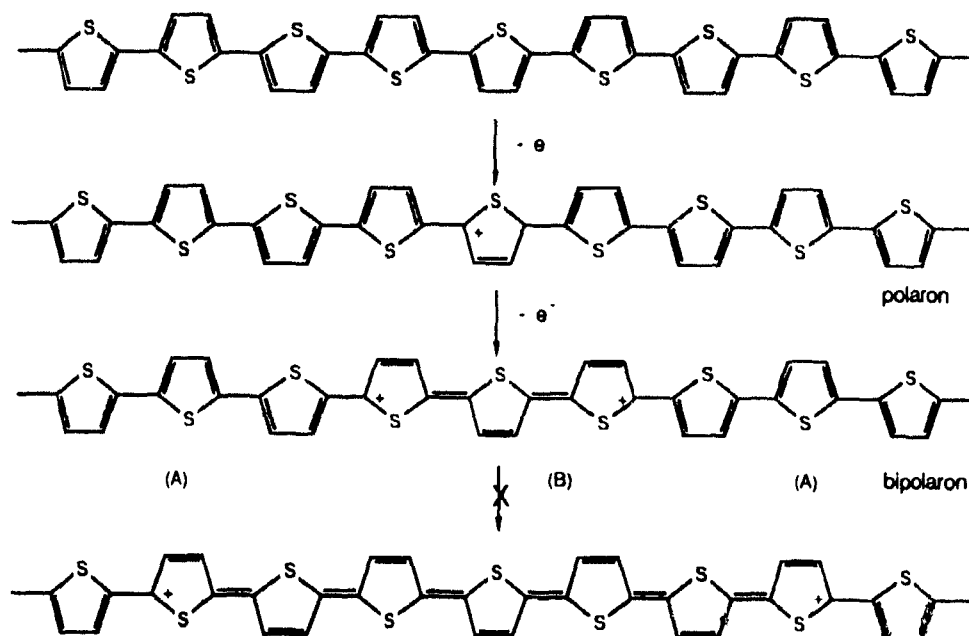
Conjugated polymers can be divided into two groups:⁸¹ those with degenerate ground states, such as *trans*-polyacetylene, and those with non-degenerate ground states, such as polythiophene and nearly all other conjugated polymers. The degenerate ground states of

trans-polyacetylene are related by the interchange of double and single bonds. The polymer can be oxidized by removal of an electron and the lattice distorts around the resulting positive charge on the polymer chain forming a polaron [Scheme 5-11]. Removal of a second electron from the same chain by further oxidation gives a bipolaron. It is energetically favorable for two polarons to form a spinless bipolaron through dimerization. Bipolarons can lower their energy further by dissociating into two isolated spinless solitons. This charge separation does not cost energy if the energy of the two polyene segments generated are the same ($A = B$). This effectively lowers the Coulombic repulsion between the two charges. However, most conducting polymers have nondegenerate ground states. For example, the thiophene units in phase A are aromatic and are lower in energy than the non-aromatic units in phase B [Scheme 5-12]. Thus, separating a bipolaron into two solitons would require additional energy since a polyene segment of higher energy would form.

The polaron-bipolaron model is a general model for conjugated conducting polymers. The presence of these excitations has been confirmed experimentally. For example, polaron, bipolaron and soliton absorptions in UV spectra have been observed. The precise mechanisms by which charges are transported in conducting polymers are still being disputed. Nevertheless, it does seem that these polarons, bipolarions or solitons act as the charge carriers and it is their movement under the influence of an applied electric field that causes electrical conductivity.



Scheme 5-11



Scheme 5-12

CHAPTER 6. Synthesis and Characterization of an Electrically Conducting Poly(3-alkylthiophene)-Iron(II) Complex.

6.1 Introduction

As discussed in Chapter 5, certain organic polymers such as polyacetylene, polypyrrole and polythiophene become electrically conductive when doped with strong oxidizing agents such as I_2 or H_2SO_4 , or with strong reducing agents such as sodium or potassium metal.^{102,118} However, most of the systems reported are unstable in the long term due to the reactive nature of the dopants. This has led to difficulties in processing these materials and in investigating their physical properties and internal structure. The technological promise of such materials has encouraged the development of additional doping techniques and reagents. Our interest in organometallic complexes embedded in polymers led us to consider them as possible dopants for polythiophene polymers. The ability of a complex to modify the electronic structure of a conjugated polymer should be a function of the metal, the organic ligands present and the mode of bonding to the polymer (for example σ or π). Hence, complexes might prove to be tunable probes to study the mechanisms of conduction in such materials. The work presented in this chapter is the preparation and characterization of a conductive 3-alkylthiophene copolymer-iron complex.

Thiophene can coordinate to transition metals *via* the S atom, but, relatively few such S-bonded complexes have been isolated.^{119,120} Recently, Goodrich and coworkers have

118. (a) Patil, A.O.; Heeger, A.J.; Wudl, F. *Chem. Rev.*, **1988**, 88, 183. (b) Kaner R.B.; MacDiarmid, A.G. *Scientific American*, **1988**, 258, 106. (c) Yamamoto, T.; Sanechika, K.; Yamamoto, A. *J. Polym. Sci., Polym. Lett. Ed.* **1980**, 18, 9. (d) Bocchi, V.; Gardini, G.P. *J. Chem. Soc. Chem. Commun.* **1986**, 148.

119. Angelici, R.J. *Acc. Chem. Res.* **1988**, 21, 394.

120. Guerchais, V.; Astruc, D. *J. Organomet. Chem.* **1986**, 316, 335.

prepared Fe-S bonded thiophene-iron complexes of the type $[\text{CpFe}(\text{CO})_2(\text{T})]\text{BF}_4$ (T = thiophene, dibenzothiophene) via displacement of isobutene from $[\text{CpFe}(\text{CO})_2(\text{H}_2\text{C}=\text{CMe}_2)]\text{BF}_4$ by thiophene and its derivatives.¹²¹ Since 3-substituted polythiophenes have shown high conductivity after being doped, a polythiophene-iron system was chosen for study. Electrochemical polymerization of thiophene^{103,104} is appropriate for the formation of conducting polymers on the surfaces of electrodes, which can become electrically insulating by reversing the potential. Soluble polymers with high molecular weight (40,000-50,000) can be synthesized in this way, but only a small amount of material can be obtained. Chemical polymerization^{101,102} is performed via magnesium induced coupling of 2,5-dihalothiophene in the presence of nickel salt promoters or by utilizing *n*-butyl lithium and copper(II) chloride induced coupling of 2,5-dihalothiophene. The resulting polymers are in their neutral form and require doping to become conducting. It is difficult to obtain high molecular weight, soluble polymers via chemical polymerization, but a large quantity of material can be obtained. The Grignard coupling method which proceeds under relatively mild conditions and usually gives the coupling product in high yield was employed in our work.^{122,123}

6.2 Experimental

3-bromothiophene(97%) was purchased from the Chemical Dynamics Co. and was used without further purification. *n*-Hexylmagnesium bromide (2.0 M solution in diethyl ether), 3-methylthiophene(99%), 2,2':5',2''-terthiophene(99%), Mg, NaBF_4 and Br_2 were obtained from Aldrich Chemical Co. I_2 and FeSO_4 were purchased from BDH. Dichloro[1,3-bis-

121. Goodrich, J.D.; Nickias, P.N.; Selegue, J.P. *Inorg. Chem.* **1987**, *26*, 3426.

122.(a) Kumada, M.; Tamao, K.; Sumitani, K. *Org. Synth.* **1978**, *58*, 127. (b) Pham, C.V.; Mark, H.B.Jr.; Zimmer, H. *Synth. Commun.*, **1986**, *16(6)*, 689.

123. Tamao, K.; Kodama, S.; Nakajima, I.; Kumada, M. *Tetrahedron.* **1982**, *38*, 3347.

(diphenylphosphino)propane]nickel(II)^{122(a)} ($\text{NiCl}_2(\text{dppp})$), $[\text{CpFe}(\text{CO})_2(\text{H}_2\text{C}=\text{CMe}_2)]\text{BF}_4$ ¹²⁴ and poly(*p*-phenylene)¹⁰⁸ were prepared according to the literature procedures. Dichloromethane (CH_2Cl_2 , Spectrograde) was distilled over P_2O_5 under N_2 . *n*-Butyl ether (*n*- Bu_2O), diethyl ether (Et_2O) and tetrahydrofuran (THF) were dried over KOH and distilled over sodium wire. Acetic acid and Spectrograde methanol (CH_3OH) were used as received.

3-Hexylthiophene.

n-Hexylmagnesium bromide (220 mL) was added *via* syringe to 3-bromothiophene (52.0 g, 0.31 mol) and $\text{NiCl}_2(\text{dppp})$ (1.0 g, 1.8 mmol) in Et_2O (500 mL) at 0°C . The reaction was then refluxed for 3 h, cooled in an ice bath, and cautiously hydrolyzed with 2N HCl. After extracting with Et_2O and drying with MgSO_4 , distillation gave 49.4 g (92.2% yield) of 3-hexylthiophene: b.p. $105^\circ\text{C}/35$ mmHg (Ref.122(b): $65^\circ\text{C}/0.45$ mmHg); $^1\text{H-NMR}$ (CDCl_3): 0.92-0.98 (m, 3H, $-\text{CH}_3$), 1.33-1.40 (m, 6H, $-(\text{CH}_2)_3-$), 1.66-1.74 (m, 2H, $\beta\text{-CH}_2-$), 2.68 (t, $J = 7.6$ Hz, 2H, $\alpha\text{-CH}_2-$), 6.95-7.02 (m, 2H, CH), 7.26-7.28 (m, 1H, CH).

2,5-Dibromo-3-hexylthiophene.

A solution of 3-hexylthiophene (49.4 g, 0.29 mol) in acetic acid (100 mL) was treated dropwise over 15 min with Br_2 (107.8 g, 0.67 mol, in 50 mL acetic acid) while cooling the reaction flask with an ice bath. After stirring a further 2 h, the product was poured onto ice, neutralized with sodium hydroxide and extracted with Et_2O . The extract was dried over MgSO_4 and fractionated to give 71.5 g (74.6% yield) of the product: b.p. $130\text{-}140^\circ\text{C}/0.3$ mmHg; $^1\text{H-NMR}$ (CDCl_3): 0.92-1.00 (m, 3H, $-\text{CH}_3$), 1.30-1.55 (m, 8H, $-(\text{CH}_2)_4-$), 2.35-2.60 (m, 2H, $\alpha\text{-CH}_2-$), 6.75 (s, 1H, CH).

124. Rosenblum, M.; Giering, W.P.; Samuels, S-B.; Fagan, P.J. *Inorg. Synth.* **1986**, *24*, 163.

2,5-Dibromo-3-methylthiophene.

A solution of 3-methylthiophene (24.8 g, 0.25 mol) in acetic acid (100 mL) was treated dropwise over 20 min with Br₂ (105.0 g, 0.66 mol, in 50 ml acetic acid) while cooling the reaction flask with an ice bath. After stirring a further 2 h, the product was poured onto ice, neutralized with sodium hydroxide and extracted with Et₂O. The extract was dried over MgSO₄ and fractionated to give 53.6 g (82.7.6% yield) of the product: b.p. 134-136°C/40 mmHg (Ref.125: 130-132°C/40 mmHg); ¹H-NMR (CDCl₃): 2.22 (s, 3H, -CH₃), 6.81 (s, 1H, CH).

3-Methyl-(3-hexylthiophene)copolymer, (COP).

Refluxing 2,5-dibromo-3-hexylthiophene (33.83 g, 0.10 mol), 2,5-dibromo-3-methylthiophene (26.55 g, 0.10 mol), magnesium (5.04 g, 0.20 mol) and *n*-Bu₂O (70mL) in THF (50mL) under N₂ for 3 h gave a homogeneous dark brown solution. After cooling to room temperature, NiCl₂(dppp) (0.57 g, 1.0 mmol) was added to the solution with vigorous stirring. The polymerization was performed for 1 h under reflux and the cooled mixture was then poured into CH₃OH (150 mL). The solid precipitate was washed repeatedly with hot MeOH and collected on a fritted-glass filter. Extraction of the copolymer with THF in a Soxhlet extractor for 2 days gave 10.0 g of the dark-red soluble copolymer. The THF insoluble fraction was 14.5 g. Total yield is 45.1%. ANAL. calcd for (C₁₅H₁₈S₂)₆(C₁₅H₁₈S₂Br₂): C, 63.16%; H, 6.36%; S, 22.48%; Br, 8.00%. found: C, 63.88%; H, 6.46%; S, 21.19%; Br, 7.94%. ¹H-NMR (CDCl₃): 0.90 (m, br, 3H, hexyl-CH₃), 1.34 (m, br, 6H, hexyl-(CH₂)₃-), 1.64 (m, br, 2H, hexyl-β-CH₂-), 2.22 (m, 1H, α-CH₃), 2.44 (m, 2H, α-CH₃), 2.56 (m, 0.5H, hexyl-α-CH₂-), 2.77 (m, 1.5H, hexyl-α-CH₂-), 6.94-6.98 (m, 2H, CH).

125. Meth-Cohn, O; Gronowitz, S. *Acta Chem. Scand.* 1966, 20, 1577.

Iodine-doping of COP.

Iodine doping was carried out at ambient temperature in a sealed glass jar containing pulverized iodine, in a similar manner to that described in Chapter 3. The disk was held 1 cm above the I₂ powder for a period of time and the uptake of dopant vapour was determined by the weight difference of the disk.

(η⁵-Cyclopentadienyl)dicarbonyl(3-methyl-(3-hexylthiophene)copolymer)iron(II) tetrafluoroborate, [CpFe(CO)₂-COP]BF₄.

The compounds [CpFe(CO)₂(H₂C=CMe₂)]BF₄ (0.20 g, 0.63 mmol) and 3-methyl-(3-hexylthiophene)copolymer (0.28 g, 2.1 mmol) were stirred vigorously in refluxing CH₂Cl₂ (12 mL) under N₂ for 80 min. The colour changed from dark-red to dark yellow-green. The reaction mixture was evaporated to a sticky residue and a solid was precipitated by adding CH₃OH; this solid was collected on a glass filter. The resulting solid was ground into a fine powder and washed with MeOH several times. It was further purified by dissolving the polymer in a small amount of CH₂Cl₂ under N₂ and precipitating it quickly by addition of MeOH. Drying the resulting solid *in vacuo* gave a brown-black powder (0.20 g). ¹H-NMR (CDCl₃): 0.96-1.67 (m, 11H, alkyl), 2.2-2.8 (m, 5H, alkyl), 5.0-5.5 (s, br, 0.6-1.0H, Cp), 6.7-7.1 (s, br, 2H, CH). IR (ν(CO)), as a film cast on the surface of a NaCl plate: 2065, 2021 cm⁻¹; (CH₂Cl₂): 2071, 2026 cm⁻¹.

(η⁵-Cyclopentadienyl)dicarbonyl(3-methylthiophene)iron(II) tetrafluoroborate, [CpFe(CO)₂(methylthiophene)]BF₄.

The compounds [CpFe(CO)₂(H₂C=CMe₂)]BF₄ (0.32 g, 1.0 mmol) and 3-methylthiophene (1.0 g, 10.2 mmol) were stirred in refluxing CH₂Cl₂ (20mL) under N₂ for 4 h. The colour changed from orange-yellow to red-purple. The reaction mixture was evaporated to a sticky solution. The solid was precipitated by adding Et₂O and collected on a glass filter. The resulting solid was purified by dissolving it in CH₂Cl₂ (5mL) and reprecipitating it by addition of Et₂O. Drying the solid *in vacuo* gave a gold-orange, microcrystalline product

(0.38g, 84.3% yield). $^1\text{H-NMR}$ (CDCl_3): 2.28 (s, 3H, CH_3), 5.49 (s, 5H, Cp), 7.07-7.12 (m, 2H, CH), 7.55-7.59 (m, 1H, CH); IR ($\nu(\text{CO})$), (solid state, ATR): 2069, 2016 cm^{-1} ; (CH_2Cl_2): 2072, 2031 cm^{-1} .

(η^5 -Cyclopentadienyl)dicarbonyl(2,2':5',2''-terthiophene)iron(II) tetrafluoroborate, $[\text{CpFe}(\text{CO})_2(\text{terthiophene})]\text{BF}_4$.

The compounds $[\text{CpFe}(\text{CO})_2(\text{H}_2\text{C}=\text{CMe}_2)]\text{BF}_4$ (0.10 g, 0.32 mmol) and 2,2':5',2''-terthiophene (0.10 g, 0.42 mmol) were stirred in refluxing CH_2Cl_2 (15mL) under N_2 for 4 h. The colour of the solution changed from orange-yellow to red-purple and a red precipitate formed. The solid was collected on a glass filter and washed with Et_2O and CH_2Cl_2 mixture solvent. Drying the solid *in vacuo* gave a red solid (93.6 mg, 57.2% yield). The resulting solid was purified by dissolving it in CH_3NO_2 and reprecipitating it by addition of ether. $^1\text{H-NMR}$ (CD_3NO_2): 5.48 (s, 1.5H, Cp), 5.52 (s, 3H, Cp), 5.57 (s, 2H, Cp), 7.16-7.75 (m, 8H, CH); IR($\nu(\text{CO})$), (solid state, ATR): 2073, 2065, 2031, 2017 cm^{-1} ; (CH_3NO_2): 2073, 2031 cm^{-1} .

Other Systems.

COP and $[\text{CpFe}(\text{CO})_2(3\text{-methylthiophene})]\text{BF}_4$ mixture.

The polymer COP (104.0 mg) was dissolved in CH_2Cl_2 (15mL) under N_2 and $[\text{CpFe}(\text{CO})_2(3\text{-methylthiophene})]\text{BF}_4$ (34.0 mg) was added. The resulting solution was stirred under N_2 for 1 min at room temperature. The solution was frozen with liquid- N_2 and freeze dried under vacuum overnight to give a powder which was then pressed into a disk.

COP- NaBF_4 , COP- FeSO_4 .

COP (104.1 mg) and NaBF_4 (105.8 mg) were stirred in refluxing CH_2Cl_2 under N_2 for about 1 h (or THF for 30 min). The salts were not very soluble in the solvents. The refluxed slurry was evaporated to dryness and pumped on overnight. The same procedure was

carried out using COP (138.9 mg) and $\text{FeSO}_4 \cdot 7\text{H}_2\text{O}$ (156.2 mg). The resulting materials were pressed into disks.

PS-[CpFe(CO)₂(H₂C=CMe₂)]BF₄, PPP-[CpFe(CO)₂(H₂C=CMe₂)]BF₄.

PS (224.5 mg) and $[\text{CpFe}(\text{CO})_2(\text{H}_2\text{C}=\text{CMe}_2)]\text{BF}_4$ (112.4 mg) were stirred in refluxing CH_2Cl_2 under N_2 for 80 min. The colour of solution changed from orange-yellow to red-purple. After cooling, the solution was evaporated and dried *in vacuo*. The same procedure was carried out using PPP (102.4 mg) and $[\text{CpFe}(\text{CO})_2(\text{H}_2\text{C}=\text{CMe}_2)]\text{BF}_4$ (74.9 mg). The conductivity was measured before and after washing by CH_3OH .

Spectroscopic Measurements.

FT-IR absorption spectra were recorded on a Bomem Michelson 100 spectrometer (see Chapter 2). The solution spectra were obtained using a NaCl liquid cell and were ratioed against neat solvents. Solid state spectra were obtained by casting CH_2Cl_2 solutions on NaCl surfaces or by the ATR technique.

The low temperature (-60°C) macro-Raman spectrum of the I_2 -doped COP was recorded on an Instruments S A. spectrometer equipped with a Jobin-Yvon U-1000 monochromator and using the 514.4nm line of an Argon laser to excite the sample (50 mW power). The sample was sealed in a capillary tube, which was mounted on the cold finger of a Cryostat using indium foil as the conducting junction. Low temperature was obtained with the aid of a Cryodyne Model 21 Cryocooler (Cryogenics Technology, Inc.) and a silicon-diode temperature sensor attached to a Cryophysics Model 4025 controller.

The proton NMR spectra were recorded on either a Varian XL-200 or XL-300 NMR spectrometer at room temperature. The data were reported in δ units (ppm) using the following abbreviations: s-singlet, t-triplet, m-multiplet and br-broad. The solvents were stored over molecular sieves before use.

UV-VIS spectra were measured on a UV-VIS instrument with a Hewlett-Packard 8451 diode array spectrophotometer equipped with a Lauda RM6 thermostat. The solution spectra

were obtained with the use of a rectangular quartz cell and were ratioed against neat solvents. Solid-state spectra were obtained by casting CH_2Cl_2 solutions on to the surface of the quartz cell.

Conductivity Measurements.

The disks (13 mm in diameter) were prepared by placing fine powder in an IR-die and pressing it in a Riic C-30 hydraulic press at 7616 kgs/cm^2 pressure at room temperature for 3-4 min. The DC conductivities of samples pressed into thin disks were measured via a standard, in-line four-probe¹²⁶ apparatus [Fig.6-1] using a Harrison 6516A DC power supply and Keithley 169 multimeters. The distance between the nearest probes (S_p) was 1.6 mm. The four probes were centered on the surface of the disks. The equipment was kept in a plastic glove bag filled with N_2 gas during the time of measurement. The measured values (voltage(V) and current(I)) were converted into the appropriate conductivity values σ ($\Omega^{-1} \text{ cm}^{-1}$) according to Eq.6-1 when $S_p / T \gg 0.2$.¹²⁶ The thickness of disk T was measured with a digital caliper (*Ultra Cal*) ($T \sim 0.3 \text{ mm}$, $\Delta T \sim \pm 0.01 \text{ mm}$).

$$\sigma = \frac{\ln 2}{\frac{V}{I} \pi \cdot T} \quad [\text{Eq.6-1}]$$

By our apparatus, the lowest current which can be recorded properly was around $1 \mu\text{A}$ and the highest voltage across the two center probes was less than 10 V. Therefore, the lowest σ which can be measured is of the order of $10^{-6} (\Omega^{-1} \text{ cm}^{-1})$. For $\sigma > 10^{-4} \Omega^{-1} \text{ cm}^{-1}$, current (I) was kept around 0.1 mA when the data were taken. $\Delta I / I$ and $\Delta V / V$ are $< 10\%$, $\Delta \sigma / \sigma$ is approximately 20%.

126. (a) Wolf, H.F. *Semiconductors*, Wiley-Interscience, Toronto, 1971, Chapter 7, p497.

(b) Uhlir, A.Jr. *BSTJ*, 1955, 34, 105.

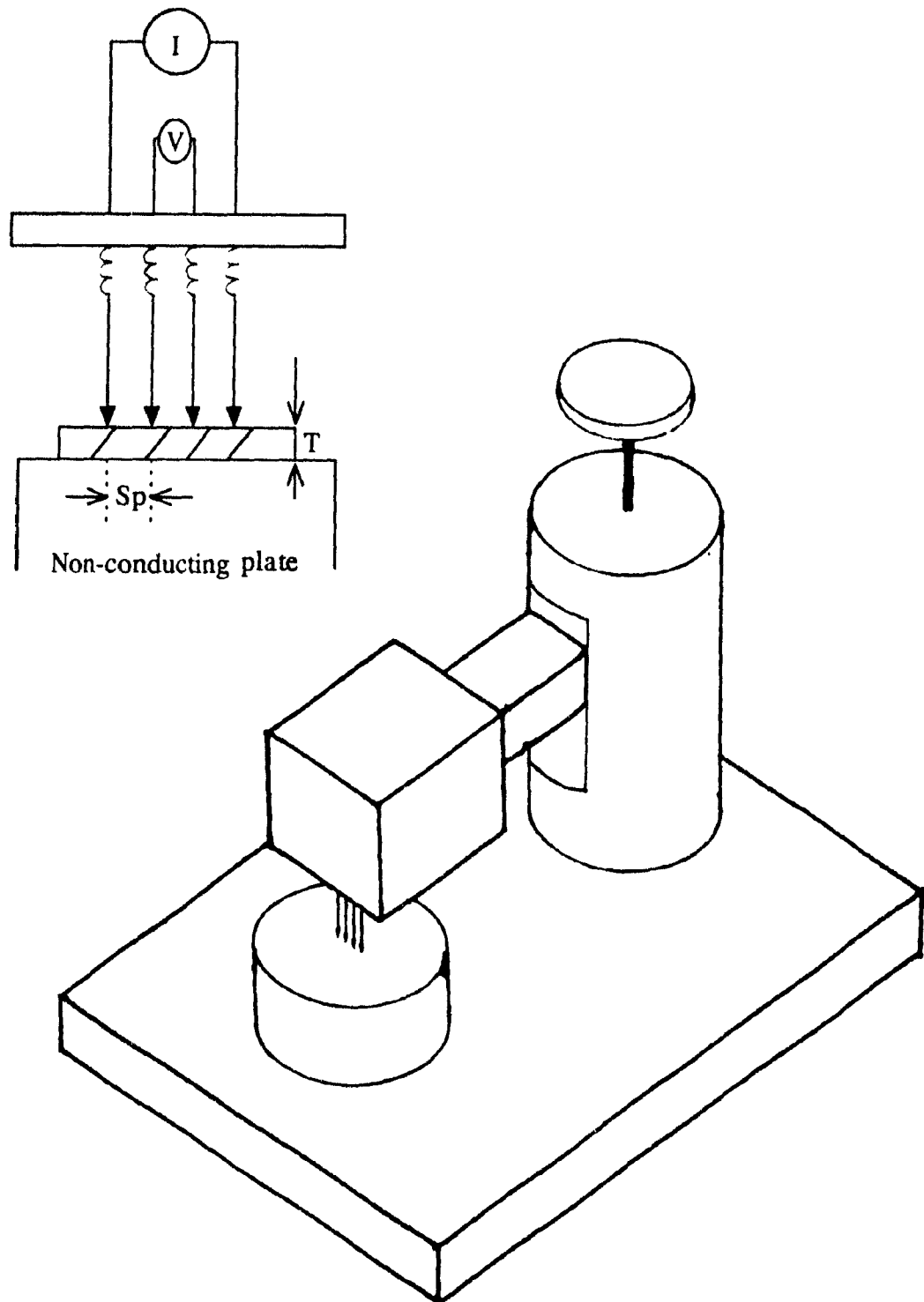


Figure 6-1 Scheme diagram of the in-line four-probe conductivity measurement apparatus.

6.3 Results

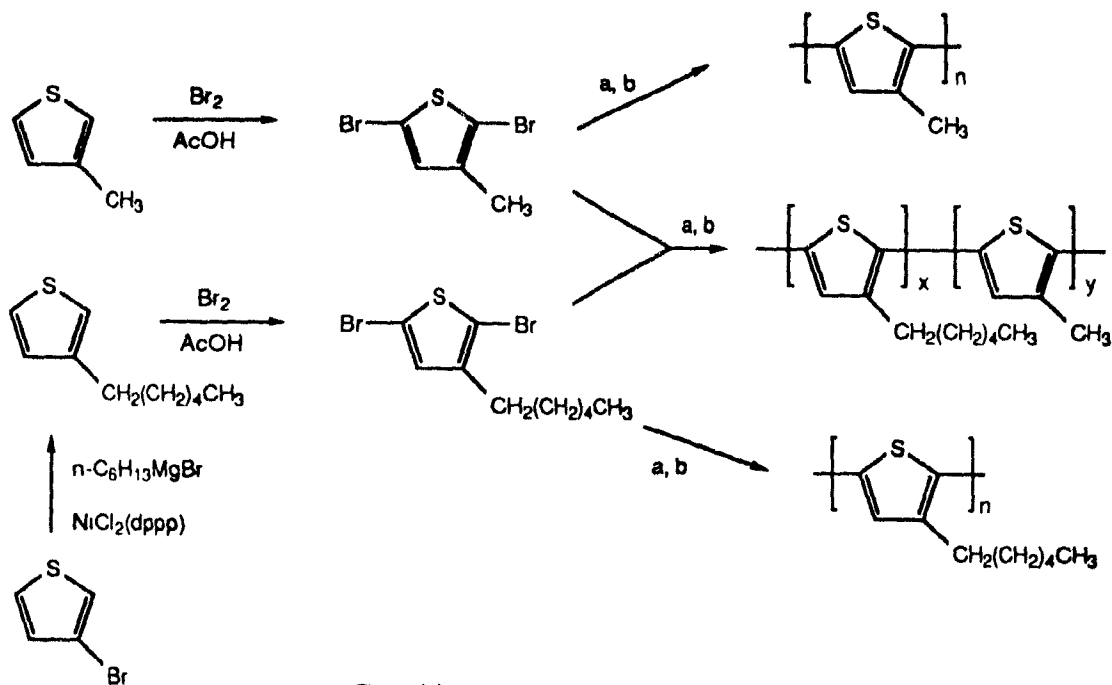
a. Preparation of 3-Alkylthiophene Polymers

Scheme 6-1 shows the synthetic route to the 3-alkylthiophene polymers. Alkylation of 3-bromothiophene with the Grignard reagent *n*-hexylmagnesium bromide in the presence of $\text{NiCl}_2(\text{dppp})$ in anhydrous Et_2O gave 3-hexylthiophene at 92.2% yield. Further treatment of 3-hexylthiophene with Br_2 in acetic acid gave 2,5-dibromo-3-hexylthiophene, which was purified by vacuum distillation. The copolymer 3-methyl-(3-hexylthiophene) (COP) was prepared by a $\text{NiCl}_2(\text{dppp})$ -catalyzed Grignard coupling of 2,5-dibromo-3-methylthiophene and 2,5-dibromo-3-hexylthiophene in a 1:1 mole ratio following a procedure similar to that reported for the synthesis of polythiophene.^{118(c)} The polymerization was performed in a mixture of THF and *n*- Bu_2O under N_2 in order to achieve a high yield.¹²⁷ The black solid obtained was washed repeatedly with hot MeOH. Soxhlet extraction of the solid with THF gave a soluble fraction with a molecular weight around 2000 (i.e., 14 rings) on the basis of elemental analysis of the residual bromo-terminal groups.¹²⁸ The material was dark red in the solid state and could be cast into a film or pressed into a disk. It was soluble at room temperature in common organic solvents such as THF, CHCl_3 and CH_2Cl_2 . In our hands, the polymer poly(3-methylthiophene) was too insoluble in those common solvents and poly(3-hexylthiophene) was too soft and rubbery to carry out the desired experiments.

The $^1\text{H-NMR}$ spectrum of the 3-methyl-(3-hexylthiophene) copolymer in CDCl_3 is shown in figure 6-2. The protons of $\alpha\text{-CH}_2$ (at 2.22 and 2.44 ppm) and hexyl- $\alpha\text{-CH}_2$ (at 2.56 and 2.77 ppm) each appears to resonate as two sets. Integration shows that one predominates

127. Yamamoto, T.; Sanechika, K.; Yamamoto, A. *Chem. Lett.* **1981**, 1079.

128. Amer, A.; Zimmer, H.; Mulligan, K.J.; Mark, H.B.Jr.; Pons, S.; McAleer, J.F. *J. Polym. Lett. Ed.*, **1984**, *22*, 77.



Conditions:

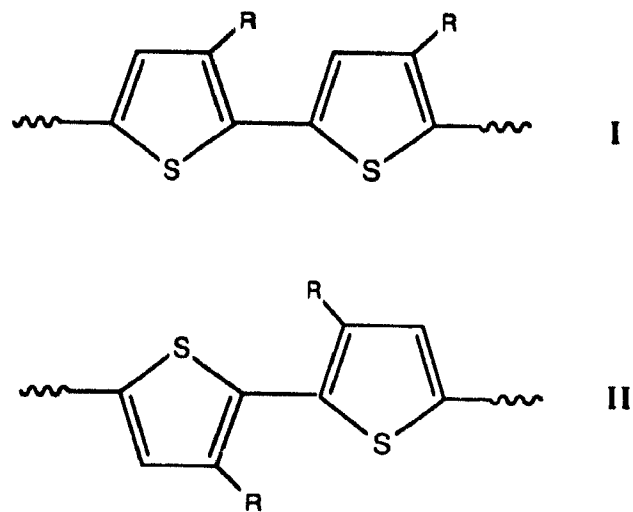
a, Mg, n-Bu₂O-THF

b, NiCl₂(dppp)

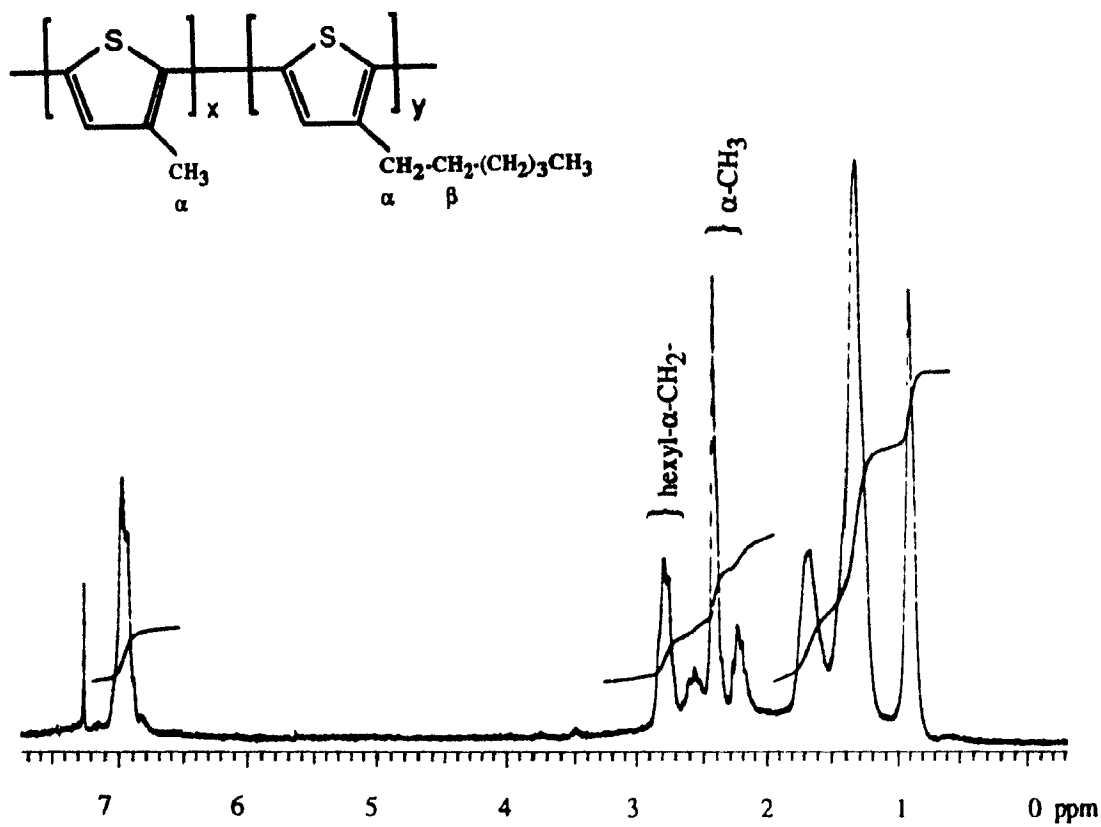
dppp = Ph₂PCH₂CH₂CH₂PPh₂

Scheme 6-1

over the other. A plausible explanation of the ¹H-NMR spectrum is the presence of a mixture of head to tail and head to head forms, I and II [Scheme 6-2]. One would assume that the probability of symmetrical coupling of the thiophene ring (II) is lower than the probability of unsymmetrical coupling (I).¹²⁸ The ratio of integration of α-CH₃ and hexyl-α-CH₂- is 3:2, which indicates that COP has a 1:1 ratio of methyl- and hexyl-thiophene in its chain.



Scheme 6-2

Figure 6-2 ¹H-NMR spectrum of 3-methyl-(3-hexylthiophene) copolymer in CDCl₃.

The IR spectrum of COP has a strong band at 800 cm^{-1} which is due to the characteristic out-of-plane C-H deformation mode of the thiophene ring;¹⁰⁸ it also shows bands at 1420 and 1490 cm^{-1} which are caused by the ring stretching vibration of 2,5-substituted thiophene [Fig.6-3].

The UV-VIS absorption spectra of COP in CH_2Cl_2 and COP cast on a quartz surface are compared in Fig 6-4. The absorption peak (λ_{max}) of the $\pi\text{-}\pi^*$ transition is shifted from 470 nm for the cast film to 450 nm for that in solution, analogous to what is observed in other 3-substituted polythiophenes.¹⁰³ This blue-shift is believed to be brought about by localization of the molecular orbitals as a result of the disorder introduced by a more random conformation of the macromolecules in solution.¹²⁹ Casting into solid films restores a more ordered backbone with an associated delocalization of the molecular orbitals. This observation implies that the solid copolymers assume a higher degree of order with longer average conjugation lengths.¹²⁹

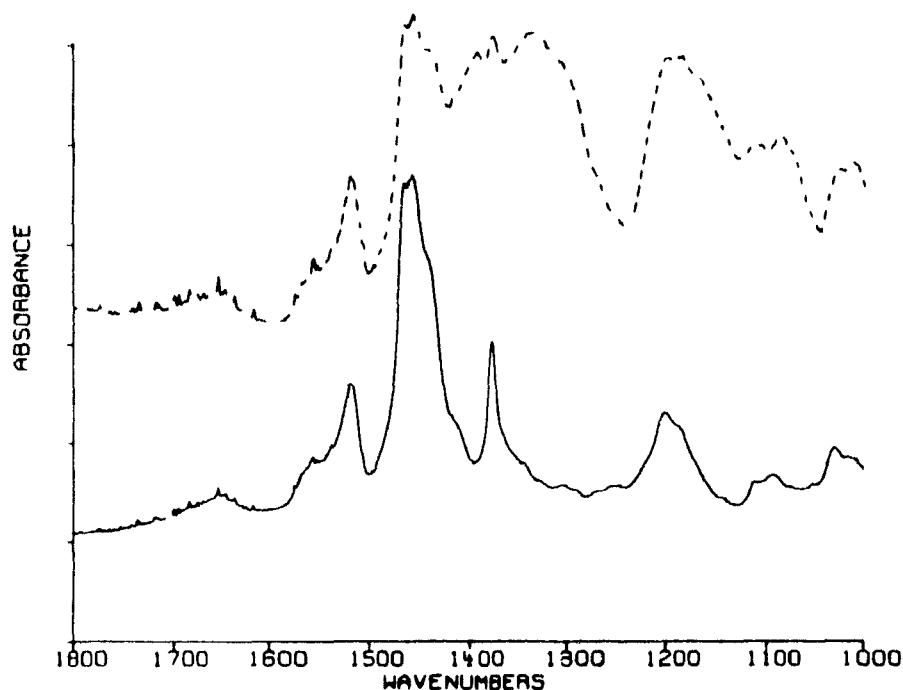


Figure 6-3 IR spectra of (—) COP and (---) I_2 -oxidized COP.

129. Hotta, S.; Rughooputh, S.D.D.V.; Heeger, A.J. *Synth. Met.* **1987**, *22*, 79.

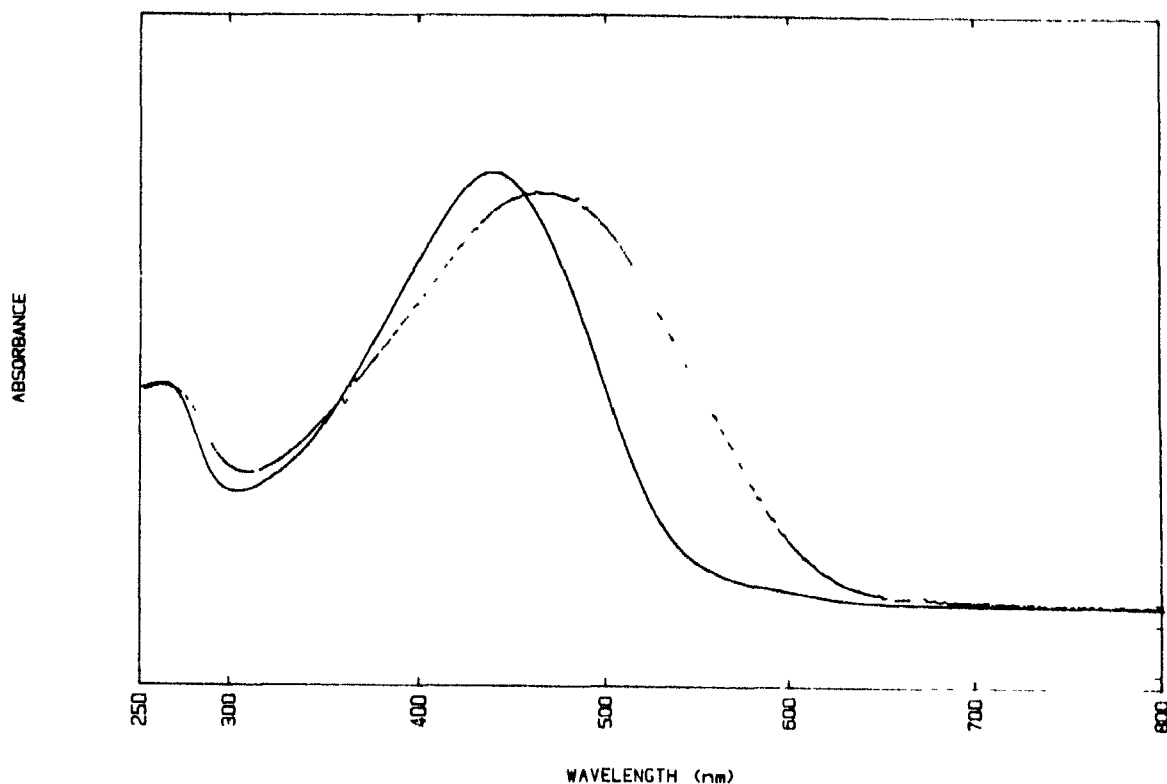


Figure 6-4 UV-VIS absorption spectra of (—) COP in CH₂Cl₂ and (...) cast on a quartz surface.

b. I₂-Doping

COP powder was pressed into a thin disk at room temperature. The sample exhibited insulating properties since the instrumentation available to us was not sensitive to conductivity values below $10^{-6} \Omega^{-1} \text{ cm}^{-1}$. Poly(2,5-thiophene) prepared in this way is reported to have conductivity values in the range 10^{-10} - $10^{-11} \Omega^{-1} \text{ cm}^{-1}$.¹²⁷

Polythiophene polymers have a high affinity towards iodine¹³⁰. When the disk or film of this copolymer was exposed to I₂ vapour, it absorbed iodine and oxidation reactions took place¹³⁰ [Eq.6-2]. At the same time, the oxidation (about 1 day in I₂ vapour) resulted in a

130. Kim, D.-U.; Reiss, H. *J. Phys. Chem.* **1985**, *89*, 2728.



characteristic increase in electrical conductivity and the weight % of the disk increased as much as 200. The absorption of I_2 was reversible. When the doped-COP was kept in air, the conductivity first increased steadily and reached a maximum value of around $5\text{-}10 \text{ } \Omega^{-1} \text{ cm}^{-1}$ (after 1-3 days), with the weight % decreasing to 50-80 %. The conductivity then fell gradually, accompanied by a further loss of iodine. On the other hand, under constant DC conditions, the current decreased rapidly at the beginning and reached a relatively constant value after a few min. The remaining residual current was relatively constant, but still gradually decreased under DC conditions.

The low-temperature (-65°C) Raman spectrum of I_2 -doped COP gave a I_3^- peak around 110 cm^{-1} and a I_2 band at 170 cm^{-1} , consistent with those reported.¹³¹ The latter peak disappeared upon prolonged scanning probably due to sublimation of I_2 from the matrix. The IR spectrum of I_2 -doped COP [Fig.6-3] showed strong new peaks around $1000\text{-}1400 \text{ cm}^{-1}$, similar to those reported by Cao¹³² and Hayes¹³³. These authors measured the IR spectra of I_2 -doped and electrochemically-doped polythiophenes and found four intense vibrational new peaks in the $1000\text{-}1400 \text{ cm}^{-1}$ region. The bands appearing in this region are mainly due to C-C, C=C and C-S ring stretching vibrations and have been attributed to the presence of the charged polythiophene chains, or the so-called charged polarons.

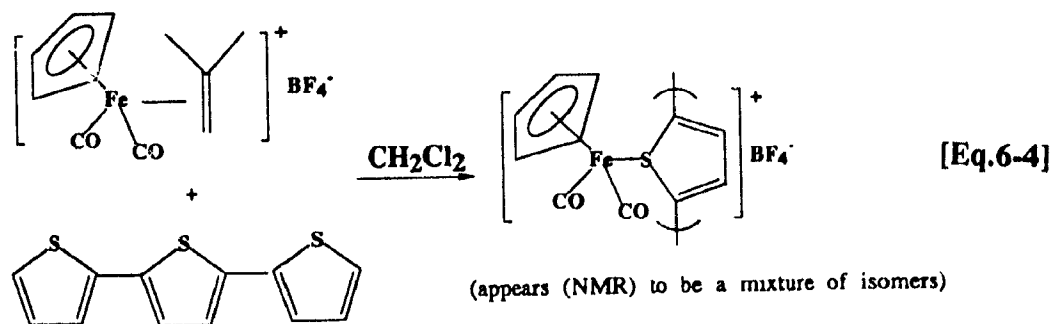
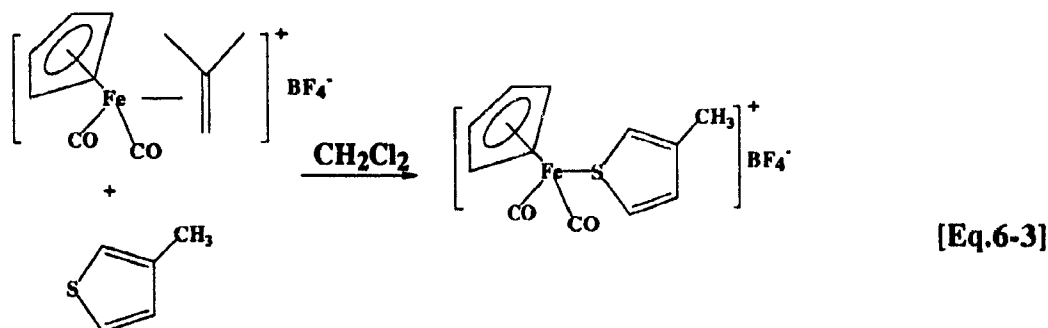
131. Ferraro, J.R.; Furlani, A.; Russo, M.V. *Appl. Spectrosc.* **1987**, *41*, 830.

132. Cao, Y.; Qian, R.Y. *Solid State Communications*, **1985**, *54*, 221.

133. Hayes, W.; Pratt, F.L.; Wong, K.S.; Kaneto, K.; Yoshino, K. *J. Phys. C: Solid State Phys.* **1985**, *18*, L555.

c. Thiophene-iron Model Complexes

When a CH_2Cl_2 solution of $[\text{CpFe}(\text{CO})_2(\text{H}_2\text{C}=\text{CMe}_2)]\text{BF}_4$ was heated in the presence of 3-methylthiophene or 2,2':5',2''-terthiophene, ligand exchange occurred, yielding respectively the orange-red $[\text{CpFe}(\text{CO})_2(3\text{-methylthiophene})]\text{BF}_4$ or the purple $[\text{CpFe}(\text{CO})_2(2,2':5',2''\text{-terthiophene})]\text{BF}_4$ [Eqs. 6-3, 6-4]. Integration of the aryl region of the $^1\text{H-NMR}$ spectrum of $[\text{CpFe}(\text{CO})_2(2,2':5',2''\text{-terthiophene})]\text{BF}_4$ relative to that of the Cp region suggested that 30% of the terthiophene had two $[\text{CpFe}(\text{CO})_2]^+$ cations attached. The IR spectra of $[\text{CpFe}(\text{CO})_2(3\text{-methylthiophene})]\text{BF}_4$ and $[\text{CpFe}(\text{CO})_2(2,2':5',2''\text{-terthiophene})]\text{BF}_4$ in CH_2Cl_2 showed two strong $\nu(\text{CO})$ bands at 2072 and 2031, and 2073 and 2031 cm^{-1} , respectively, which are very close to those reported for analogous complexes. The two complexes were very soluble in polar solvents, such as CH_3NO_2 and MeOH, and were fairly stable in the solid state under N_2 or in a vacuum, but decomposed in air at room temperature. Heating the complexes to 80°C gave the decomposed product $\text{CpFe}(\text{CO})_3\text{BF}_4$.¹²¹



Freshly prepared $[\text{CpFe}(\text{CO})_2(\text{H}_2\text{C}=\text{CMe}_2)]\text{BF}_4$ and $[\text{CpFe}(\text{CO})_2(3\text{-methylthiophene})]\text{BF}_4$ were pressed into disks and their conductivities were measured. The conductivities of these materials were below the detection limit of the instrumentation ($<10^{-6} \Omega^{-1} \text{ cm}^{-1}$). Under 500 V DC power supply, only very low initial currents were detected (about 1 μA), which disappeared in about 5-10 seconds. Similar results were also obtained for $[\text{CpFe}(\text{CO})_2(2,2':5,2''\text{-terthiophene})]\text{BF}_4$. The disks became soft and the conductivities increased after standing in air, but the current of these disks decreased very rapidly under the DC conditions.

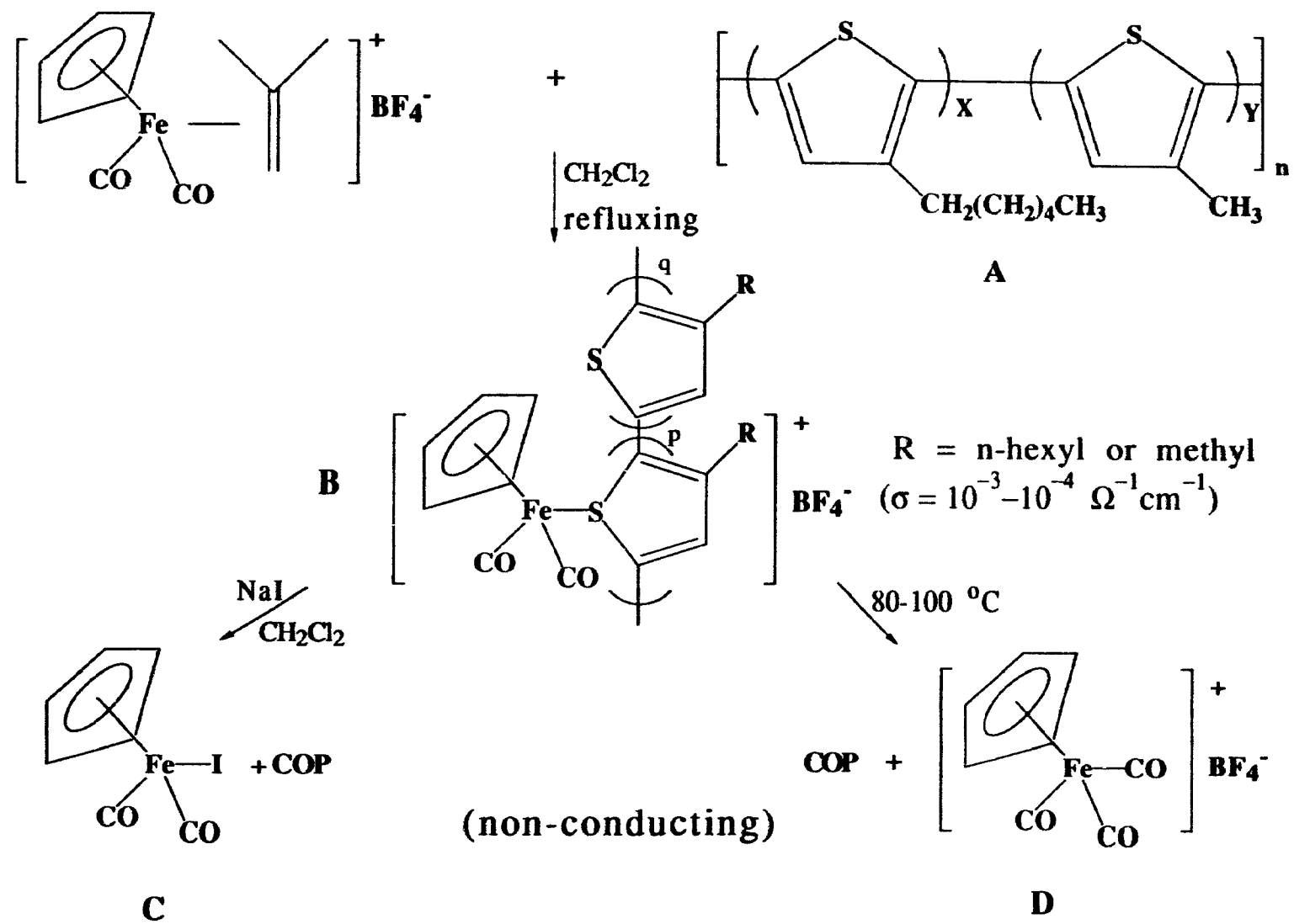
d. $[\text{CpFe}(\text{CO})_2]^+$ -doping

The COP was treated with the iron(II) complex $[\text{CpFe}(\text{CO})_2(\text{H}_2\text{C}=\text{CMe}_2)]\text{BF}_4$ (3:1 mole ratio) under N_2 in refluxing CH_2Cl_2 for 80 min following a procedure similar to that for preparing $[\text{CpFe}(\text{CO})_2(\text{thiophene})]\text{BF}_4$.¹²¹ The colour of the solution changed from dark-red to dark-yellow-green. The residue upon evaporation of CH_2Cl_2 was washed with CH_3OH and dried under vacuum to give the brown-black material $[\text{CpFe}(\text{CO})_2\text{-COP}]\text{BF}_4$. The conductivity of the disk pressed from this material was of the order of $10^{-3}\text{-}10^{-4} \Omega^{-1} \text{ cm}^{-1}$.

The $[\text{CpFe}(\text{CO})_2\text{-COP}]\text{BF}_4$ complex in CH_2Cl_2 exhibited two strong IR bands in the $\nu(\text{CO})$ stretching region at 2071 and 2026 cm^{-1} , consistent with the presence of the $\text{CpFe}(\text{CO})_2$ residue [Fig.6-5]. Interestingly, there were a few new strong bands in the 1000-1400 cm^{-1} region which were also observed in the IR spectrum of the conducting, I_2 -doped copolymer but which did not appear in the spectrum of pure COP. The percentage of the thiophene rings of COP attached to organoiron cations was determined by integration of the ^1H NMR spectrum. Integration of the aryl and alkyl regions of the NMR spectrum relative to that of the Cp region suggested that 7% of the thiophene rings were attached to an organoiron cation. Comparison of the UV-VIS spectrum of the $[\text{CpFe}(\text{CO})_2\text{-COP}]\text{BF}_4$

complex to that of pure COP [Fig.6-6] revealed that the single broad band at 470 nm observed for COP was split into two bands with λ_{max} at 400 nm and approximately 570 nm due to complexation. Clearly, the attachment of the organoiron cation perturbs the electronic configuration of the copolymer.

The de-doping process was done by either stirring $[(\text{CpFe}(\text{CO})_2\text{-COP})\text{BF}_4]$ with NaI in CH_2Cl_2 under N_2 at room temperature for about 30 min, or by heating the disks at 80-100°C for 3 h. Heating solid $[(\text{CpFe}(\text{CO})_2\text{-COP})\text{BF}_4]$ to 100°C gave a non-conducting material whose IR spectrum [Fig.6-5] was characteristic of $[(\text{CpFe}(\text{CO})_3)\text{BF}_4]$ in the $\nu(\text{CO})$ stretching region (2123, 2068 and 2006 cm^{-1}), which is similar to the thermal decomposition of $[(\text{CpFe}(\text{CO})_2(3\text{-methylthiophene}))\text{BF}_4]$ or decomposition in solution.¹²¹ The dark-red colour of the original pure COP returned. Treatment of $[(\text{CpFe}(\text{CO})_2\text{-COP})\text{BF}_4]$ in CH_2Cl_2 with NaI gave, upon evaporation of solvent, a dark-red, non-conducting residue, whose IR spectrum [Fig.6-5] in the carbonyl region (2044 and 2002 cm^{-1}) is characteristic of $\text{CpFe}(\text{CO})_2\text{I}$ embedded in COP and whose $^1\text{H-NMR}$ spectrum in CDCl_3 is consistent with a mixture of $\text{CpFe}(\text{CO})_2\text{I}$ and COP. Its UV spectrum in CH_2Cl_2 is the same as that of COP [Fig.6-6]. This further indicates that the original COP had been regenerated. The thiophene ligand of the complex has been substituted by I^- , which is consistent with the result reported that thiophene ligands of $[(\text{CpFe}(\text{CO})_2(\text{T}))\text{BF}_4]$ are labile and can be displaced by ligands such as CH_3CN or acetone.¹²¹ The preparation of $[(\text{CpFe}(\text{CO})_2\text{-COP})\text{BF}_4]$ and its subsequent transformations are depicted in Scheme 6-3. It is reasonable to conclude that the $[(\text{CpFe}(\text{CO})_2)^+]$ residues bind to the sulfur atoms of some of the thiophene rings of the copolymer backbone.



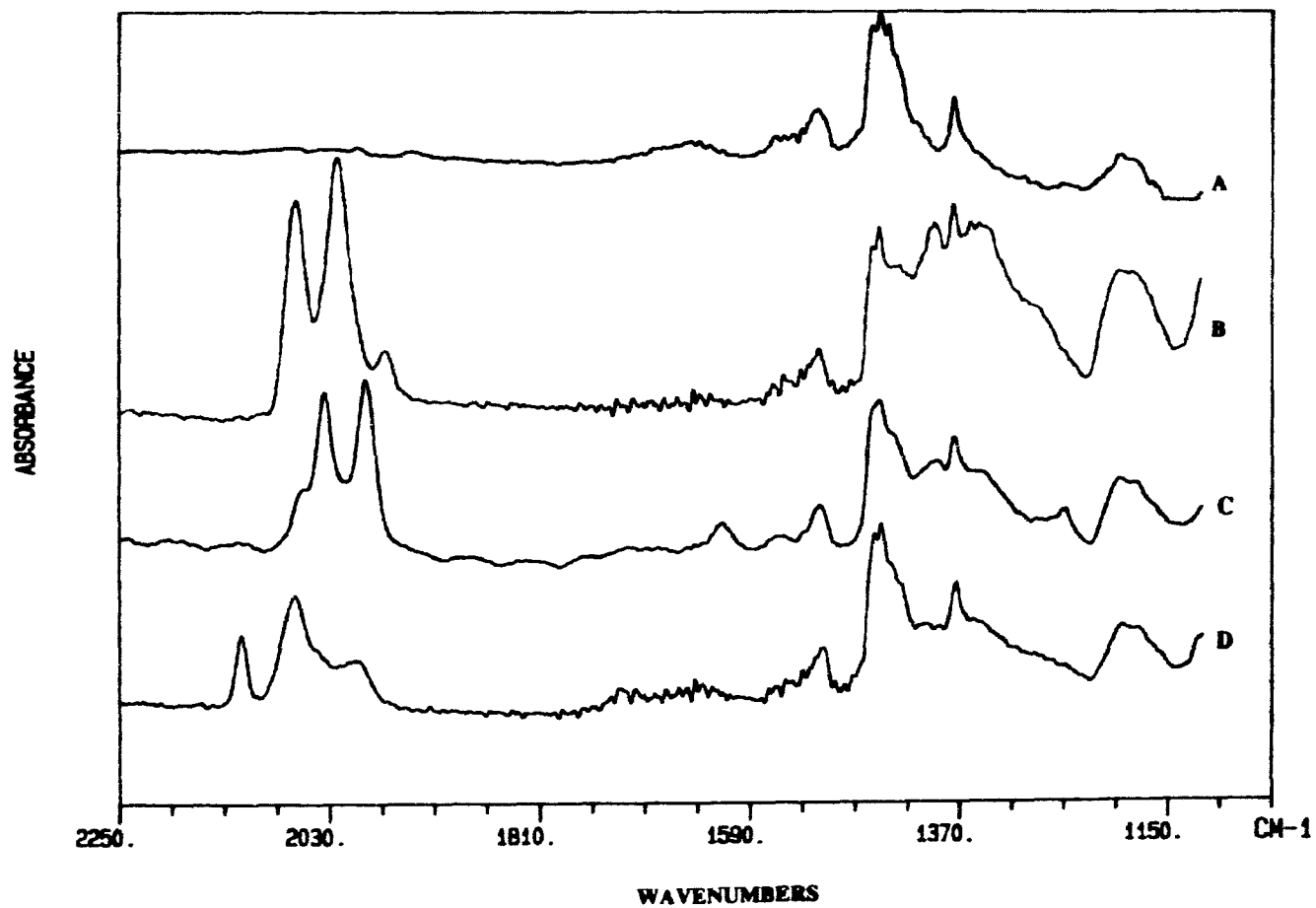


Figure 6-5 The IR spectra of (a) COP, (b) $[\text{CpFe}(\text{CO})_2\text{-COP}]\text{BF}_4$, (c) $\text{CpFe}(\text{CO})_2\text{I-COP}$ and (d) $\text{CpFe}(\text{CO})_3\text{BF}_4\text{-COP}$

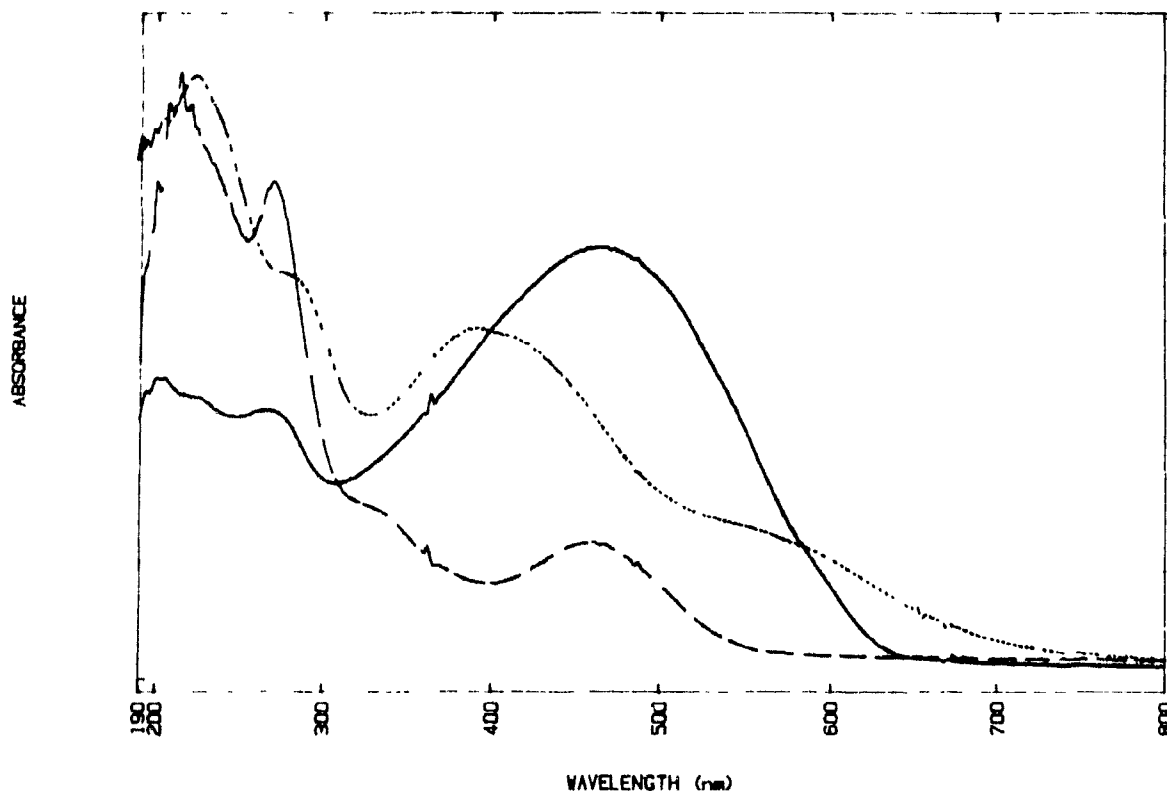


Figure 6-6 UV-VIS spectra of (....) $[\text{CpFe}(\text{CO})_2\text{-COP}]\text{BF}_4$, (---) $[\text{CpFe}(\text{CO})_2(3\text{-methylthiophene})]\text{BF}_4$ and (—) COP.

Changing the ratio COP : $[\text{CpFe}(\text{CO})_2(\text{H}_2\text{C}=\text{CMe}_2)]\text{BF}_4$ in the preparation of $[\text{CpFe}(\text{CO})_2\text{-COP}]\text{BF}_4$ changes the number of iron-functionalized thiophene rings. Figure 6-7 shows the $\log \sigma$ as a function of the number of $[\text{CpFe}(\text{CO})_2]^+$ groups attached to every 100 thiophene rings. The conductivity reached its maximum value at relatively low loadings (about 3-5%). These correspond to 6-10 weight percentage of iron doping agent. The conductivity only decreased slightly from $8 \times 10^{-4} \Omega^{-1} \text{cm}^{-1}$ to $3 \times 10^{-4} \Omega^{-1} \text{cm}^{-1}$ after the disk had been stored *in vacuo* at room temperature for 6 months. The conductivity decreased dramatically after the disk was exposed to water vapour in a sealed flask

containing some liquid water for about 1 week, while the conductivity increased slightly following storage in air.

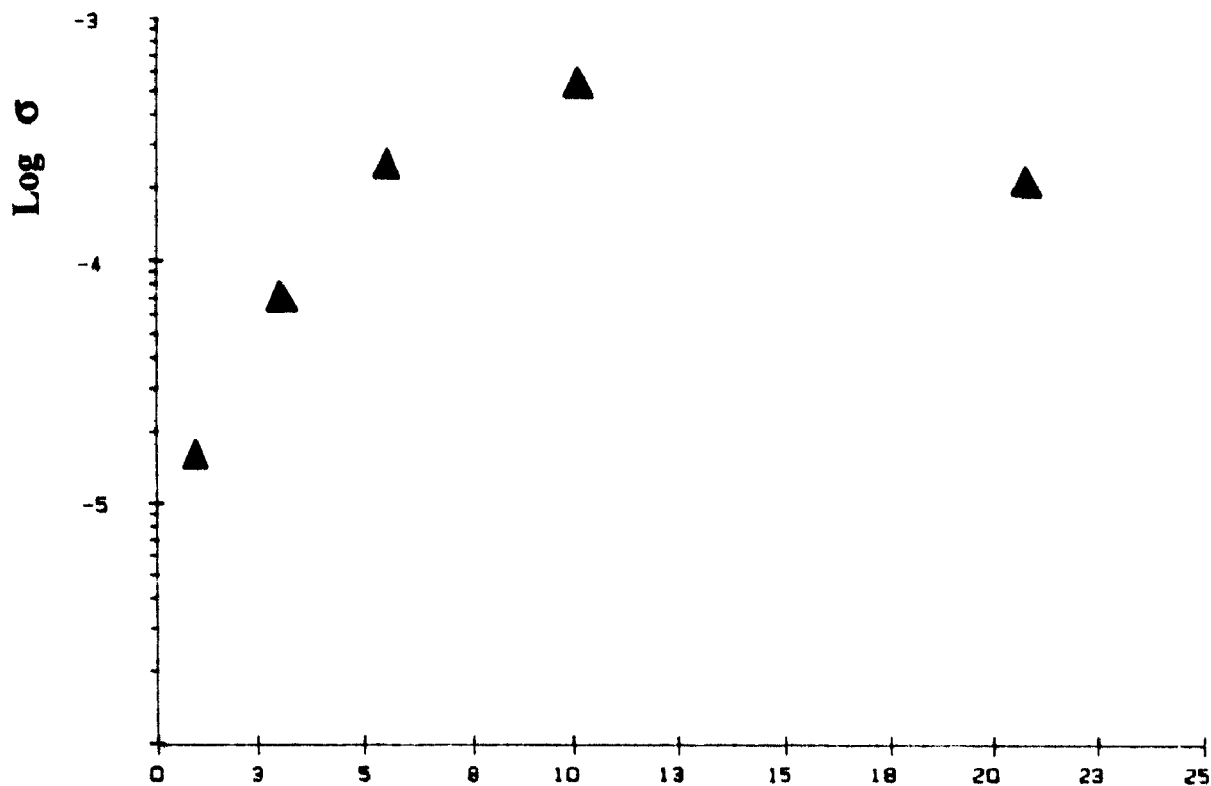


Figure 6-7 $\text{Log } \sigma$ as a function of the number of $[\text{CpFe}(\text{CO})_2]^+$ attached to every 100 thiophene rings.

Under constant DC conditions the current carried by a disk of $[\text{CpFe}(\text{CO})_2\text{-COP}]\text{BF}_4$ decreased rapidly at the beginning [Fig.6-8]. This decrease moderated for the next few hours and then the current stabilized at a relatively constant value although a gradual decrease continued. However, the conductivity of this material remained relatively stable. This behaviour was similar to that of I_2 -doped COP.

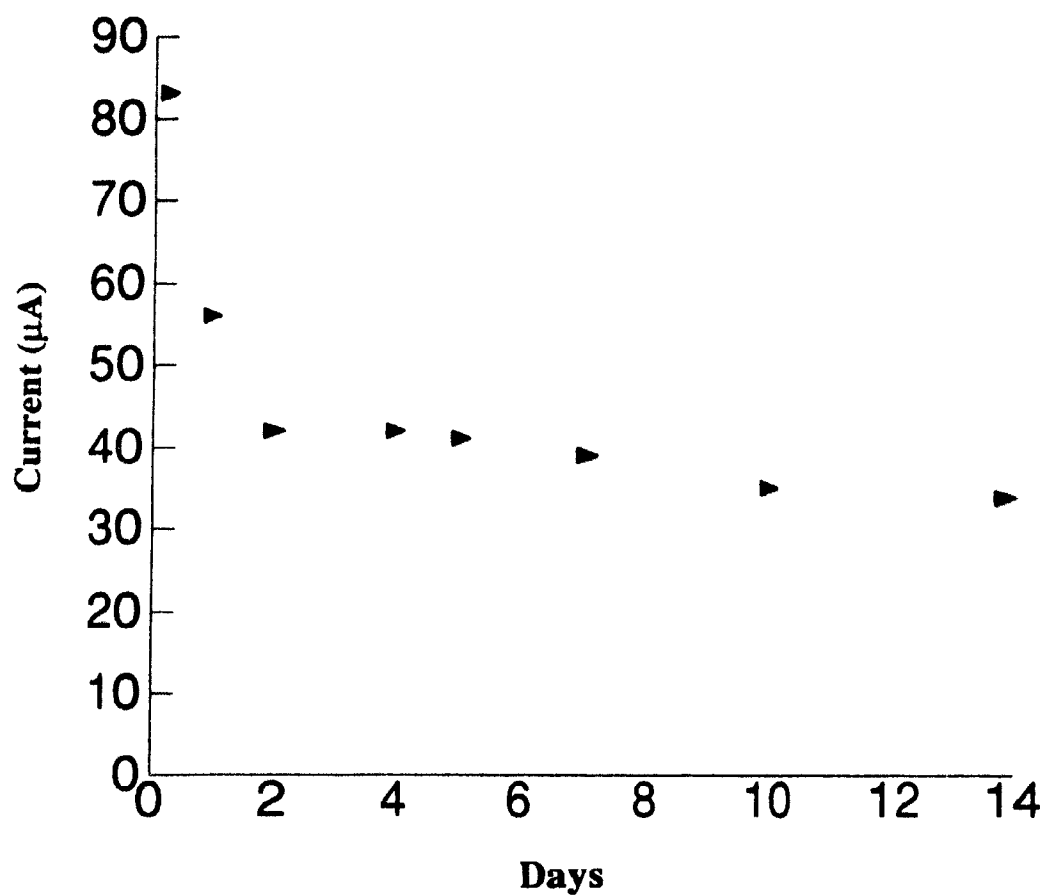


Figure 6-8 The current of $[\text{CpFe}(\text{CO})_2\text{-COP}]\text{BF}_4$ as a function of time under constant DC conditions (200 V).

Several other experiments were performed for comparison purposes.

1) Refluxing COP with finely powdered NaBF_4 or FeSO_4 , in CH_2Cl_2 or THF, gave non-conducting residues upon evaporation of solvent. No colour or IR spectral changes were noted.

2) COP and freshly prepared $[\text{CpFe}(\text{CO})_2(3\text{-methylthiophene})]\text{BF}_4$ (3:1 weight ratio) were stirred in CH_2Cl_2 under N_2 for 1 min and freeze-dried under vacuum. No detectable conductivity of the disk of this mixture was measured.

3) Refluxing PS and $[\text{CpFe}(\text{CO})_2(\text{H}_2\text{C}=\text{CMe}_2)]\text{BF}_4$ in CH_2Cl_2 under N_2 gave a red residue. The colour was very easily extracted by CH_3OH , eventually giving a colourless solid which had no absorption in the $\nu(\text{CO})$ region of its IR spectrum and no peak in the Cp region of its $^1\text{H-NMR}$ spectrum. This solid material was an insulator.

4) Upon refluxing PPP (soluble) and $[\text{CpFe}(\text{CO})_2(\text{H}_2\text{C}=\text{CMe}_2)]\text{BF}_4$ in CH_2Cl_2 under N_2 for 2 h, the colour of solution changed from orange-yellow to red-brown. The residue upon evaporation of this solution was dried under vacuum and pressed into a disk. Very low conductivity was detected which disappeared after a few seconds. Similarly, the colour of the residue was easily extracted by CH_3OH . The washed material was an insulator and showed no absorption in the $\nu(\text{CO})$ region of its IR spectrum and no peak in the Cp region of its $^1\text{H-NMR}$ spectrum.

6.4 Discussion

In the case of $\text{CpFe}(\text{CO})_2(\text{T})\text{BF}_4$ model complexes and several other systems, (i.e., COP- $[\text{CpFe}(\text{CO})_2(3\text{-methylthiophene})]\text{BF}_4$ mixture, refluxed PS- $[\text{CpFe}(\text{CO})_2(\text{H}_2\text{C}=\text{CMe}_2)]\text{BF}_4$ and PPP- $[\text{CpFe}(\text{CO})_2(\text{H}_2\text{C}=\text{CMe}_2)]\text{BF}_4$), the DC conductivity measurements show very low initial currents which disappear after a few seconds. As discussed in Chapter 5, ionic conductivity of most dielectric materials, decays with time. The current diminishes after a few seconds or a few minutes under DC conditions.^{116(a)} Therefore, the materials behave as low ionic conductors and the initial currents are likely due to the contribution of ionic carriers.

For I_2 -doped COP and $[\text{CpFe}(\text{CO})_2]^+$ -doped COP, under a constant DC power supply, the current decreased quickly in the first few minutes. Ionic carriers probably carry part of the current at the beginning, but they are swept out of the disk soon under DC conditions.

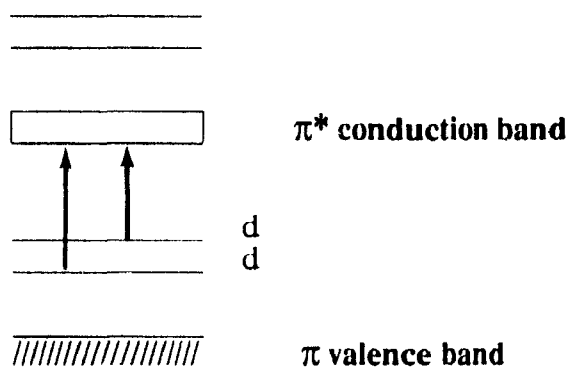
The remaining conductivities are relatively stable for I_2^- and $[\text{CpFe}(\text{CO})_2]^+$ -doped COP. The origin of the electrical conductivity of I_2 -doped polythiophene polymers has been widely studied. As mentioned in Chapter 5, the most acceptable mechanism is that the doping process creates polarons and bipolarons, which act as charge carriers. The UV spectra of doped polythiophene polymers have shown bands due to the absorptions by polaron and bipolaron species.^{81,118(a)} However, the exact mechanism of the conductivity is still not clear.

It is difficult to determine the mechanism of conduction of $[\text{CpFe}(\text{CO})_2\text{-COP}]\text{BF}_4$ based on the data in hand. However, its conductivity is relatively stable under the constant DC power conditions. This indicates that the conductivity of $[\text{CpFe}(\text{CO})_2\text{-COP}]\text{BF}_4$ is likely to be via an electronic mechanism.

The IR spectrum of $[\text{CpFe}(\text{CO})_2\text{-COP}]\text{BF}_4$ shows several new bands around 1000-1400 cm^{-1} . These bands are also observed in the IR spectrum of I_2 -oxidized COP and

electrochemically-doped polythiophene and have been assigned to the charged polythiophene chains or the so-called polarons and bipolarons.^{132,133} The UV spectrum of the oxidized-polythiophene shows a new band around 750 nm with a large decrease of the $\pi \rightarrow \pi^*$ absorption of the polymer around 470 nm.^{118(a)} Following doping of COP with $[\text{CpFe}(\text{CO})_2]^+$, the band at 470 nm splits into two new bands at 400 and 570 nm. Because of this spectroscopic similarity, the $[\text{CpFe}(\text{CO})_2]^+$ residue may be regarded as mimicking the action of an oxidizing agent such as I_2 on COP leading to improved electrical conduction.

The introduction of $[\text{CpFe}(\text{CO})_2]^+$ moieties into the conjugated COP chain may lead to the interaction of the d-electrons of the metal with the π -electron system of the polymer.¹³⁴ The lowest energy bands of the complexes $[\text{CpFe}(\text{CO})_2(\text{T})]\text{BF}_4$ in the UV-VIS spectra [Fig.6-6] shift from 460 nm (T = methylthiophene) to 570 nm (T = COP). It is not clear if the bands are due to the CT (charge transfer) absorptions. However, the CT bands have been observed for the complexes such as $\text{CpMn}(\text{CO})_2(\text{pyridine})$.¹³⁵ It is possible that the d-electrons can be excited into the conduction π^* band of COP to carry electron flux [Scheme 6-4].^{134,135}



Scheme 6-4

134. Ashby, M.T.; Enemark, J.H.; Lichtenberger, D.L. *Inorg. Chem.* **1988**, *27*, 191.

135. Geoffroy, G.L.; Wrighton, M.S. *Organometallic Photochemistry* Academic Press, Toronto, **1979**.

The $[\text{CpFe}(\text{CO})_2\text{-COP}]\text{BF}_4$ may also be viewed as a complex with a long conjugated ligand whereby conduction occurs *via* a combination of inner- and outer-sphere redox reactions.¹³⁶

6.4 Conclusions

Treatment of an electrically non-conducting copolymer of 3-methyl- and 3-hexylthiophene with $[\text{CpFe}(\text{CO})_2(\text{H}_2\text{C}=\text{CMe}_2)]\text{BF}_4$ gave $[\text{CpFe}(\text{CO})_2\text{-COP}]\text{BF}_4$, a material with a relatively stable conductivity ($\sigma = 10^{-3}\text{-}10^{-4} \Omega^{-1} \text{cm}^{-1}$). The presence of $[\text{CpFe}(\text{CO})_2]^+$ residues covalently bonded to the thiophene-sulfur atoms of 5-10% of the rings of the polymer has been established. The attachment of the organoiron cations perturbs the electronic configuration of the copolymer in a manner not yet understood. However, it is clear that the $[\text{CpFe}(\text{CO})_2]^+$ residues, attached to the thiophene rings of the copolymer backbone, are the source of the improved conductivity.

6.5 Suggestions for Future Work

One possibility is to vary doping reagents, such as $[\text{CpRu}(\text{CO})_2]^+$, $[(\text{R}_5\text{Cp})\text{Fe}(\text{CO})_2]^+$, to see if these can form more stable metal-S bonded complexes and also improve the conductivity. Variation of conjugated polymers, such as the polypyrrole type polymers, is another possibility to form a $\text{CpFe}(\text{CO})_2\text{-N}(\text{pyrrole})$ complex in order to induce conductivity in polypyrrole.

136. Cotton, F.A.; Wilkinson, G. in *Advanced Inorganic Chemistry*, Fifth edition, Wiley-Interscience, Toronto, 1988, p1307-1316.

SUMMARY AND CONTRIBUTIONS TO KNOWLEDGE

PART I

- 1) A variety of polymer films (PS, PMMA and PSAN) containing monomeric and dimeric metal carbonyl complexes were prepared through hot-pressing. The technique was simple, general and reasonably non-destructive. Films generated were examined by IR, ATR-IR, Raman and microscopy techniques. They were uniform and transparent and the organometallics embedded were highly dispersed in the polymer matrices.
- 2) Infrared data of metal carbonyls in polymer films were recorded in the $\nu(\text{CO})$ stretching region. The polymers PS, PMMA and PSAN appeared to approximate the common solvents toluene, ethyl acetate and acetonitrile, respectively, in their influence on the shapes and positions of the IR bands of metal carbonyls.
- 3) Several of the films were subjected to UV irradiation and some of the photoproducts formed were identified by IR spectroscopy and were subsequently isolated. Irradiation of the embedded complexes led to decomposition, rapidly in PS and slowly in PMMA. The PSAN polymer was capable of stabilizing photogenerated intermediates by coordination of pendant nitrile groups to form organometallic polymers such as $\text{W}(\text{CO})_5(\text{PSAN})$, $\text{CpMn}(\text{CO})_2(\text{PSAN})$ and $\text{Mn}_2(\text{CO})_9(\text{PSAN})$. These are useful for the synthesis of organometallic polymers and unstable complexes in the solid state.
- 4) Iodine oxidation of dimeric complexes in PS, PMMA and PSAN matrices gave $\text{CpFe}(\text{CO})_2\text{I}$, $\text{CpMo}(\text{CO})_3\text{I}$ and $\text{Mn}(\text{CO})_5\text{I}$. The oxidation rate was dependent on the polymer, with the reaction in PS being the fastest and that in PMMA the slowest.
- 5) The addition reactions of *trans*- $\text{Ir}(\text{CO})\text{Cl}(\text{PPh}_3)_2$ embedded in PS with CO , H_2 , SO_2 , O_2 and I_2 gases were monitored by IR and appeared to be similar to those reactions in

toluene. These reactions demonstrate additional methods of transforming organometallic complexes in solid polymer films.

6) A polarized IR spectral study indicated that $\text{Mn}_2(\text{CO})_{10}$ can be partially oriented by stretching a PE film doped with the complex. This technique is useful for vibrational band assignments.

Part II

Treatment of an electrically non-conducting 3-methyl-(3-hexylthiophene)copolymer with $[\text{CpFe}(\text{CO})_2(\text{H}_2\text{C}=\text{CMe}_2)]\text{BF}_4$ gave the new conducting material $[\text{CpFe}(\text{CO})_2\text{-COP}]\text{BF}_4$ ($\sigma = 10^{-3}\text{-}10^{-4} \Omega^{-1} \text{cm}^{-1}$). The IR, UV and NMR spectra of this material and of model complexes suggested that $[\text{CpFe}(\text{CO})_2]^+$ residues, which were attached to the sulfur atoms of the thiophene rings of the COP backbone, induced the improved conductivity. The result opens a new avenue for the development of conducting polymers.

PUBLICATIONS

(1) A. Shaver, I. S. Butler, A. Eisenberg, J. P. Gao, Z. H. Xu, B. Fong, H. Uhm and D. Klein, "Complexes in polymers: FT-IR spectra and photochemistry of some monomeric organometallic carbonyl complexes in polystyrene, poly(methylmethacrylate), polystyrene-poly(methylmethacrylate) and polystyrene-polyacrylonitrile copolymer", *Appl. Organomet. Chem.* **1987**, *1*, 383-392.

(2) A. Shaver, J. P. Gao and I. S. Butler, "Complexes in polymers II: FT-IR spectra, iodine oxidation, and photochemistry of $[(\eta^5\text{-C}_5\text{H}_5)\text{Fe}(\text{CO})_2]_2$, $[(\eta^5\text{-C}_5\text{H}_5)\text{Mo}(\text{CO})_3]_2$ and $\text{Mn}_2(\text{CO})_{10}$ in polystyrene, polymethylmethacrylate, and polystyrene-polyacrylonitrile copolymer", *Appl. Organomet. Chem.* **1988**, *2*, 9-15.

(3) A. Shaver, J. P. Gao and I. S. Butler, "Complexes in polymers III: Addition reactions of CO, H₂, SO₂ and O₂ to *trans*-Ir(PPh₃)₂(CO)Cl embedded in polystyrene", accepted by *Appl. Organomet. Chem.*

(4) A. Shaver, J. P. Gao and I. S. Butler, "Electrical conductivity in a polythiophene induced by complexation with $[(\eta^5\text{-C}_5\text{H}_5)\text{Fe}(\text{CO})_2]^+$ ", *Organometallics* **1989**, *8*, 2079.

(5) I. S. Butler, J. P. Gao and A. Shaver, "Polarized IR spectra of decacarbonyldimanganese(0) and decacarbonyldirhenium(0) oriented in stretched polyethylene films", accepted by *Appl. Spectrosc.*

(6) I. S. Butler, H. Q. Li, J. P. Gao and A. Shaver, "A comparison of the photoacoustic, attenuated-total-reflection and transmission FT-IR spectra of some solid organoiron(II) carbonyl complexes", manuscript in preparation.